COINCIDENCE STUDIES WITH THE ACTIVE DEPOSITS OF RADIUM AND THORIUM

A Thesis

submitted by

K. W. Ogilvie, B.Sc.

for the degree of

Doctor of Philosophy

University of Edinburgh,

November, 1952.

LIST OF CONTENTS.

Chapter No.		Page No.
I	The Half-Life of Radium C'.	1
II	Scintillation Counters and Coincidence Circuits.	19
III	Measurement of the Half-Life of ThC' using Scintillation Counters.	31
IV	The Theory of Coincidence Experiments.	44
V	A Simple High Speed Coincidence System.	58
VI	An Attempt to put an upper limit to the Half-Life of one of the Long-Range α Particle Groups emitted by ThC'.	79
Appendix	The Efficiency of a Scintillation Counter as a γ Ray Detector.	90
References	1 to 52.	93.

Chapter I.

THE HALF-LIFE OF RADIUM C'.

Introduction.

RaC' is formed from RaC by β disintegration and decays by α emission. Several determinations of the half-life of this substance have been published, and all except the latest have given mutually consistent results of about 150 ± 5 μS. These have been obtained by two methods of coincidence counting. The first, called the integral method, examines the variation of coincidence counting rate with the resolving time of the mixer circuit. Dunworth (1), Ward (2) and Rotblat (3) have made such determinations. Dunworth's was an early experiment, of relatively low accuracy, giving the result 150 ± 20 μS. Ward, using a single counter, containing Radon, for both the α and β particles, obtained the result 148 ± 6 μS. Gamma rays follow the β particles from RaC with negligible delay, so α-γ coincidences may be used to determine the half-life of RaC'. Rotblat obtained 155 ± 20 μS in this way, as well as a value 145 ± 5 μS by α-β coincidences.

In the second method, the β pulses are electrically delayed, for a time which may be varied, and then put into coincidence with those due to the α particles in a mixer circuit of fixed resolving time. This differential method has been used by Jacobsen and Sigurgiesson (4) to obtain a result 155 ± 5 μS.

The latest determination, by Von Dardel (5, 6) was made using a twenty channel delay discriminator. In this apparatus the pulse from the β particle counter operates a gate circuit which opens, for a short period, each of the twenty recording channels in turn. The subsequent α particle pulse is accepted by that channel which is open when it occurs. The method is equivalent to a delayed coincidence experiment where counting is carried out using twenty different time delays simultaneously. It is capable of great accuracy when the electronic engineering is good and Von Dardel obtained 163.7 ± 0.2 μ S for the half-life. In his paper (6) there is a reference (his reference 8) to an unpublished account of an experiment carried out by Berthelot, Chaminade and Wahl, using a method similar to his and leading to results in good agreement with those obtained by earlier workers. The error quoted is, however, much larger than that of Von Dardel, and similar to that of Jacobsen.

While Von Dardel's result is not definitely inconsistent with those of other authors, it was thought that a new determination, using both the older methods, but paying more attention to details of electronic technique, might eliminate a possible small systematic error and lead to better agreement.

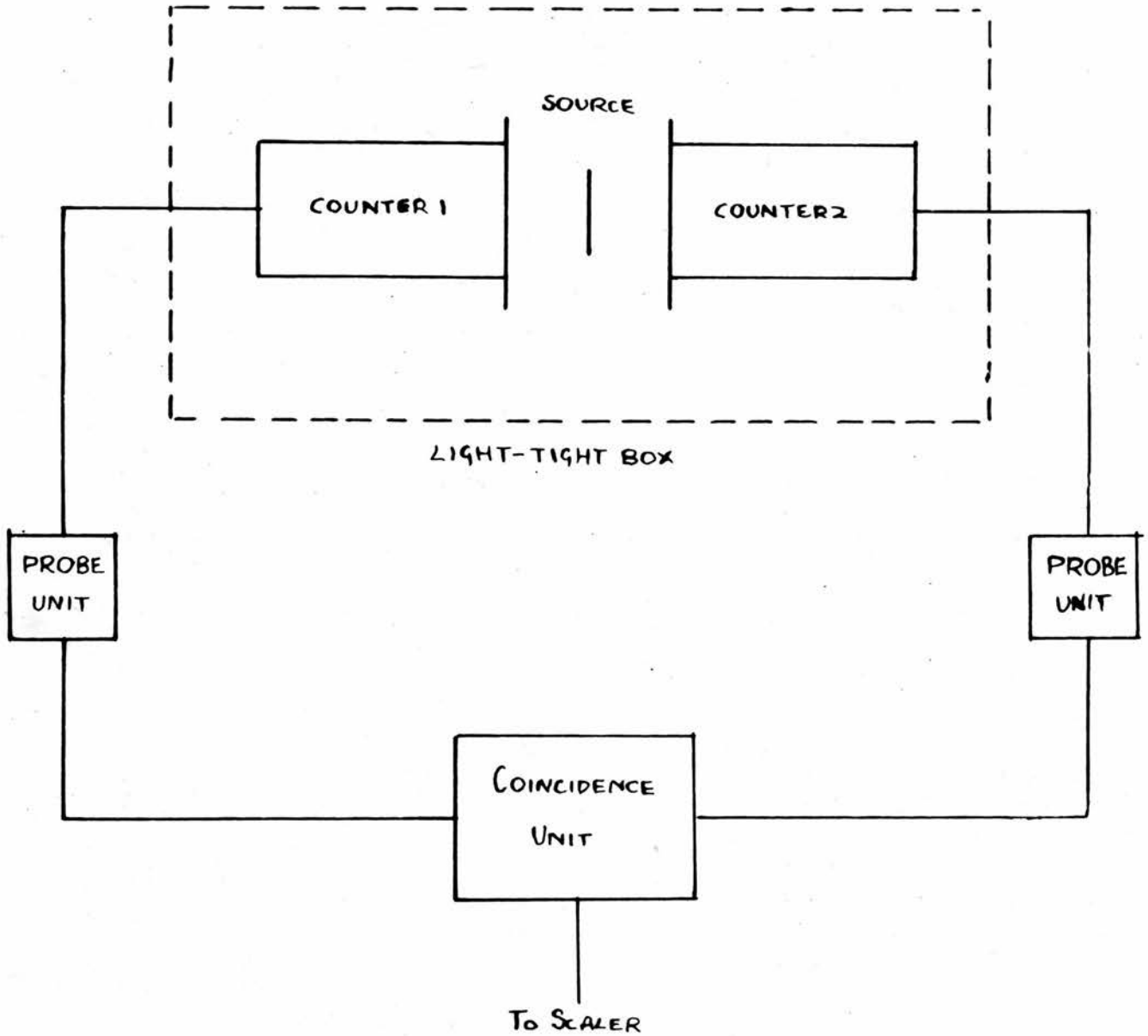

Figure 1. Block diagram of apparatus to determine the half-life of RaC'.

Description of Apparatus.

A diagram of the arrangement of the apparatus used for the experiments is given in Fig. 1 . Geiger counters were used, the α counter being a G.E.C. type E.H.M.2 and that for the β particles a G.E.C. type G.M.4. Since the α particle counter was found to be light-sensitive it was necessary to enclose the source and counters in a wooden box. Preliminary experiments were made to show that the effect of scattering from the walls of this box was negligible. The source was so fixed between the counters that it could easily be changed and replaced in the same position. Each counter was operated from a stabilized E.H.T. supply in conjunction with an A.E.R.E. probe unit type 1014A. This unit incorporates a circuit which lowers the potential of the counter anode by approximately 300 volts for a short and accurately known period of time after each discharge. This was necessary, both to allow the calculation of the correct counting rate, and also for a reason to be discussed below. The period of time during which the counter is made insensitive is known as the 'paralysis' - or 'dead' - time.

The pulses obtained from the probe units were fed directly into the coincidence circuit. The block diagram is shown in Fig. 2, and the circuit in Fig.

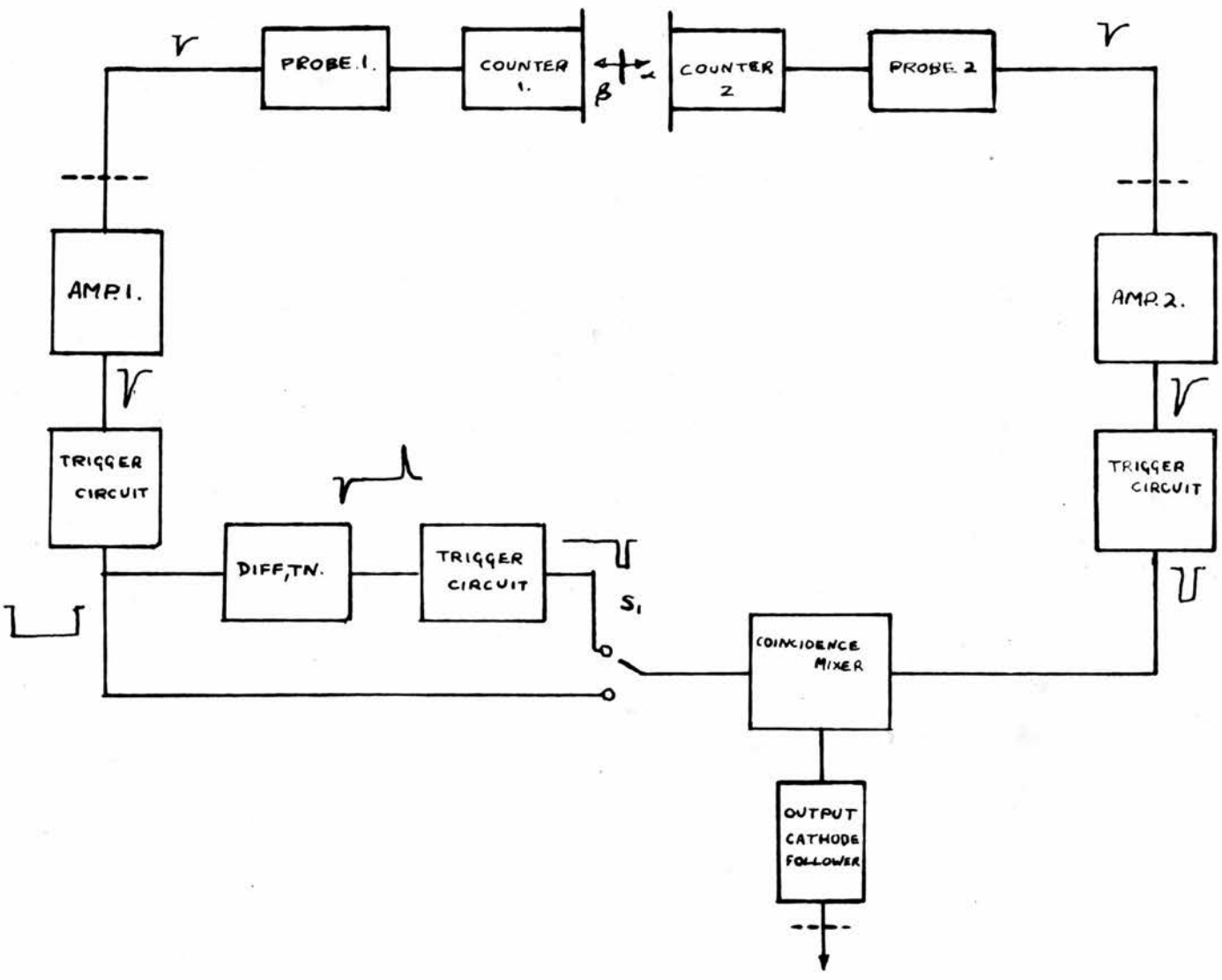

Figure 2. Block diagram of coincidence unit.

3. The same circuit was used for the integral method with switch S_1 in the lower position, and for the differential method with this switch reversed. Valves 1 and 2 amplified the pulses from the β counter probe unit which were applied to input I. Valves 3 and 4, connected in a cathode-coupled trigger circuit, were operated by these amplified pulses fed through the diode V_{12}. Large negative-going rectangular voltage pulses were thus fed to the grid of V_4, and their duration was controlled over a wide range by selecting the value of capacitor 4, resistor 14 being fixed in value. With S_1 in the lower position, these pulses were placed directly upon the grid of valve 5, which formed a cathode-coupled coincidence mixer together with valves 6 and 7.

Input II carried the pulses from the α counter probe unit, and these were amplified by valves 11 and 10. They were then converted to large negative-going rectangular voltage pulses by valves 8 and 9 in a similar way to that described above for the β pulses. However C_8, controlling their duration, was kept fixed in magnitude throughout the experiments. These standard pulses were applied through C_7 to the grid of the coincidence mixer V_6. The resolving time was the sum of the α and β pulse widths, and the β pulse width was varied by switching different values of C_4 into the circuit.

The coincident pulse output was obtained across R_{18} and was delivered to the scaler by the cathode follower V_{18}. The cathode resistors of valves 2 and 10 were not bypassed by capacitors, and so the voltage pulses appearing there were used to give the individual counting rates of the α and β counters.

For the differential method, the block diagram Fig. 2 was the same, and the same counters and source arrangement were used, but with the switch S_1 placed in the upper position. This modified the operation of the circuit in the following manner. The large pulses derived from valves 3 and 4 were now differentiated by C_5 and R_{16}. The positive-going rear edges were thus converted to positive-going delayed pulses, whose time delay was given by the duration of the pulses which had been differentiated. This delay could of course be varied by altering the value of C_4. However, it was found that the positive pulses so obtained were insufficiently constant in length and size as C_4 was varied, to be used in the coincidence mixer directly. It was thus necessary to introduce valves 14, 15 and 17 in order to convert them to standard shape. Valves 14 and 15 formed a cathode-coupled trigger circuit which was triggered through diode 16 by the (negative) output of valve 17. The resultant standard pulses were connected by the lower contact of switch S_1 to the grid of V_5.

No.	Value
	Resistors
1	250K Λ
2	10K
3	200
4	250K
5	2.5K
6	20K
7	150K
8	100K
9	30K ÷
10	100K ÷
11	20K
12	10K
13	10K
14	1250K ÷
15	250K
16	500K
17	5K ⁂
18	1K
19	50K ÷
20	250K
21	80K ÷
22	75K ⁂
23	1500K ÷
24	10K
25	10K
26	20K
27	100K ⁂
28	30K ⁂
29	2.5K
30	20K
31	10K
32	250K
33	200
34	250K
35	1000K ÷
36	10K
37	20K
38	10K ⁂
39	500K pot. ⁂
40	
41	100K pot. ⁂
42	
43	10K
44	1K
45	250K
46	2.5K
47	2.5K

No.	Value
	Capacitors
1	75 pf
2	75 pf
3	75 pf
4	Switched
5	40 pf
6	75 pf
7	75 pf
8	40 pf
9	75 pf
10	75 pf
11	75 pf
12	40 pf
13	75 pf
14	0.01 μf

	Valves
1	8D3
2	½ 6SN7
3	½ 6SN7
4	½ 6SN7
5	½ 6SN7
6	½ 6SN7
7	½ 6SN7
8	½ 6SN7
9	½ 6SN7
10	½ 6SN7
11	8D3
12	EA50
13	EA50
14	½ 6SN7
15	½ 6SN7
16	EA50
17	½ 6SN7
18	½ 6SN7

N.B.

⁂ denotes Wire Wound

÷ denotes High Stability

Figure 4. Table of Component Values.

Thus the delay introduced was controlled by the magnitude of C_4 and the resolving time was the sum of the widths of the pulses derived from the two trigger circuits comprising valves 9 and 10, and 14 and 15 respectively. From the list of components, Fig. 4 , it will be seen that good stability was assured by the use of high-stability and wire-wound resistors, at critical points. H.T. supply was obtained from a stabilized unit, and was independent of mains input variations.

It has been found that if such trigger circuits are operated by pulses occurring at regular intervals, the output pulse length remains constant and equal to the value given by calculation using the known component values, unless the pulse repetition frequency becomes large. When the time between two triggering pulses approaches the duration of the output pulse normally given by the circuit, this is shortened, and the circuit operates irregularly. The circuit is triggered by a pulse, and the effect of the next one is then often to extend the output pulse, giving one of greater length rather than two of the correct duration. This effect could occur in the present circuit if either counting rate, particularly that in the β counter, became high. The presence of the probe units prevents it and the experiments were carried out with the paralysis time of each fixed substantially larger than the duration of the longest pulse to be obtained from the trigger

circuits which followed them.

Tests carried out upon the Apparatus.

(i) Integral Method.

Eight values of C_4 were used in the experiment and the appropriate values of resolving time were obtained by the two source method. A β -ray source was placed in front of each counter and shielded to prevent it affecting the other. The chance coincidence counting rate N_c was observed, and when the separate counting rates in each counter, N_1 and N_2, had been found, the formula $N_c = 2N_1N_2T$ was used to find the resolving time $2T$. ($2T$ is equal to the sum of the α and β pulse widths at the mixer stage.) The results are summarised in Table 1.

The second and third columns show the figures for two separate experiments, carried out over a period of two weeks, using each of the values of C_4. The fourth column sets out the time of counting required to give the degree of accuracy shown in columns 2 and 3. More than two determinations were carried out for the smaller values of resolving time, in order to test the stability of the circuit over periods of time similar to that of one experimental run. The length of the pulse due to the β counter was also determined by a calibrated oscilloscope and the results form column 5 of the Table. These figures are subject to the uncertainty of the

calibration of that instrument, which is about 2%. The final resolving times used in the calculation of the results are given in column 6.

Table 1.

C_4 No	Run 1	Run 2	Time of Counts	β pulse width	2T
1	58 ± 2.3 61 ± 2.4	65 ± 3.2	60	54	61.3 ± 2.5
2	111 ± 4.4 115 ± 4.6	124 ± 3.7 119 ± 3.6	30	110	117 ± 4.0
3	200 ± 6	222 ± 6.6 200 ± 6	20	193	200 ± 5
4	287 ± 11	302 ± 9	25	287	294 ± 10
5	412 ± 12	412 ± 12	10	405	412 ± 12
6	476 ± 14	490 ± 15	10	476	483 ± 14
7	575 ± 17	550 ± 16.5	8	556	563 ± 16
8	757 ± 23	723 ± 22	7	-	-
	μS	μS	min.	μS	μS

During these experiments the paralysis times of the probe units, operating in conjunction with the β and α counters, were 1550 μS and 500 μS respectively.

A capacitor which gave a value of 2T of approximately 1250 μS was next inserted in the position of C_4. The table below shows that the β probe unit was operating correctly, because the resolving time obtained by the two source method did not vary with the

counting rate in the β counter,

N_1	N_2	$2T$
3866	4835	1240 ± 37 μS
3915	9923	1210 ± 30 "
3934	21884	1210 ± 12 "
3434	30269	1105 ± 55 "

providing it was not greater than about 22,000 per minute.

(ii) Differential Method.

Before calibrating the time delays, it was necessary to ensure reproducible values of resolving time at each delay setting.

The first column of Table 2 shows the numbers assigned to the positions of the switch which controlled the values of C_4 for this experiment. The variations in the resolving times for different values of C_4 on different occasions with the original circuit, shown in columns 2, 3, and 4 of Table 2, made it necessary to introduce valves 14 and 15, as mentioned above.

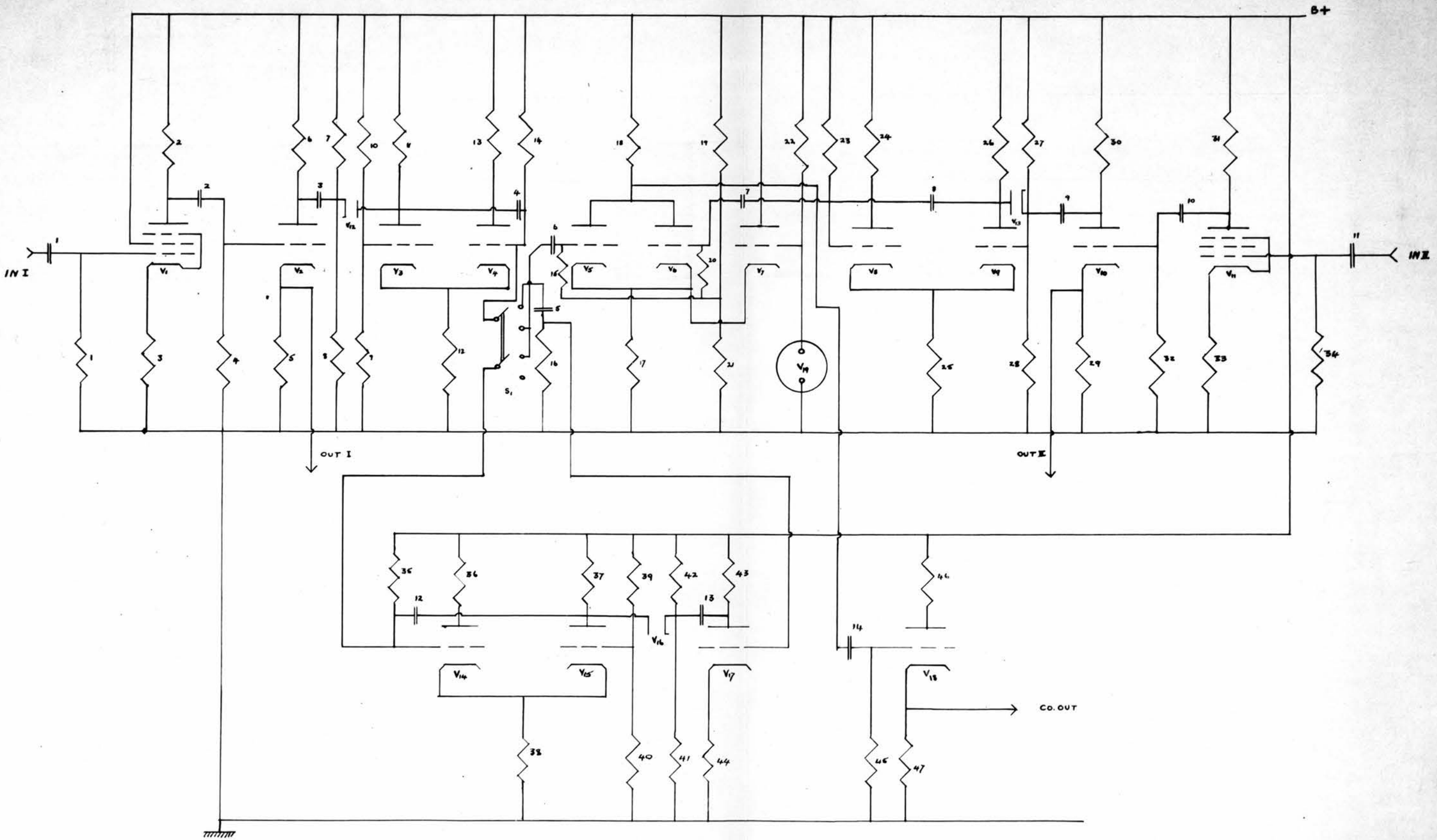

Figure 3. Circuit diagram of Coincidence Unit.

COINCIDENCE UNIT. Fig 3.

Table 2.

C_4No	2T run 1	2T run 2	2T run 3	2T	Delay
1	57 ± 1.7	40.6 ± 1.6	40.4 ± 1.6	30.9 ± 1	95
2	52 ± 1.7	-	39.2 ± 1.6	30.8 ± 1	200
3	55 ± 1.7	41.4 ± 1.6	38.3 ± 1.6	30.7 ± 1	290
4	51 ± 1.7	41 ± 1.6	38.8 ± 1.6	29.7 ± 1	455
5	56 ± 1.7	40.3 ± 1.6	36.4 ± 1.6	28.0 ± 1	475
6	52 ± 1.7	38 ± 1.6	39.4 ± 1.6	27.3 ± 1	695
7	48 ± 1.7	38 ± 1.6	33.6 ± 1.6	25.5 ± 1	950
8	46 ± 1.7	41 ± 1.6	-	24.7 ± 1	995
					μs

When this modification had been made, the results shown in column 5 were obtained, reproducible to within the limits of error. The decrease in resolving time as the delay is increased is due to the similarity in duration between the triggering pulse and the output pulse from valves 14 and 15. In these circumstances a variation in the characteristics of the triggering pulse causes a slight variation in the width of the output pulse. This effect necessitates a small correction to the results of the delayed coincidence experiments.

The delay times were found by measuring the duration of the pulse in the β channel, by a method illustrated by the diagram in Fig. 5. A 100 Kcs crystal

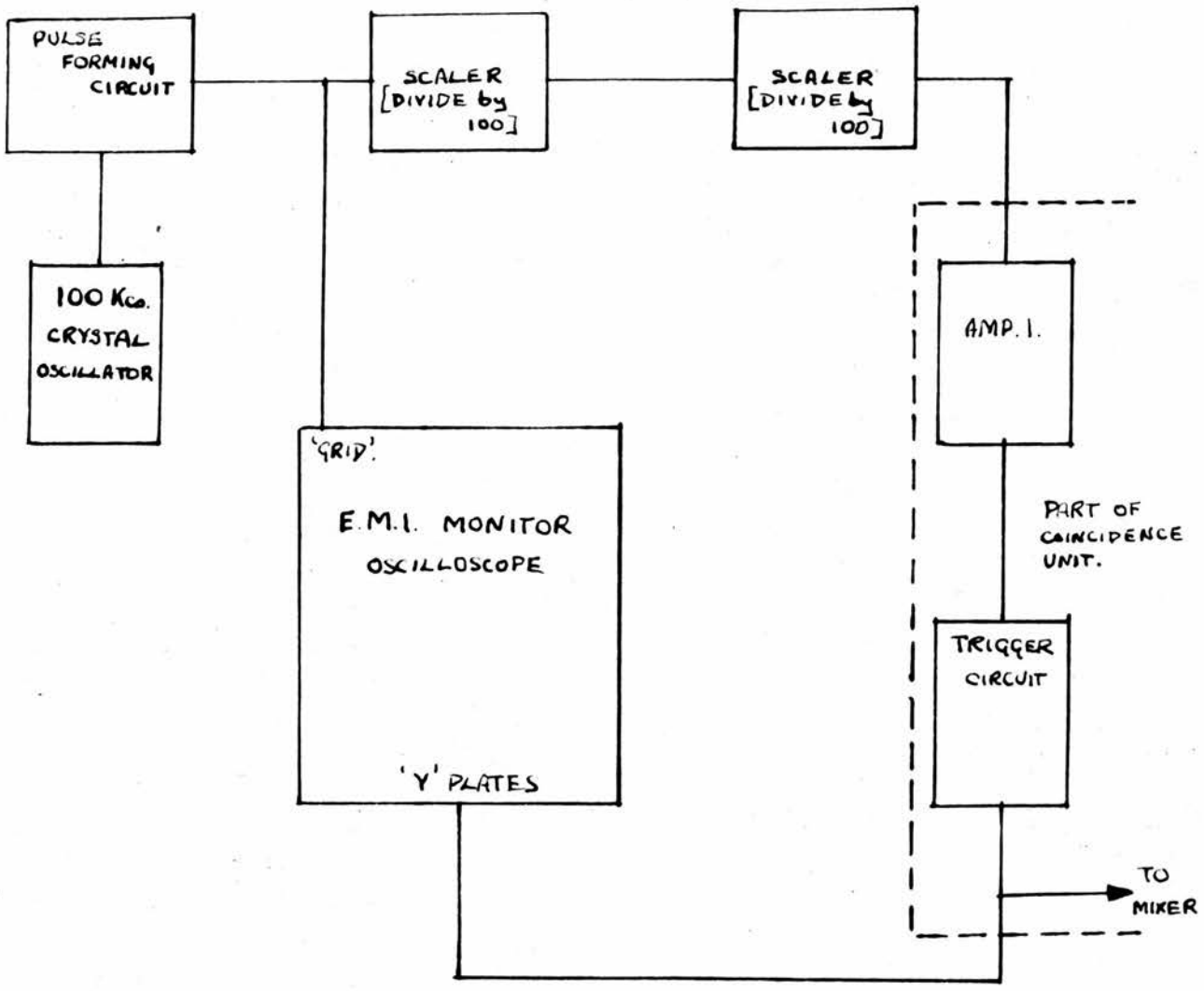

Figure 5. Block diagram showing arrangement of apparatus for calibration of time delays.

oscillator was used to trigger a pulse generator, and the frequency of these pulses was divided by 10^4 using two scalers in series. The resulting pulses, with a frequency of 600 per minute, were applied to the circuit through the β probe unit. The output from the trigger circuit comprising valves 3 and 4, was displayed upon an oscilloscope whose grid was modulated with the 100 Kcs pulses directly. A dotted trace was thus observed, and the length of the long pulses obtained by counting the dots, and interpolating between the last two. This arrangement was found to be very stable, and to give reproducible readings, of an accuracy of $\pm$ 3 microseconds, or better. The final values are given in column 6 of Table 2.

The Source.

A diagram of the transformations occurring in the short-lived active deposit of Radium is given in Fig. 6 together with a table given by Hevesy and Paneth (7) in their book, "Manual of Radioactivity". Radium C' is formed as a result of 99.96% of the disintegrations of RaC, so that for the present purpose the transformations occurring in the source can be represented by

$$\text{RaB} \xrightarrow{\beta,\alpha} \text{RaC} \xrightarrow{\beta} \text{RaC'} \xrightarrow{\alpha} \text{RaD}.$$

This ignores the γ radiation, for which the counters have a relatively low efficiency. The α particle counter detects α and β particles, but the β

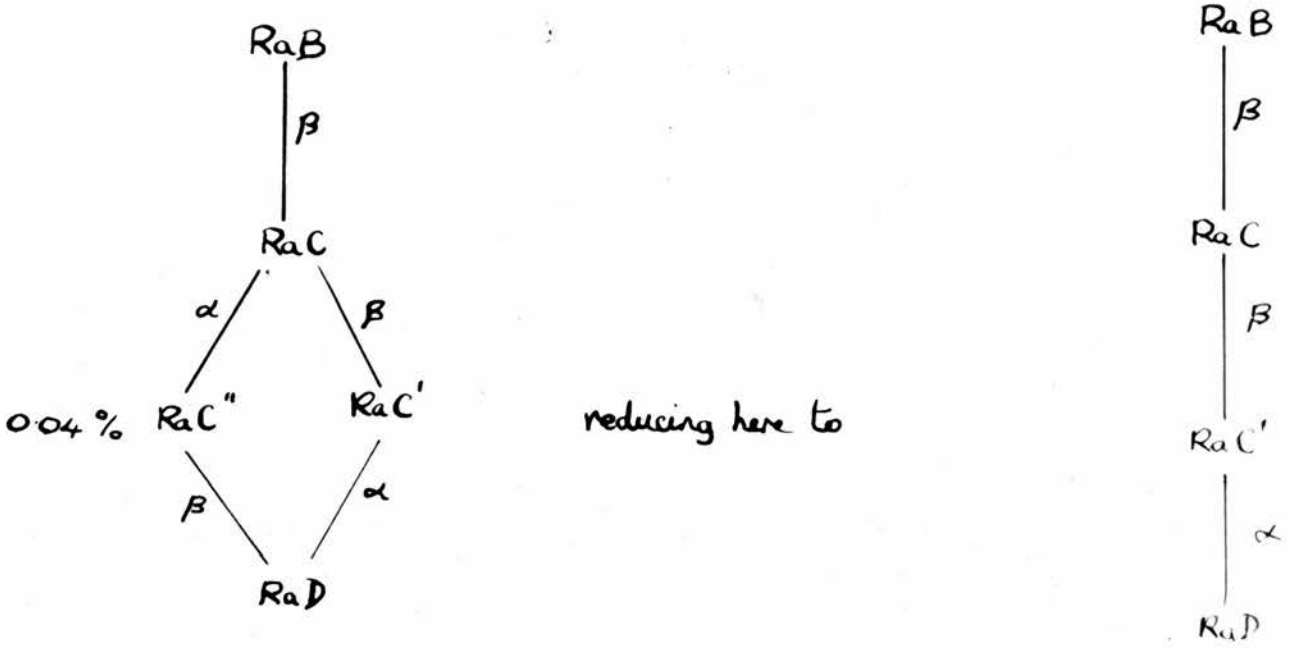

SUBSTANCE	RaB		RaC		RaC'	RaC"
HALF-LIFE	26·8 m		19·7m.		—	1·32m.
RADIATION	β, γ		α, β, γ		α	β
RANGE – α			4·1cm		6·96cm.	
ABSORBTION COEFFICIENT cm^{-1} in Al.	β	γ	β	γ		
	890 77 13	230 40 0·57	50 13	0·23 0·127		

Figure 6. Diagram of disintegrations in the active deposit of Radium.

counter window does not transmit α particles. Thus the α particle counting rate should be about 50% more than that of the β particles. This was observed.

The source was deposited by recoil from Radon, on to 1 sq. cm. at the centre of a strip of Aluminium foil 5 cm. long and 1 cm. wide. The thickness of this foil was 11 mg./sq. cm. After removal from the activation apparatus the source was allowed to decay for three hours. This was necessary to give a suitable counting rate, and it also ensured that the source decay was accurately exponential in form. Table 3 shows a typical set of readings of β counting rate corrected for decay of the source and for the paralysis time of the probe unit. The figures in the fourth column are constant within 2½%.

Table 3.

Time (min.)	C_4No	Counting rate (per min.)	Corrected rate
0	1	20,169	21,800
8½	2	17,415	22,650
17	3	14,351	22,150
27½	4	11,882	22,150
38	5	9,858	22,800
48½	6	7,883	22,500
60	7	6,329	22,500

One minute counts were taken at the times shown in column 1. This was the procedure during an experiment.

The strip bearing the source was attached across the diameter of a brass ring with cellulose glue. This ring was mounted upon a rod which was held in a standard position between the counters. The active deposit faced the α counter, the β particles having to pass through the foil. The distance between the foil and either counter was approximately 1 cm.

Experimental Procedure and Results.

In each experiment counting was done according to a carefully drawn-up time table, so that accurate normalization for source decay could be carried out. Table 3 shows that this was successful. Each experimental run took 70 minutes, and the results were deduced from the total of counts obtained during seven runs. The short resolving time readings were taken when the source was fresh so that the number of coincidence counts dropped by less than a factor of two as the source decayed during the experiment.

Integral Method.

If $w(t)$ is the number of coincidences counted when using resolving time T, then

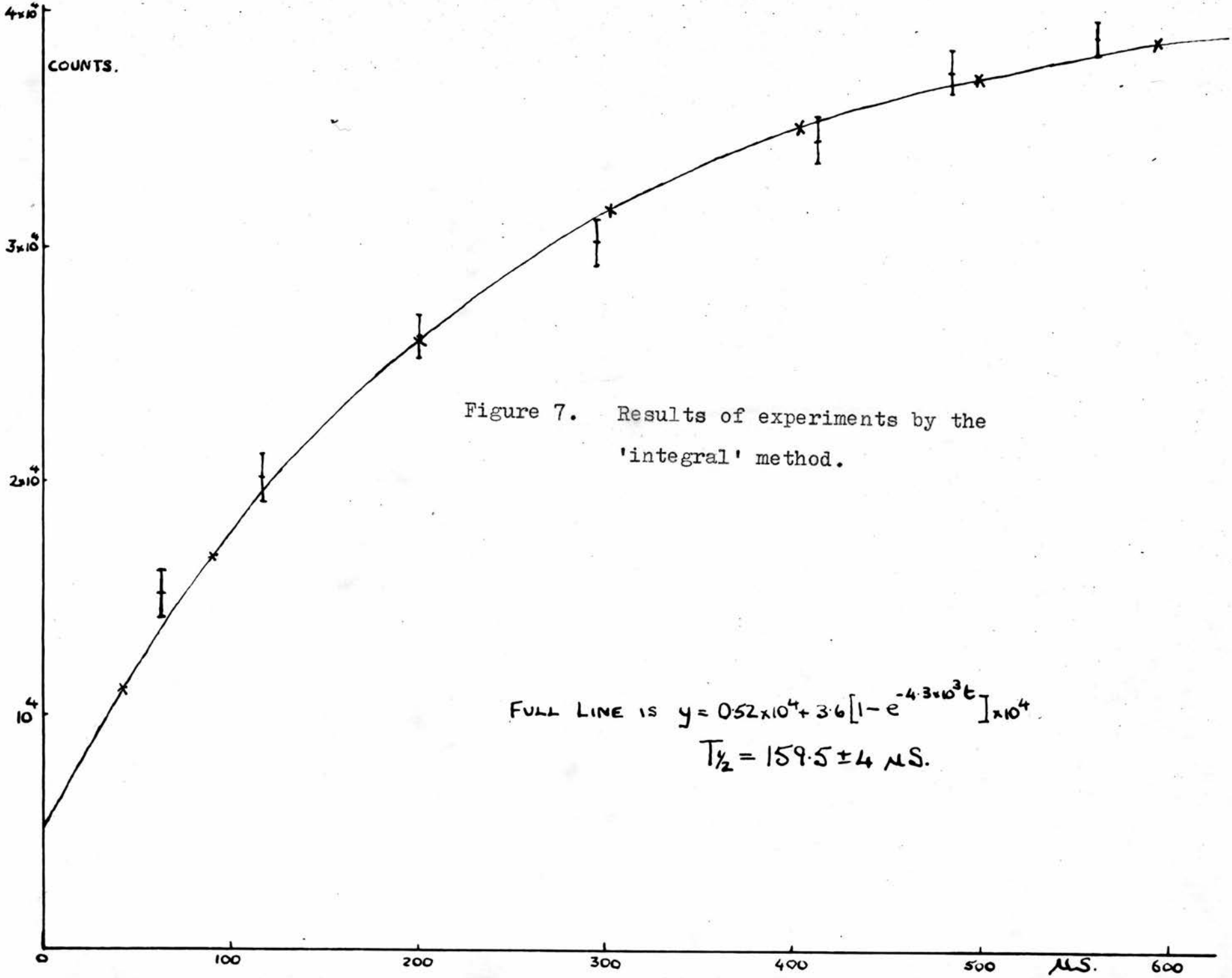

Figure 7. Results of experiments by the 'integral' method.

FULL LINE IS $y = 0{\cdot}52\times10^4 + 3{\cdot}6\left[1 - e^{-4{\cdot}3\times10^3 t}\right]\times10^4$

$T_{1/2} = 159{\cdot}5 \pm 4\ \mu S.$

$$W(t) \propto \left(1-e^{-2\lambda T}\right) \qquad (1)$$

Assuming some instantaneous coincidence radiations to be present, which will be counted for all resolving times, we may write

$$W(t) = A - Be^{-2\lambda T} \qquad (2)$$

Thus when the readings obtained in a number of experimental runs had been added up, for each value of resolving time, a relation of the form (2) was fitted to them by the least squares method (8). Fig. 7 shows the resulting curve, which had the equation

$$y = 0.52 \times 10^4 + 3.6 \times 10^4(1 - e^{-4.36 \times 10^3 t}).$$

This was drawn through the points indicated by crosses. The experimental points are shown as dots, together with the errors. The half-life obtained is 159.5 $\pm$ 4 μS. This represents the results of seven experiments, several runs being rejected because the test, described above (Table 3), did not lead to a constant number of corrected counts. Some of these were due to faulty counters, and the others due to a fault in the coincidence unit power supply causing anode voltage variations. The instantaneous coincidences observed are discussed below.

Differential Method.

With this method the number of coincidences per second is given by the relation

$$D = 2N\epsilon_{1\beta}\epsilon_{2\alpha}e^{-\lambda t_d}\sinh\lambda T \qquad (3)$$

where N is the number of disintegrations per second of the source.

$\epsilon_{2\alpha}$ is the efficiency of the α counter to α particles, $\epsilon_{1\beta}$ that of the β counter to β particles, and td the delay time which is introduced. Also the number of accidental coincidences is given by the relation

$$N_c = 2N_1N_2T \qquad (4).$$

The counters and counting procedure were the same as in the Integral Method discussed above, but two corrections had to be applied. The first of these was for instantaneous coincidences (9). If the source emits two radiations whose separation in time is very small, these will be counted in the single rates, but not in the delayed coincidence rate.

Let the number of such coincidences which were counted be C per second, and assume that they are due to the source, and therefore decay with it. The two equations (2), and (3), must therefore be replaced by

$$N_c = 2(N_1 - C)(N_2 - C)T \qquad (5)$$

and

$$D = 2(N\epsilon_{1\beta} - C)\epsilon_{2\alpha}e^{-\lambda t_d}\sinh\lambda T \qquad (6)$$

where $N_1 = N\epsilon_{1\beta}$.

and $N_2 = N(\epsilon_{2\alpha} + \epsilon_{2\beta})$.

N_1 is the counting rate in the β counter. N_2 is the counting rate in the α counter, and $\epsilon_{2\beta}$ is the efficiency of the α counter to β particles. (C is the number of instantaneous coincidences between the

Figure 8. Results of experiments by the 'differential' method.

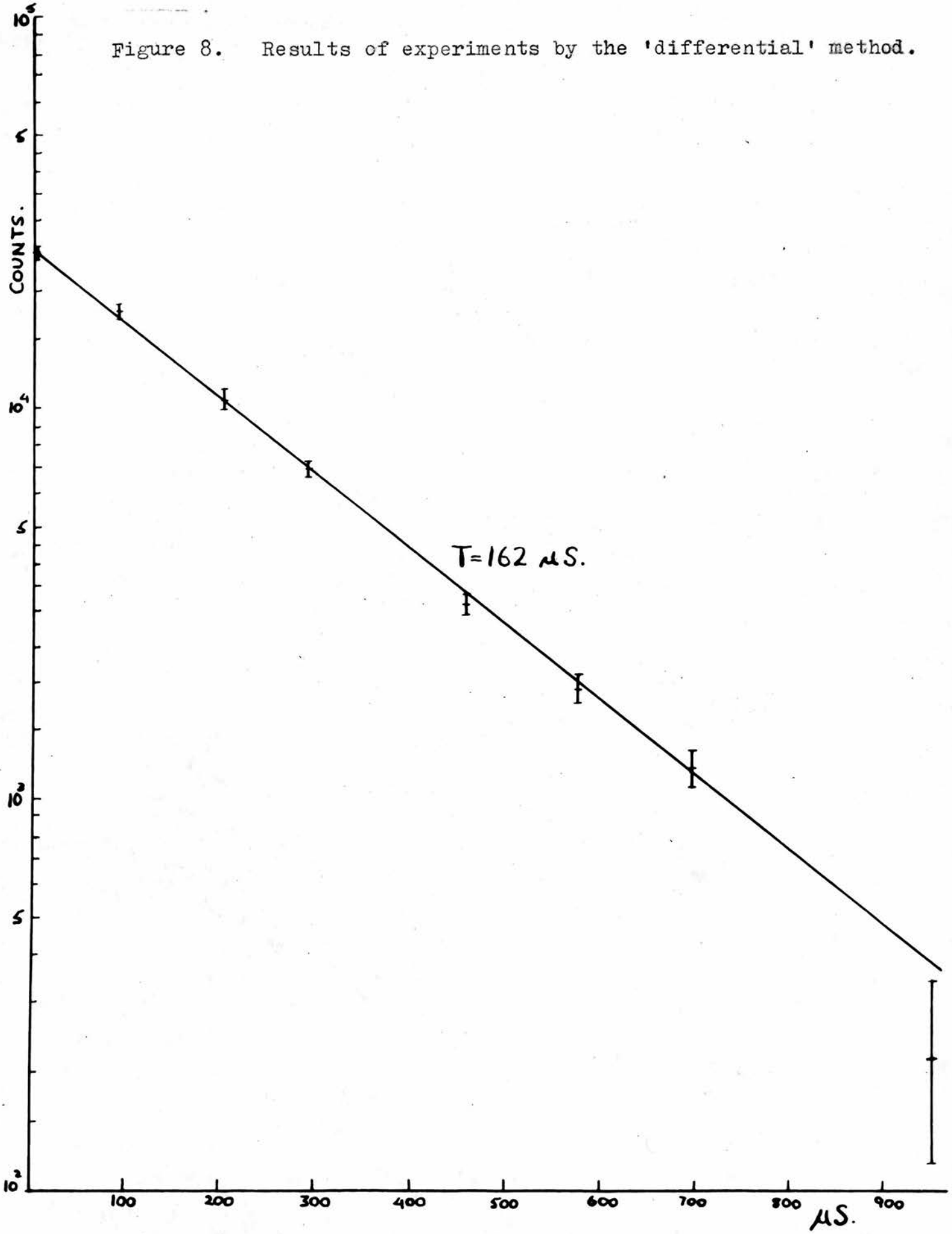

two detectors). This quantity may be calculated for each experimental run assuming that when the longest time delay is in use, all the counted coincidences are accidental.

Thus from (2) we have,

$$c^2 - c(N_1 + N_2) + (N_1N_2 - \frac{Nc}{2T}) = 0$$

and so $$c = \frac{N_1 + N_2}{2} - \sqrt{\frac{N_1 + N_2}{2} + \frac{N_c}{2T}} .$$

The longest time delay used was 950 μ S justifying the assumption made above, especially since the correction is small. In a typical case when the α counting rate was approximately 2×10^4 per minute C was 800 counts per minute. The number of immediate coincidences observed here was similar to that found in the experiment by the integral method. There was a second correction, due to the decrease of resolving time with delay time already referred to above. This consisted in normalizing the readings to a standard resolving time of 30 μ S using equation (6). Near our value of λT, $\mathrm{Sinh}\,\lambda T$ varies only slowly with its argument.

Fig. 8 shows a plot of the results of eighteen experiments with errors indicated, together with the straight line deduced by least squares. This leads to a value for the half-life of 162 ± 3 μ S.

Discussion.

The results obtained here are in better agreement

with that of Von Dardel than the earlier values referred to in the introduction. Also the present experiments indicate a possible reason for the discrepancy.

Previous authors do not mention the deliberate use of paralysis times such as are introduced by the probe units employed here. Ward has discussed the question of dead time, but the use of one counter for both α and β particles complicated the situation in his experiment. Assuming for the time being that the value obtained by Von Dardel is correct within his quoted error, the values of λ deduced by previous workers are too high. Thus for the delayed coincidence experiments they obtained too few counts at the longer delays, and for the integral method their curves were above the correct curve for the smaller values of resolving time. In the first case, this is the effect which would occur due to irregular operation of trigger circuits at longer delays as discussed above. If too few counts were registered at large resolving times during experiments by the integral method, those parts of the curve corresponding to short resolving times would be relatively too high. The equation of the curve of counting rate against resolving time would not then be

$$W(t) = A - Be^{-2\lambda T}$$

However, in an experiment of moderate accuracy, the best fit with such an equation would give too high a value

of λ . Thus, loss of counts due to irregular operation at large resolving times would again lead to a high value of λ .

Von Dardel (10) is of the opinion that the disagreement is due either to the cause outlined above, or to the source decay correction, which is eliminated in his experimental method.

Table 4 below shows the results which have been obtained by the various authors.

Table 4.

Author	Date	Method	Result	Ref.
Dunworth	1939	Integral	150 ± 20 μs	1
Ward	1942	Integral	148 ± 6 "	2
Rotblat	1941	Integral	145 ± 5 "	3
Rotblat	1941	Integral	150 ± 20 "	3
Jacobsen	1942	Differential	155 ± 5 "	4
Von Dardel	1950	Differential	163.7 ± 0.2 "	5, 6.
Ogilvie	1951	Integral	159.5 ± 4 "	
Ogilvie	1951	Differential	162 ± 3 "	

Chapter II.

SCINTILLATION COUNTERS AND COINCIDENCE CIRCUITS.

Introduction.

The performance of a scintillation counter is determined both by the properties of the photomultiplier and by those of the scintillating material or phosphor.

A photomultiplier consists of an evacuated envelope inside which are placed electrodes (dynodes), maintained at successively higher potentials with respect to the photocathode. The last of these is the anode or collector plate. For every electron reaching the first dynode from the cathode, σ electrons are emitted towards the second dynode, where σ is the secondary emission ratio of the dynode material. If several electrons are emitted by the cathode within a short time, each is represented by a small pulse of charge which arrives at the anode after an interval called the transit time of the tube. This is what occurs when a particle to be counted enters the phosphor and causes it to emit several photons in rapid succession. If the phosphor emitted all its light in an infinitesimally short time, these elementary pulses could be integrated by a very short time constant in the anode circuit, and a single pulse with an infinitely rapid rise and a decay governed by this time constant would

result. However the emission of light from a phosphor takes place according to an exponential law

$$I = I_0 e^{-t/T_1}$$

T_1, the decay time of the phosphor, is defined analogously to the mean life of a radioactive substance. Therefore the spacing of the elementary pulses is decided by the phosphor decay time and not by the time of traverse of the particle through the phosphor, or that of the pulse through the multiplier.

Thus a time constant of at least the same order as T_1 is required to integrate the elementary pulses to give an output pulse whose height varies with the number of photons originally emitted. It is to be noted that the rise time of this integrated pulse will be equal to the decay time of the phosphor and its fall-off will be controlled by the time constant of the anode circuit.

The elementary pulses, each of which can be thought of as being due to one photon, consist of a small number of electrons, especially during the early stages of the multiplication process. The secondary emission ratio σ is a mean-value, and any given electron may give rise to more or fewer secondaries. Thus the output pulses due to equal numbers of photons vary in size about a mean value to form a distribution. An additional cause of this phenomenon is that in the passage of the burst of electrons through the tube

some will be lost.

Two types of construction have been employed for photomultipliers. The Venetian blind type uses grid electrodes erected parallel to each other and perpendicular to the axis of the tube, so that the electrons travel in approximately straight lines from the photocathode through this structure to the anode. For the second system, as used in the American 931, electrostatic fields focus the beams of electrons along a complicated path from dynode to dynode. Because of this focussing the properties of the second type are in some ways superior, fewer electrons being lost from each pulse. The rise of the elementary pulses is not instantaneous, firstly because the transit time is variable, the actual paths followed by individual electrons being of variable lengths; and secondly because the electrons are emitted with different initial velocities. In this respect also the focussing type multiplier tube is superior to the other.

Even at room temperature the photocathode and dynodes of a multiplier tube emit electrons. Because of the high gain which is available, these are the progenitors of pulses which occur at the output in the same way as signal pulses and may be confused with them. This is especially likely if low energy radiation is to be counted although the scintillation counter will respond to β particles of a few kilovolts

energy. One method of overcoming this defect is to lower the temperature of the cathode. Close to room temperature the dark pulse rate may be halved for every 10 degree centigrade decrease in temperature. (11) However the time constant referred to above, which is used to integrate the elementary signal pulses when they arrive at the anode, acts so as to increase the signal-to-noise ratio (12). This is because it modifies the very rapid rise of the dark "noise" pulses with the result that their amplitudes are decreased with respect to those of the slower signal pulses. In a discussion of the value to be employed for the output time constant of a scintillation counter Coltman (12) shows that a good compromise value is equal to the decay time of the phosphor. To illustrate the orders of magnitude which occur, Anthracene, a phosphor which is often used, has a decay time of approximately 1.5×10^{-8} sec. (13), (14) while both theoretical calculations (12) and experiments (13) (15) give less than 5×10^{-9} sec. as the rise time of a noise pulse in a phototube of the focussed type. In general, cooling of the tube is only necessary when low energy radiation is to be counted.

When fast pulses, that is to say pulses with a rapid rise, are to be used, it is a great advantage if they leave the multiplier at a high level. Several

volts are often required to operate coincidence mixer circuits, and the only available amplifiers which attain the necessary band width (> 100 Mcs) are of the so-called 'distributed' type (16), (17). These are difficult to construct and uneconomical, and it is desirable to avoid their use. The gain of available multiplier tubes is 10^6 to 10^7 times, and multipliers of much higher gain have been built (18), (11). A 14 stage multiplier photocell with a gain of 10^9 has lately become commercially available.

The output stage of a Scintillation Counter.

The stray capacity at the anode of a photomultiplier tube is fixed, so that as the load resistance is raised in value, the magnitude of the output pulse and the output circuit time constant are also increased. When the load resistor becomes comparable with the internal impedance of the tube, the size of the output pulses are almost independent of its value, and this condition begins to occur with a load resistance of approximately 10^5 ohms. Thus the output impedance of the device is high, and as the input impedance of the circuits which follow may be low, a cathode follower is placed between them. An important method of producing short pulses of regular shape, illustrated by the circuit diagram in Fig.9 , is easily adapted to such an arrangement. The cathode load resistor of

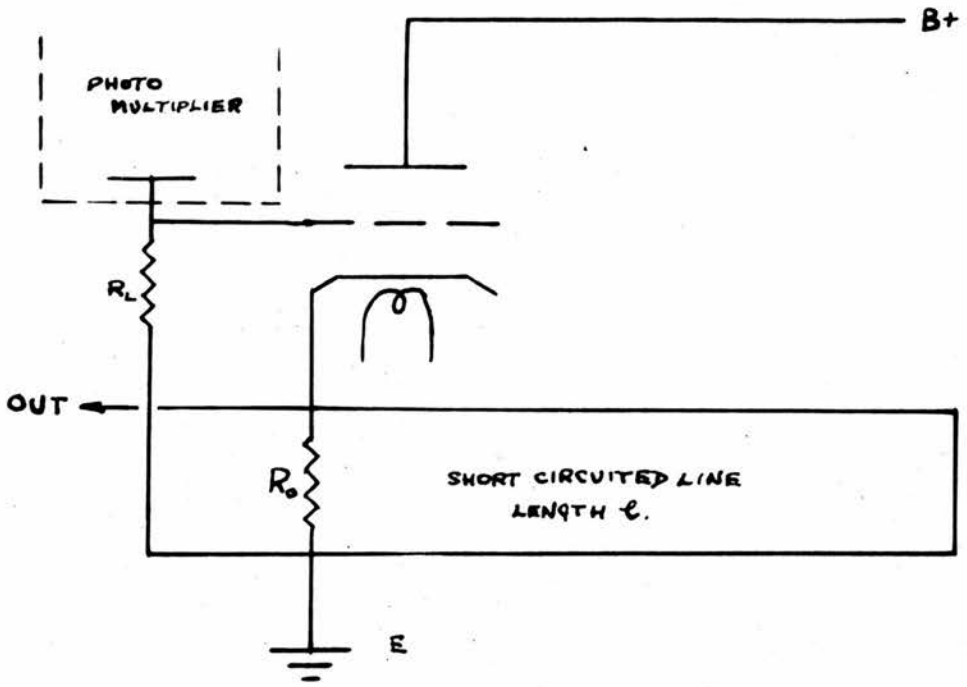

Figure 9. Circuit diagram of the cathode follower used in the short-circuited line method for reducing the duration of pulses from a photomultiplier.

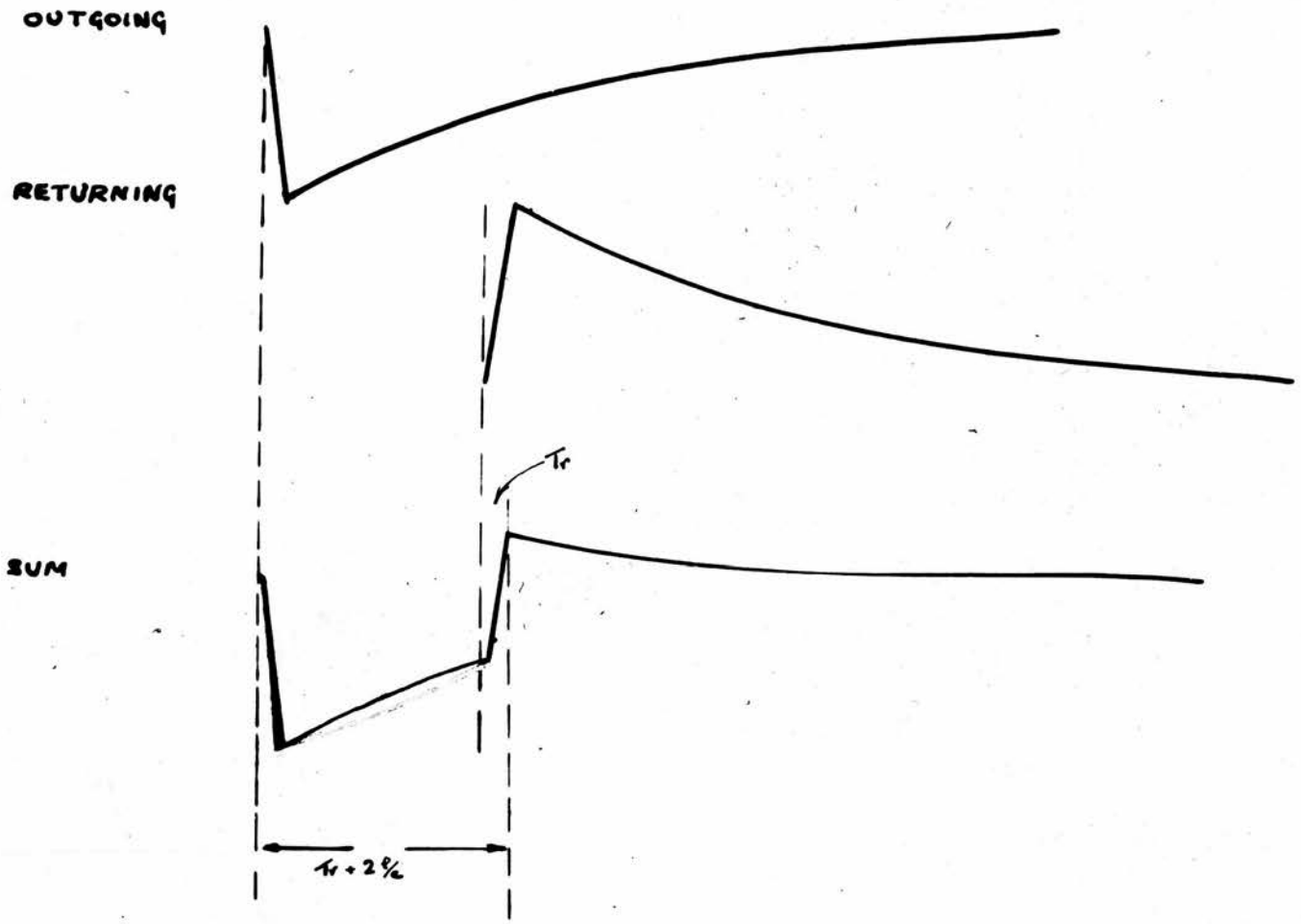

Figure 10. Diagram showing the method of operation of the short-circuited line method of pulse shortening.

the cathode follower is made equal to the characteristic impedance R_o of a transmission line. A length of the line, short-circuited at the far end, is now connected across this resistor. When a voltage pulse occurs at the grid of the valve, a current pulse ΔI flows through the load, and a voltage pulse $R_o \Delta I$ travels from the cathode end of the line with velocity $v < c$. Since the other end is short-circuited the reflected pulse is reversed in sign and arrives back at the cathode after a time $2\ell/v$. Fig. 10 shows how this shapes the voltage pulse at the cathode, and can be used to give a more or less rectangular shape with a duration of $\geqslant 2T_r$, T_r being the time of rise of the current pulse ΔI.

High Speed Coincidence Circuits.

The coincidence circuit introduced by Rossi can be made to operate satisfactorily down to resolving times of the order of 10^{-8} sec. The resolving time of such a circuit is approximately equal to the sum of the durations of the two sets of pulses which are fed to it. A block diagram of a typical coincidence system is given in Fig. 11 . As the duration of the input pulses is reduced, the resolving time is not correspondingly reduced, and the ability of the circuit to reject large single pulses is impaired. Due to the great spread in size of pulses obtained from a photomulti-

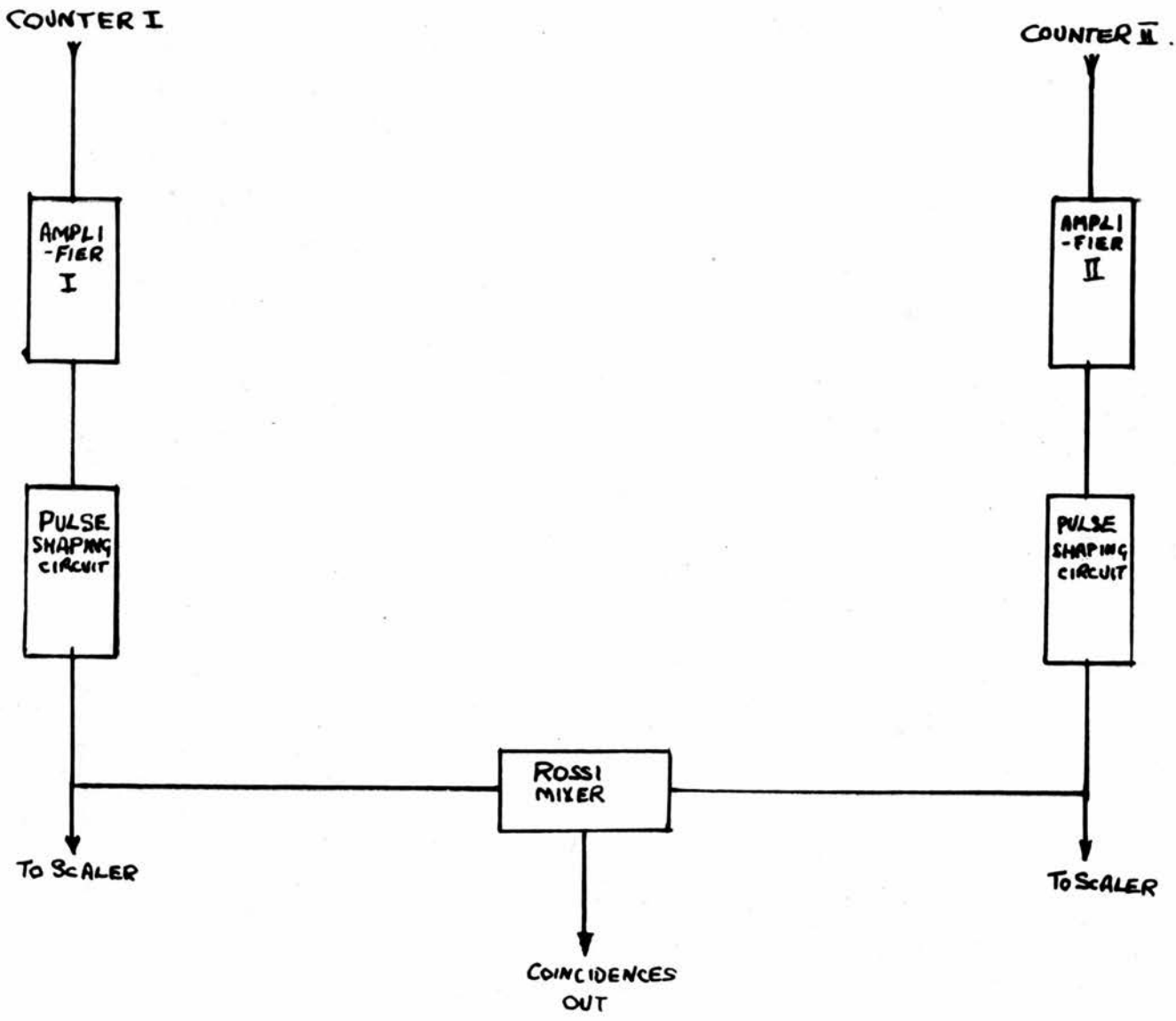

Figure 11. Block diagram of a Rossi coincidence system.

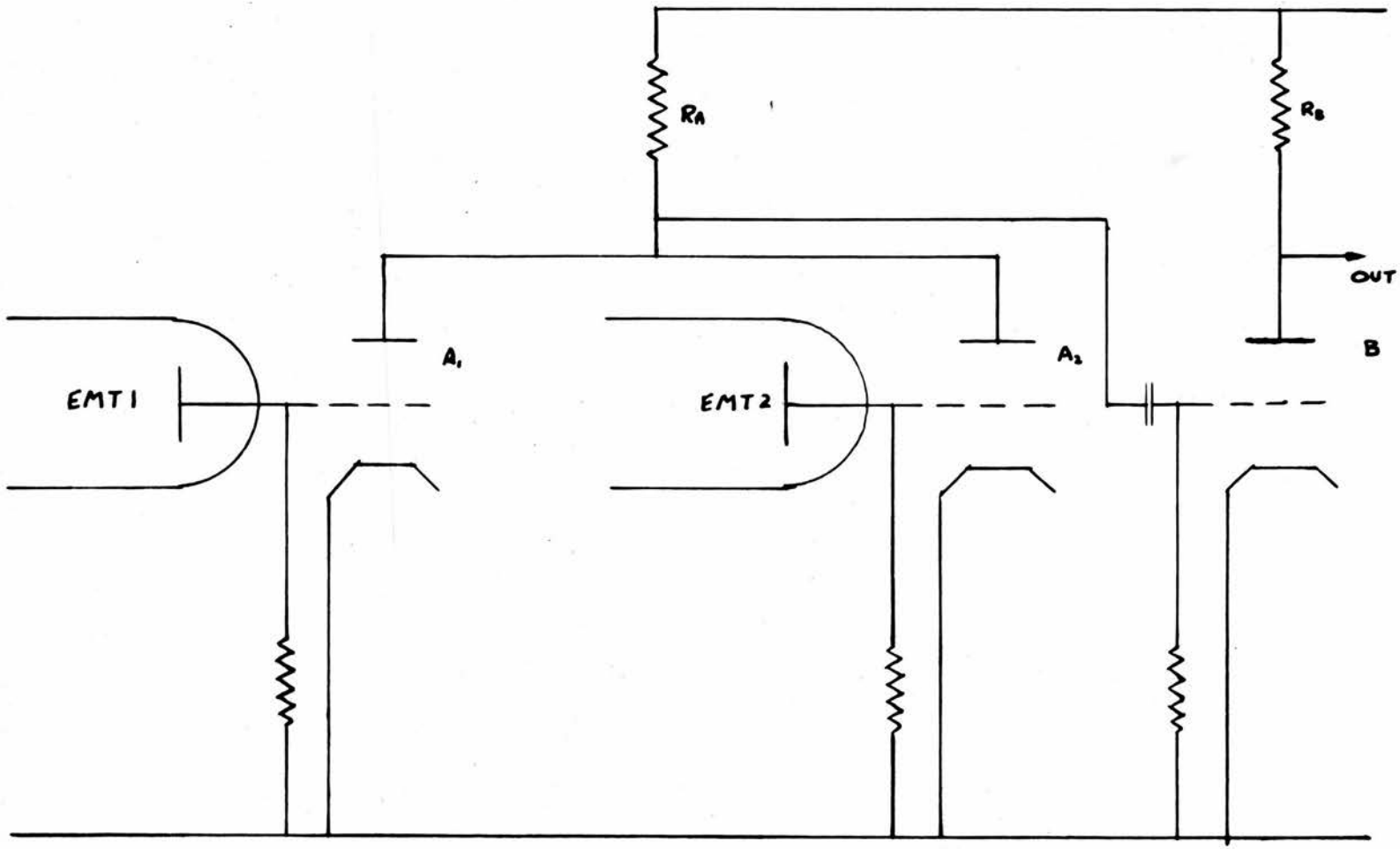

Figure 12. The coincidence system of Bay and Papp.

plier, this is particularly important for us. Two methods have been proposed for overcoming this defect of the Rossi circuit, which is caused by the grid-anode capacity of the valves (20).

Bay and Papp (19) have used the circuit given in Fig. 12 . The multiplier output pulses are equalized in size by valves A_1 and A_2, which are short grid-base pentodes of high mutual conductance, and the common anode load is very low (50 Ω). The electron multipliers used, which counted the particles directly without preliminary conversion of energy into light, have very high gain, $\sim 10^9$. Direct multipliers have two advantages over photomultiplier counters. Firstly, the time of rise of their pulses is determined by the properties of the multiplier and not by a (slower) crystal, and secondly, the signal-to-noise ratio can be higher due to the absence of a photocathode. Bearing these in mind, it seems unlikely that the resolving time of 5×10^{-9} sec., which the authors quote for this circuit, could be obtained by photomultipliers, with an adequate rejection of large noise and signal pulses from the single channels.

In the circuit due to Garwin (20), Fig. 13, the effect of capacitance feed-through from grid to anode is removed by the action of diode a. Garwin has obtained a resolving time of 0.005 μ S and reports completely reliable operation at 0.05 μ S. A somewhat

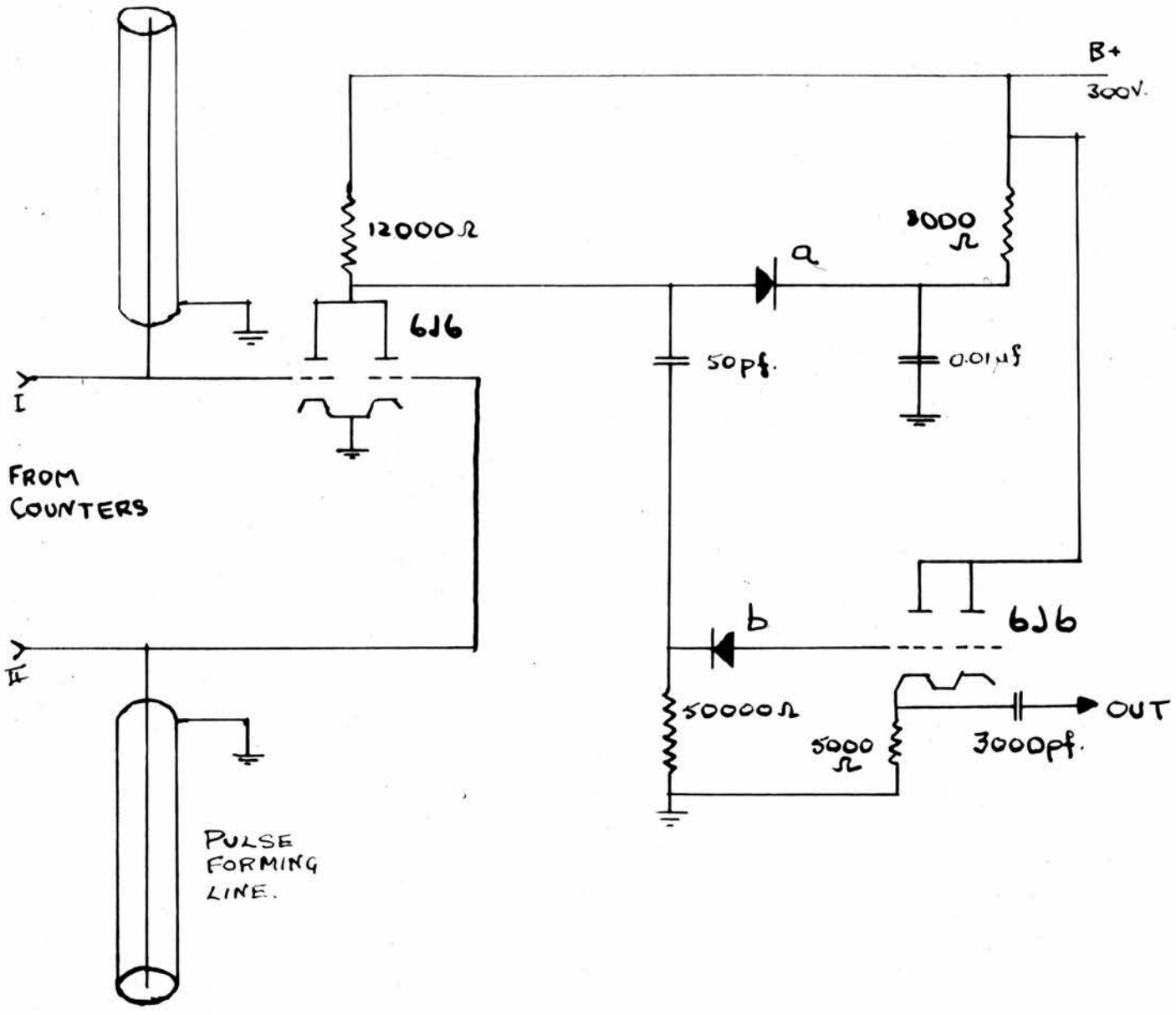

Figure 13. The coincidence circuit of Garwin.
Diode a reduces the effect of the anode-cathode capacitance of the valve.
Diode b is a pulse-lengthener.

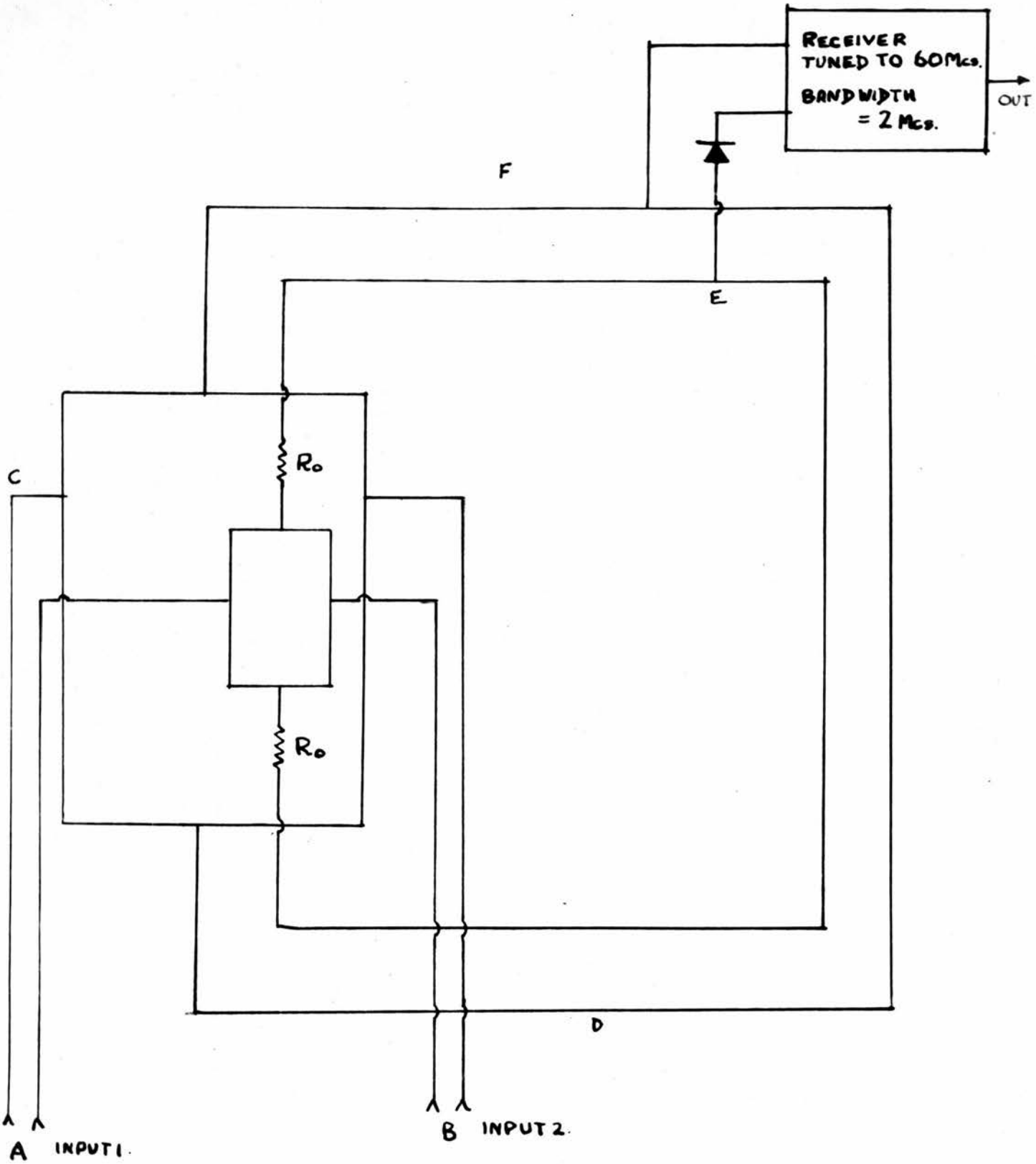

Figure 14. The coincidence system of Dicke.

large input pulse of 3v is required however.

Before considering the circuits using germanium diodes there are two other high resolution coincidence devices which deserve attention. Wiegand (21) has described a coincidence circuit using the travelling wave principle which is utilised in the design of amplifiers of large bandwidth. He has obtained a resolving time of 10^{-8} sec. This idea should be suitable for development, but at present the circuit requires input pulses of 10v amplitude. The second circuit is one which is of interest because it operates on a different principle from all the others. It has been described by Dicke (22), (23) and a schematic diagram is given in Fig. 14 . The input pulses are fed into coaxial cables at A and B, and travel along them to the junction C. The cables have a difference in length equal to one half wave length at 60 Mcs. Signals from C travel along cable CFE and CDE, also differing in length by one half wave length as before, to the crystal located at E. The output from the crystal is connected to the input of a radio receiver having a bandwidth of 2 Mcs. When a single pulse enters the circuit at A two pulses arrive at the crystal as indicated by the solid curve in Fig. 15 . Only those Fourier components of the pulse near 60 Mcs influence the receiver, and as the pulses are very short, their Fourier components in this region are large. Due to

Figure 15. Explanatory diagram of the operation of the Dicke circuit.

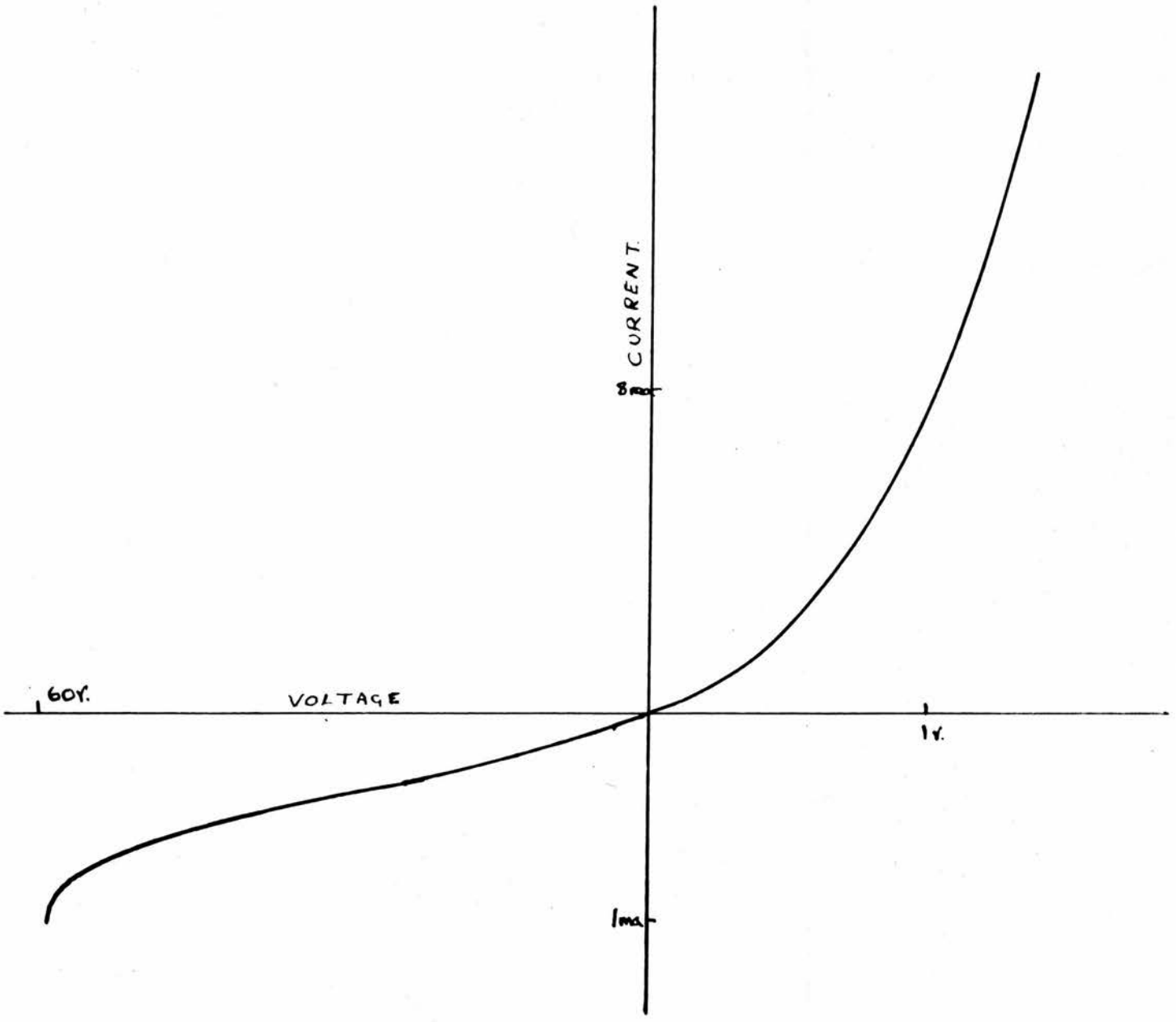

Figure 16. A typical germanium diode current-voltage characteristic curve.

the half wave path difference, however, these are out of phase, and the output from the receiver is zero. Simultaneous pulses at each input give rise to three pulses at the crystal, the solid and dotted curves in Fig. 15. The output then contains considerable 60 Mcs components derived from the two almost superimposed pulses. Dicke quotes a resolution time of a few times 10^{-9} sec., and a ratio $\frac{\text{Coincident pulse amplitude}}{\text{Output due to a single pulse}}$ of 400. It seems likely that this circuit could be developed to show a gain in sensitivity over the conventional circuits, as well as higher resolution.

Germanium diodes are very small in size so that their stray capacity is approximately 1 pf, have a forward resistance of 50 ohms, and a reverse resistance of about 10^5 ohms at 1v input potential. The type of characteristic curve which is obtained is given in Fig.16. Using these rectifiers it is possible to design a coincidence circuit to operate at the low level of the output of a conventional phototube. The resolution time is then equal to slightly more than twice the duration of an input pulse. Most of the circuits which have been described are in the form of a bridge balanced initially and unaffected by single pulses, but considerably unbalanced when both inputs are fed with a pulse simultaneously. A simple circuit of this type is described by Elmore (24) and is illustrated in Fig. 17. This has been tried out by the present

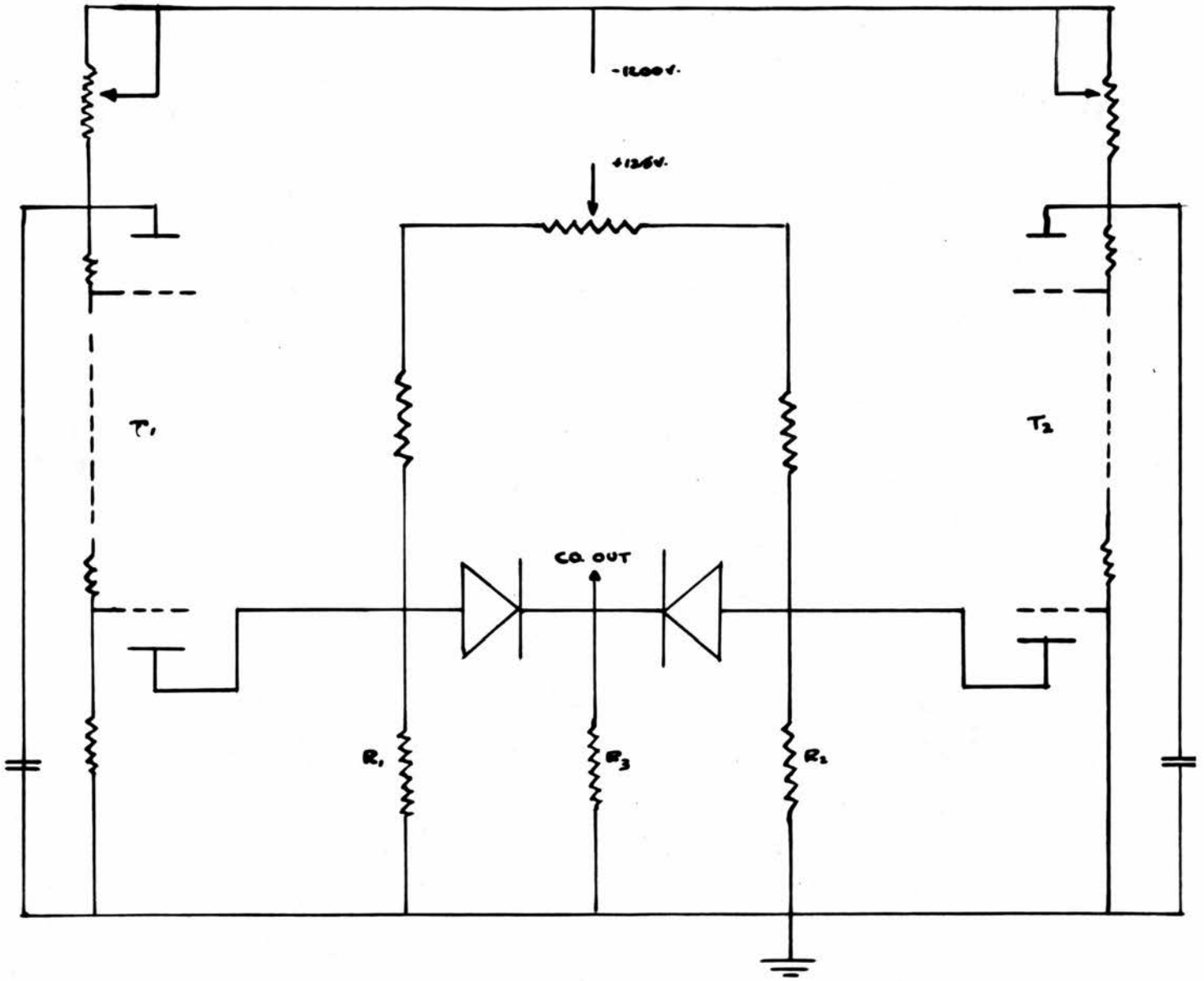

Figure 17. The coincidence circuit of Elmore. The author could detect no difference in the operation of the circuit when the 125 V. supply was disconnected.

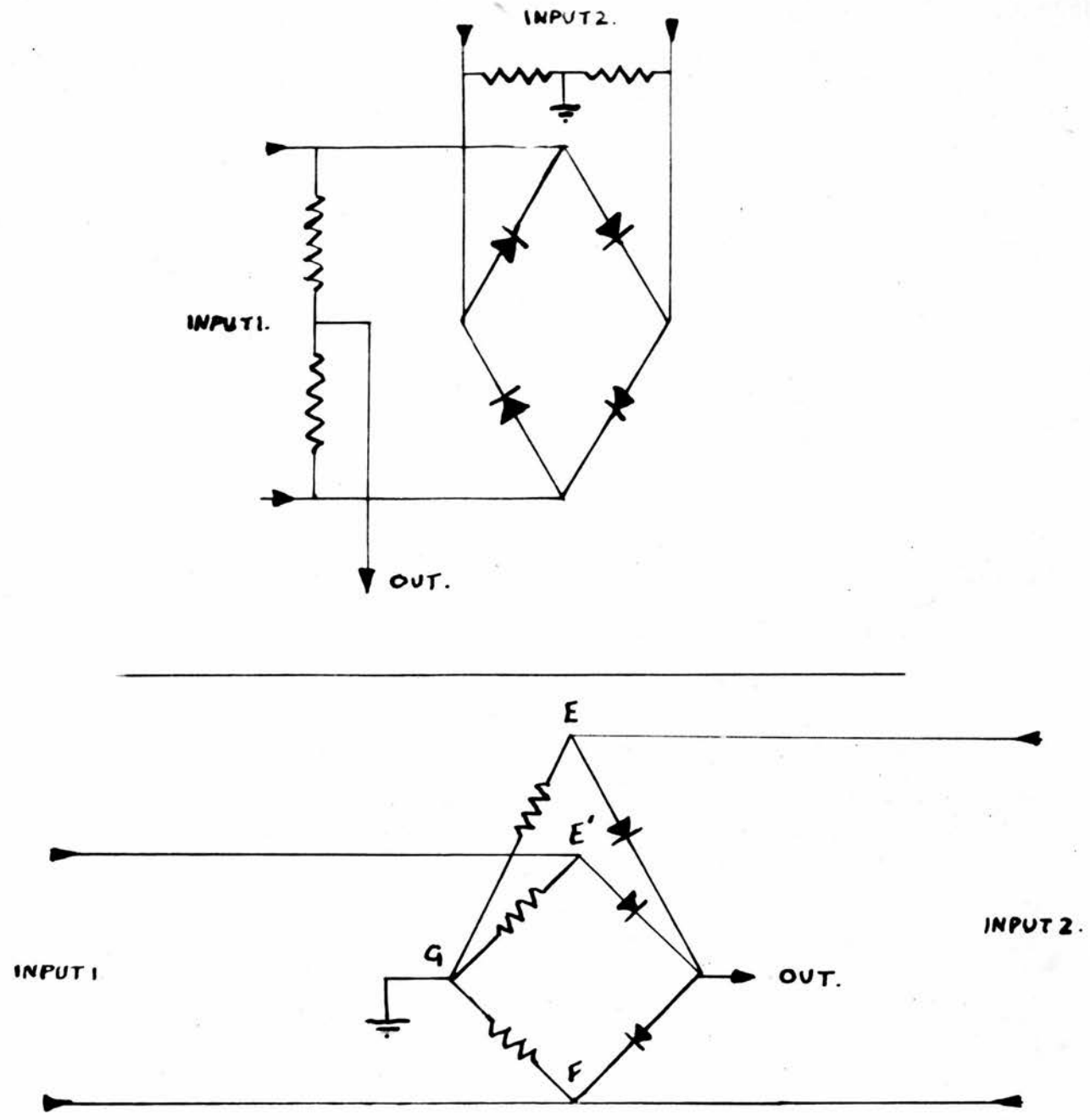

Figure 18. Coincidence circuits used by Baldinger, Huber and Meyer.

writer and the results of Elmore repeated, but was not used because of the better rejection ratio offered by the arrangement due to Bay described below. Other bridge connections have been described by Schrader (25) and Baldinger, Huber and Mayer (26), Fig. 18 . The chief disadvantage of this type of coincidence device is the necessity for balancing the bridge very accurately for the maximum rejection of single pulses, and this can only be carried out for a limited range of pulse sizes. Moreover it is only possible if the bridge is fed exclusively between the points E and F and E' and F. This means that earth currents to point G must be avoided by decoupling the dynodes of the multipliers.

Since besides short resolving time it is very desirable for a coincidence circuit to be reliable, easily set up, and stable, one of the most satisfactory of the circuits described above is that of Garwin. Because it is relatively insensitive it cannot be used with normal photomultipliers and no additional amplification. A circuit due to Bay (27), which can be so used, and has been employed by the writer for work to be described below, is given in Fig. 19 . Its operation is easily understood by referring to Fig. 20 . Capacitor C is charged by diode D if a difference of potential exists between A and B, after which it discharges through R and R_b in series. This forms an anticoincidence circuit, operated by pulses of very

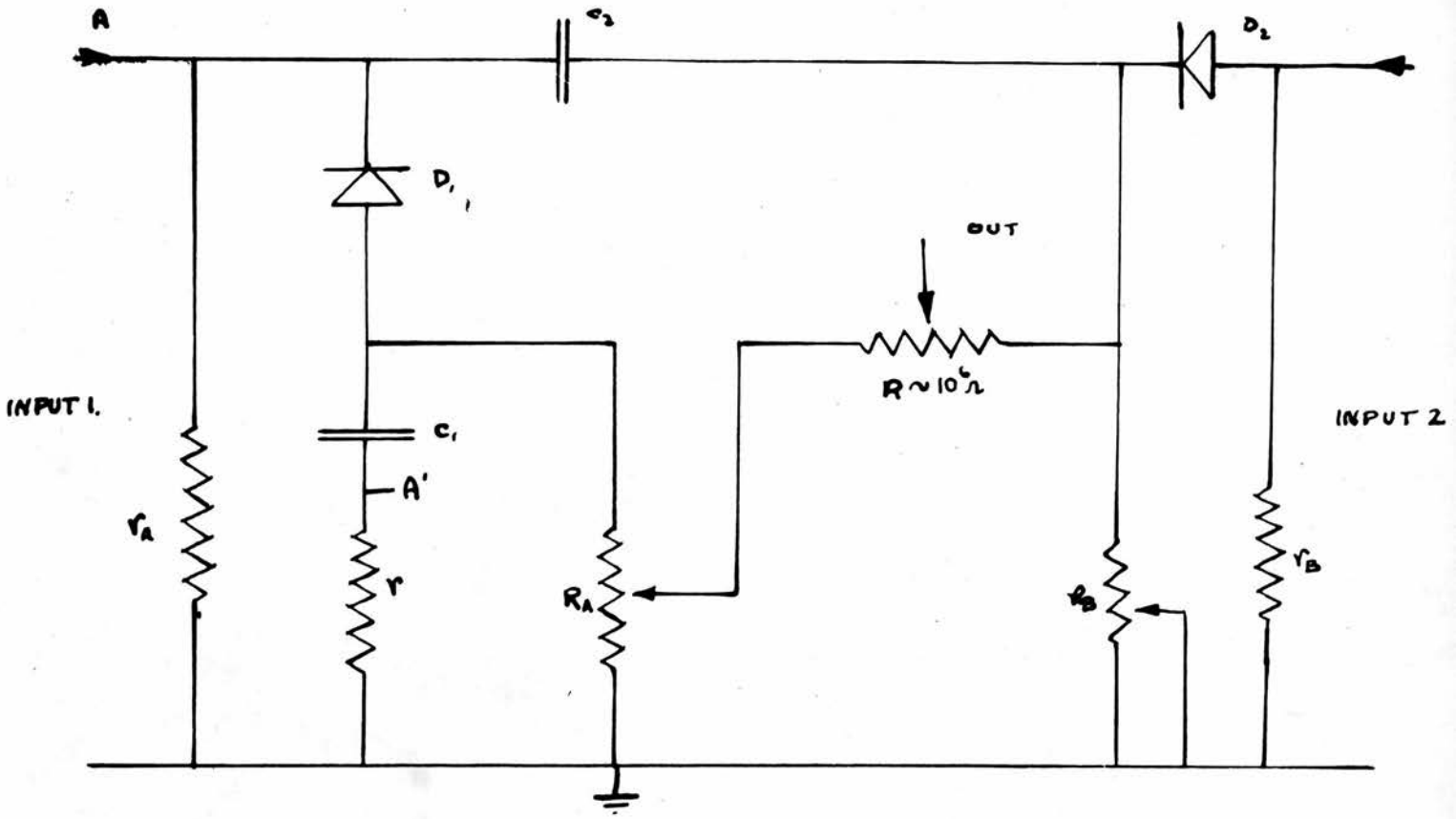

Figure 19. The coincidence circuit, due to Z. Bay, used by the author.

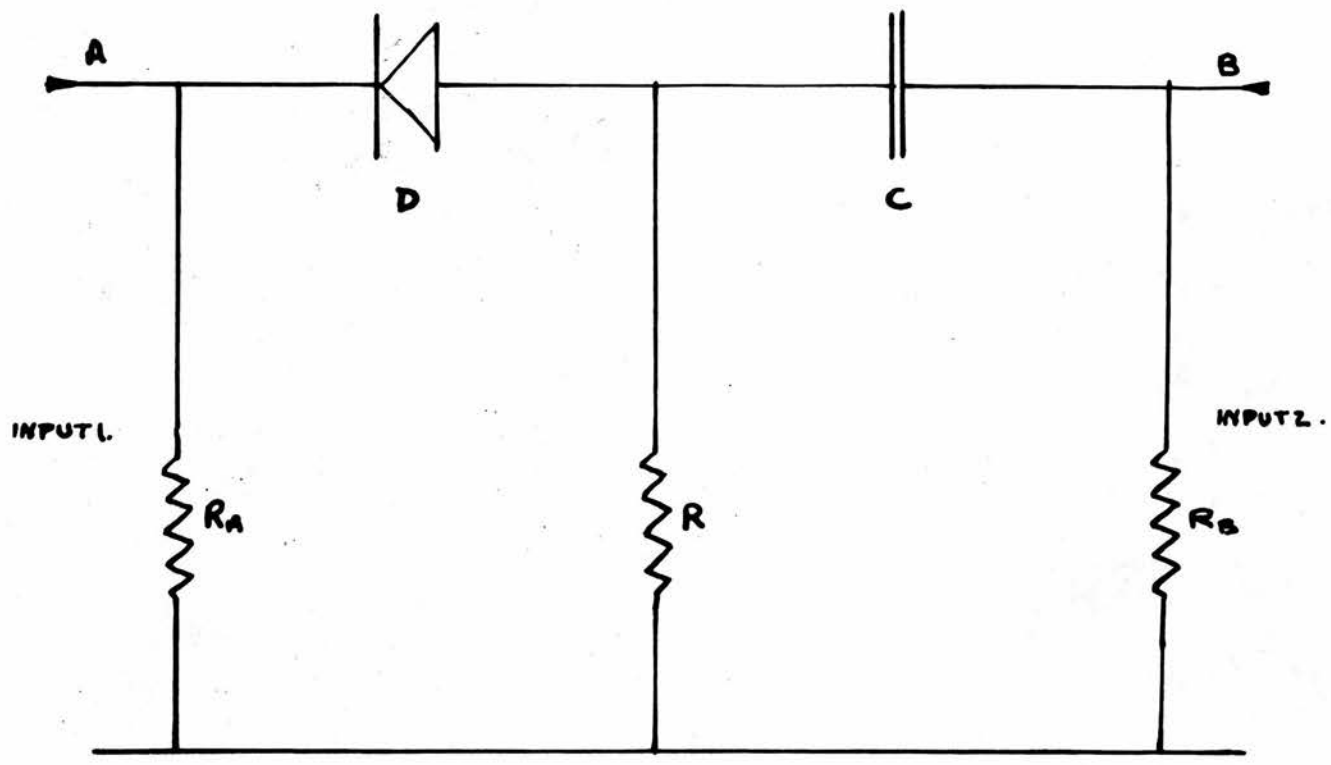

Figure 20. An anti-coincidence circuit,
two of which form the circuit of Fig. 19.

short duration, and giving output pulses lasting much longer, which may easily be separated from the former by integrating in the succeeding amplifier. Until the finite forward resistance of the diodes and their stray capacitance limits the operation of the circuit, it is improved by shortening the input pulses. In Fig. 19 D_1, C, r, R_A and r_A form one anti-coincidence circuit and the other components a similar one, the difference of their outputs being taken to the amplifier. If the pulses from channel A are applied at A", a negative pulse results from a coincidence, while if at A' the coincidence output is positive.* A discussion of the practical operation of the circuit is given below.

Thus, for coincidence counting the Rossi circuit may be used, by suitable simple modifications, down to a resolving time of approximately 5×10^{-8} sec., either with high gain photomultipliers connected directly, or with low gain photomultipliers and amplifiers. If this resolving time is too long, then a factor of 10 at least can be gained, using photomultipliers of the focussed type in conjunction with diode coincidence circuits such as that of Bay or de Benedetti and Richings (28). For very high speed counting and short resolving times, there is considerable advantage to be gained by using direct multipliers rather than photomultipliers, since they are not limited in speed of

* for negative pulses at inputs 1 and 2.

response by a crystal, and give a high signal-to-noise ratio. Valuable reviews of the whole subject of high speed counting are given by Wells (29) and in the accounts of the Scintillation Counter Symposium, Washington, January 1952, published in Nucleonics (30).

Chapter III.

MEASUREMENT OF THE HALF-LIFE OF ThC' USING SCINTILLATION COUNTERS.

Introduction.

In order to gain experience with scintillation counters it was decided to make a determination of the half-life of ThC' using them.

Several authors have described experiments by delayed coincidence and other methods to measure this half life. Dunworth (31) and Bradt and Scherrer (32) used a method involving the variation of the resolving time of their coincidence circuits. Dunworth's experiment, performed early in the development of electronic technique, was of low accuracy, but Bradt and Scherrer obtained the result $2.6 \pm 0.4 \times 10^{-7}$ sec. These authors analysed the effect of the variable delays which occur between the entry of a particle into a Geiger counter and the subsequent output pulse. They corrected for these random delays, assuming them to be distributed about their mean value according to a Gaussian error law.

Van Name (33) used the delayed coincidence method, correcting his results for random time delays in the emergence of the pulses from the counters. He assumed that these delays were distributed in a triangular manner, the most probable delay being zero, and the number of pulses delayed by δ t decreasing linearly

with increasing δt, until for some definite value it became zero. He obtained one parameter for this theory by means of a subsidiary experiment in which particles transversed both counters, but could not perform the parallel experiment with β particles. The second parameter had therefore to be inferred from other work. Van Name's final equation, used to deduce λ, was

$$C = \frac{8T e^{-\lambda t_d}}{\lambda^3 A^2 B^2} (\cosh \lambda A - 1)(\cosh \lambda B - 1) \quad (9)$$

where A is the half-width of the α counter delay distribution, the first parameter, and B is a similar constant for the β counter. λ is determined from the slope of the curve at large delays, and this is unaffected by the value of A and B if they remain constant as the delay varies.

The discrepancy between the value obtained by this author (2.2×10^{-7} sec.), and those of the other workers, may be due to one of the following causes.

(1) The triangular distribution of pulse delay times, although supported by experiments with the counters used, was not employed by Bradt and Scherrer. In this connection Fig. 21 shows data upon the time lags occurring in counters, obtained by Mandansky and Pidd (34), to which Van Name refers. The experimental points are given as circles and the solid line was obtained by the writer by fitting a straight line to

Figure 21. Showing how the results upon counter delays obtained by Mandansky and Pidd may be represented as well by a Gaussian curve as by a straight line.

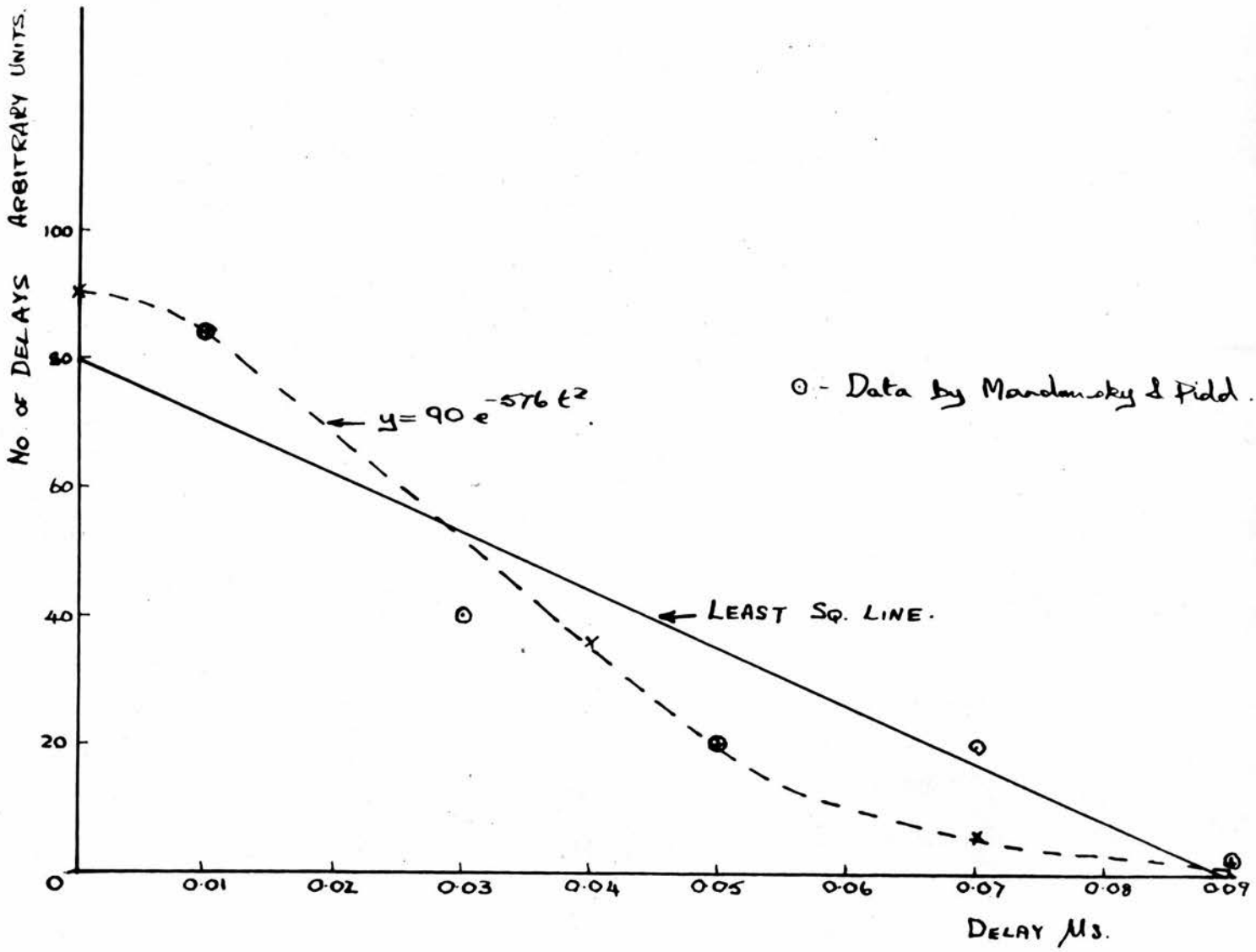

them by least squares. The dotted curve is an error function also fitted to the points, and it will be seen that it fits the somewhat meagre data at least as well as the linear law. More data on this subject is provided by Stevenson (35).

(2) The delay line used consisted of a helical coil, the output pulses being picked up by a second short coaxial coil which could be moved along the axis of the first. Variation in B might result due to attenuation at longer delays, and no description is given in (33) of the method used to calibrate this delay line.

(3) Van Name gives as his error $\pm$ 0.1 x 10^{-7} sec., but this was apparently estimated rather than calculated.

Hill (36)overcame the effect of other coincidences of very short lifetime which occur in the Thorium B decay scheme by working at a least delay long enough to avoid recording them. The least value of delay was determined by a subsidiary experiment and Hill showed that this precaution also avoids the necessity for correcting for variable counter delays. There was, of course, a considerable loss of counting rate at these delays.

Bunyan, Lundby and Walker (37) carried out a determination by delayed coincidences with carefully designed electronic equipment and obtained

$3.04 \pm 0.04 \times 10^{-7}$ sec.

In a delayed coincidence experiment, apart from variable counter delays, the accuracy of the result depends upon the calibration of the delay line and constancy of the resolving time at different delays and with time. Bearing this in mind the above value and that of Hill ($3.0 \pm 0.15 \times 10^{-7}$ sec.) can be taken as the most reliable available, and a description of a new determination agreeing with these, but using scintillation counters, is given below.

Description of Apparatus.

Scintillation counters and an A.E.R.E. type 1036 coincidence unit were used. A block diagram is shown in Fig. 22.

(a) The Scintillation Counters.

The two counters were identical, and a diagram of the construction is given in Fig. 23. The phototube A, together with its associated voltage dividing potentiometer, is enclosed in a brass case consisting of two tubes B and C, and three discs D, E, and F. F is the backplate, and carries the paxolin framework which supports the resistors. As it also carries the input plug and the gain control, while the phototube base forms part of the paxolin frame, all the electrical parts are securely attached to it. This form of construction ensures a very compact and well screened

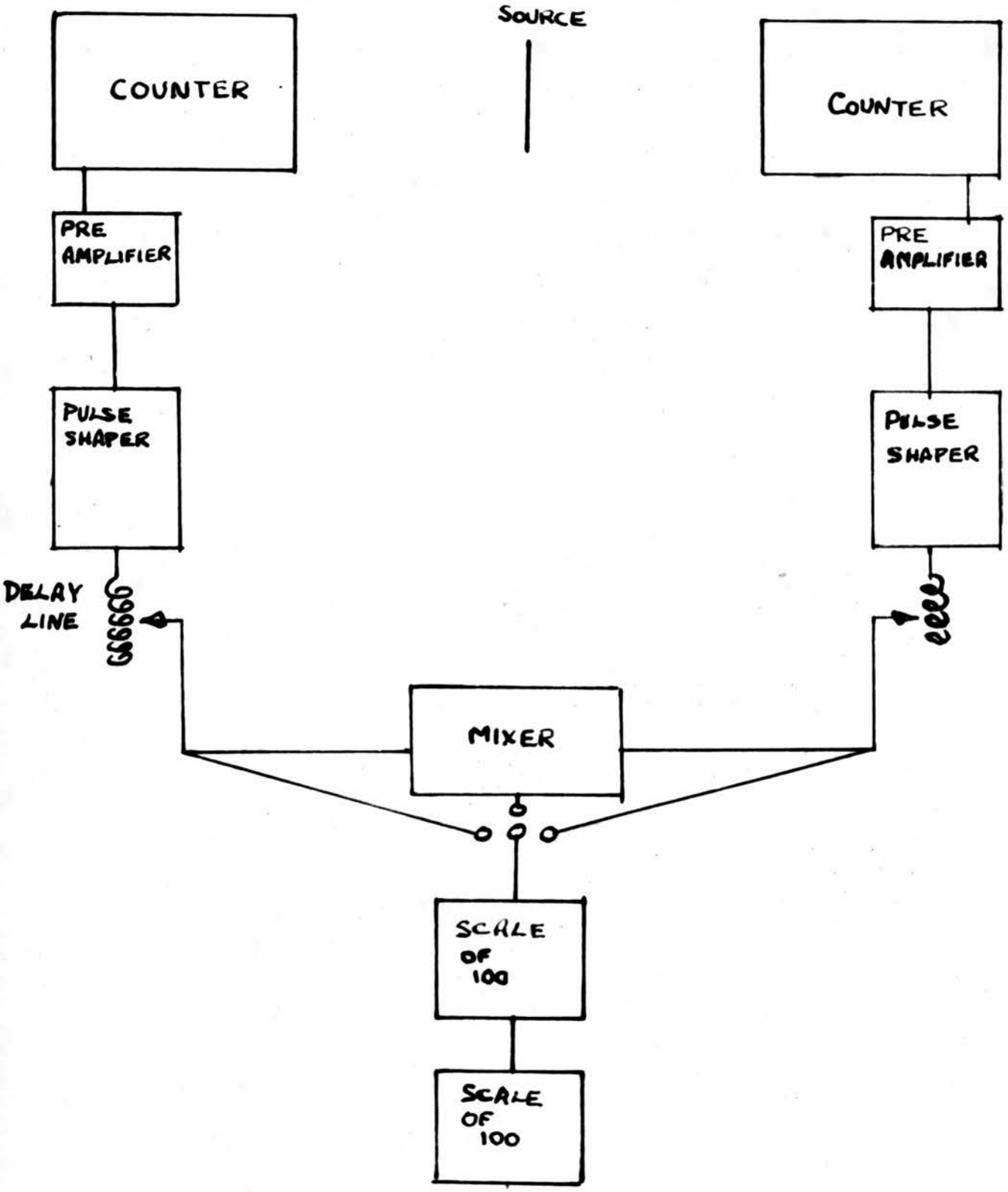

Figure 22. Block diagram of coincidence arrangement for the experiments upon the half-life of ThC'.

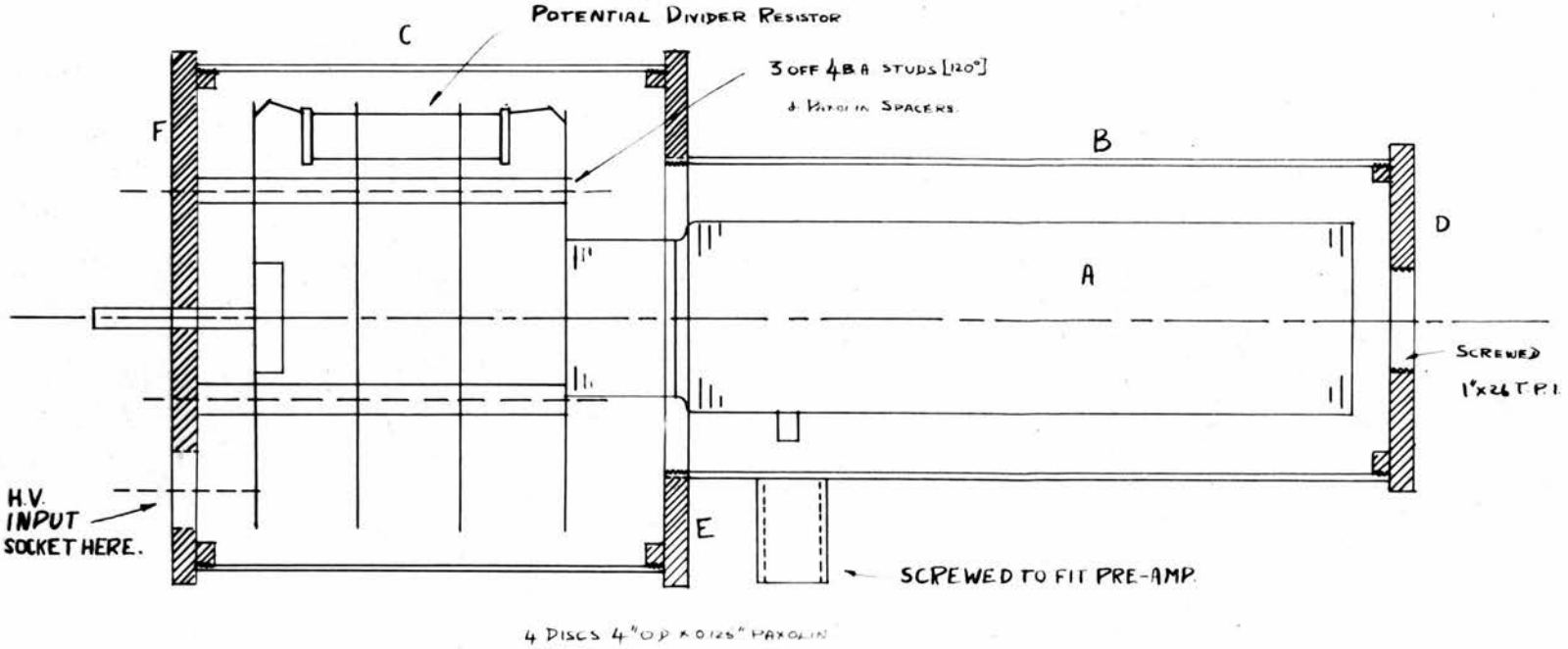

Figure 23. Diagram showing the construction of the scintillation counters.

system. Tube C screws on to a male thread F and disc E joins tubes C and B, the latter having an internal thread to accommodate D. A 1 in. diameter threaded hole in the centre of disc D allows various crystal systems to be placed opposite the cathode of the phototube, which on the tubes used here (EMI type 5060), is $\frac{3}{8}$ in. diameter and at the centre of the end face.

This mounting has been found to conform to the very high degree of light-tightness and electrical screening necessary for quantitative measurement. It allows the cathode of the tube to be either at earth or a high negative potential with equal facility.

The signal output from the tube appears at a connection in the side of the glass envelope. Thus a side tube is necessary to allow the extraction of the signal with a low capacitance to ground. This side tube is screwed into the wall of tube B in a radial direction and carries a thread at its outer end fitting that of the preamplifier input plug. The preamplifier is thus securely attached to the counter case.

(b) Electrical Circuits.

Fig. 24 shows the electrical supply circuit of the phototube. D.C. power at the appropriate voltage, 1 - 2 Kv, is supplied by a voltage stabilized power pack and is fed to the resistor chain R_1 - R_{12}, which

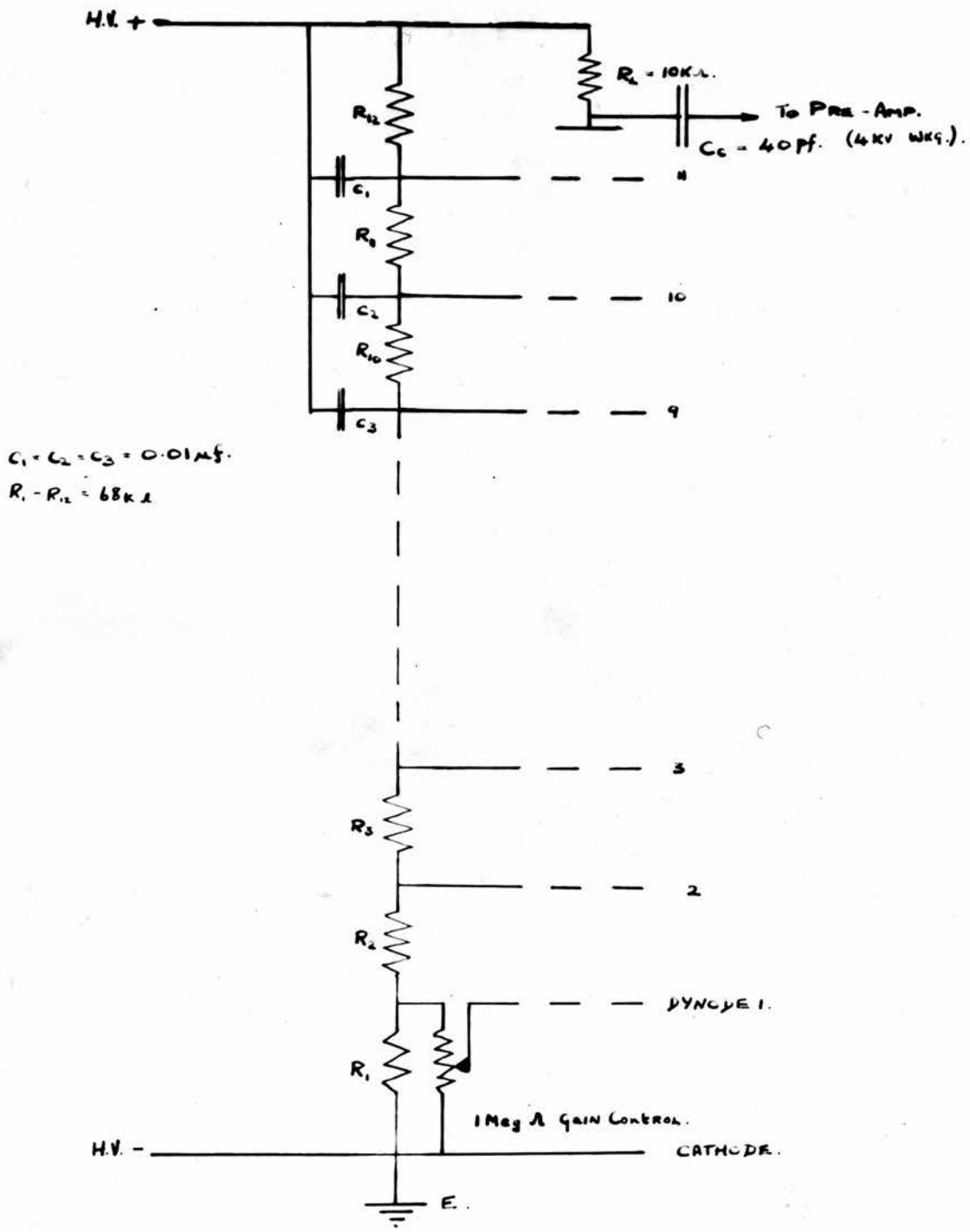

Figure 24. The high-voltage supply of the scintillation counter.

supplies the dynodes. This power pack must be of high quality and particular attention must be paid to low hum level, good stability of output, and lack of spurious disturbances. The power packs used were constructed by the author from a circuit supplied by Messrs. E.M.I. Research Laboratories Limited. The gain of the photomultiplier varies as a high power of the total applied voltage, and increase of the first dynode potential increases the gain, and the efficiency of collection of photo-electrons, but decreases the signal-to-noise ratio. The drop in gain caused by a reduction of first dynode potential can easily be offset by an increase of the overall potential, so the first dynode potential should be as low as is possible consistent with high collection efficiency. There is some evidence that a small difference of potential between the last dynode and the collector plate gives an increase in signal-to-noise ratio due to saturation on the faster noise pulses.(19). However, for these experiments not requiring great signal-to-noise ratio, the first dynode potential was variable, but all the others fixed.

The negative end of the resistor chain was connected to earth, so that a blocking capacitor, C_c, was required between the phototube collector and the preamplifier input.

Fig. 25 shows the circuit of the preamplifier

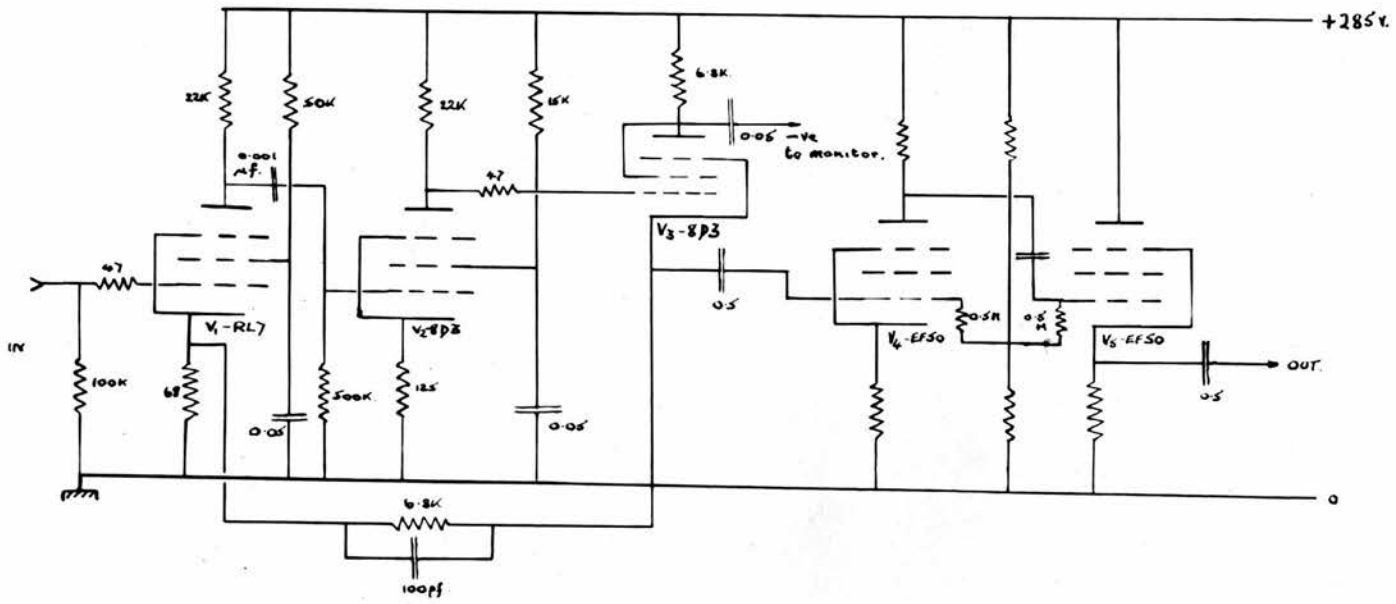

Figure 25. Circuit diagram of Pre-amplifier.

which was used to raise the 0.5 v output of the phototube to 50v. The first three valves form a feedback amplifier of gain 50, and were actually in the form of an A.E.R.E. type 1008 H.F. head amplifier. Valve V_4 is an inverting stage of gain 2 and V_5 an output cathode follower. These two valves were on a sub-chassis mounted on the preamplifier case.

Power supplies for these amplifiers were obtained from a stabilized power pack. A pulse generator for testing was built on the same chassis as this power pack.

The preamplifier had a passband, between points at which the voltage gain was 3 db below the maximum, of 2 Kcs to 700 Kcs; thus the rise time was less than 0.5 μ S. The load resistance of the multiplier tube was 10^4 ohms and 50v pulses of about 2.0 μ S duration were obtained at the coincidence unit.

It was found that the phototube load resistor was especially susceptible to leakage to the brass case. This was finally overcome by screening its lead and returning the screen to the H.T. terminal, to give a guard ring system.

(c) Arrangement of a Pair of Counters.

Fig.26 shows how the two counters were mounted upon a pair of parallel rods, as on an optical bench. One counter was fixed in position and the other free to slide on a carriage, so that its axis coincided

Figure 26. Diagram showing the arrangement of two scintillation counters for coincidence experiments.

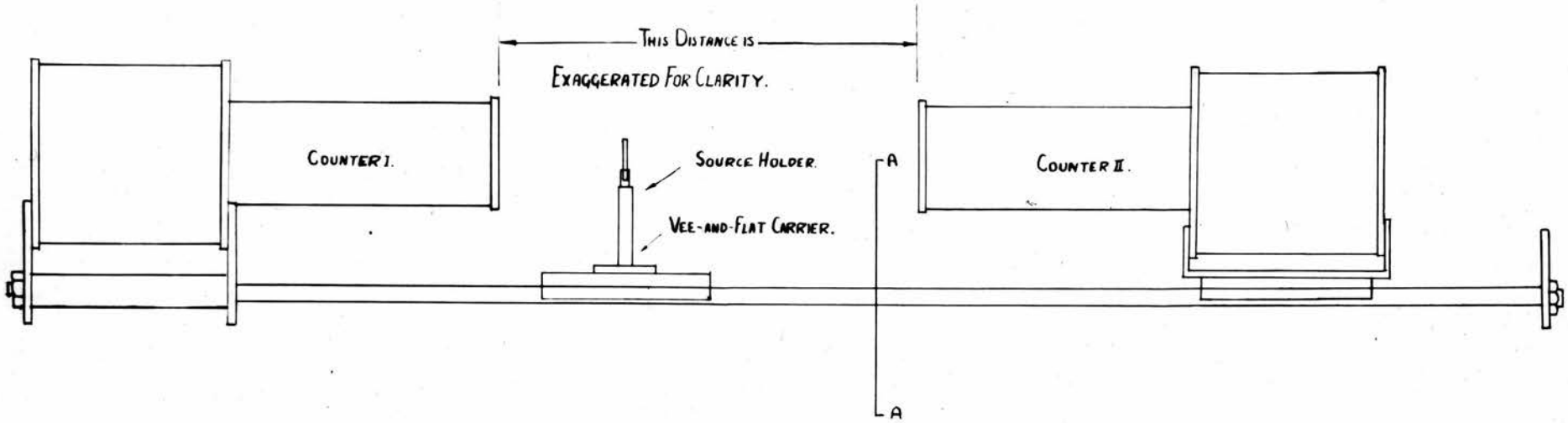

with that of the fixed counter. The source holder, in the form of a brass ring whose centre height could be adjusted, was mounted with its plane at right angles to the counter axes upon a sliding carriage. Both moving carriages could be clamped and the counters were normally separated by a distance of about 1 cm. This mounting made the replacement of sources easy.

The Source.

The source was deposited by recoil in a Thorium "pot" of normal design, upon one side of a piece of Aluminium foil 1 cm. x 5 cm. The activated region covered an area of 1 sq. cm. in the middle of the strip, the active side facing the α counter. About 15 minutes activation gave a source of strength a few microcuries. The foil was then fixed across the horizontal diameter of the source ring with a little cellulose glue at its ends.

Fig. 27 shows a diagram of the transformations occurring in Thorium B and C. The β counter counted only the β particles, but the α counter was affected by both α and β particles. Thus the α particle counting rate should be greater than that of the β counter, as was observed. The ratio α counting rate/β counting rate varied slightly during different experimental runs, but the mean value was 1.74. Calculation of the expected ratio is difficult due to the

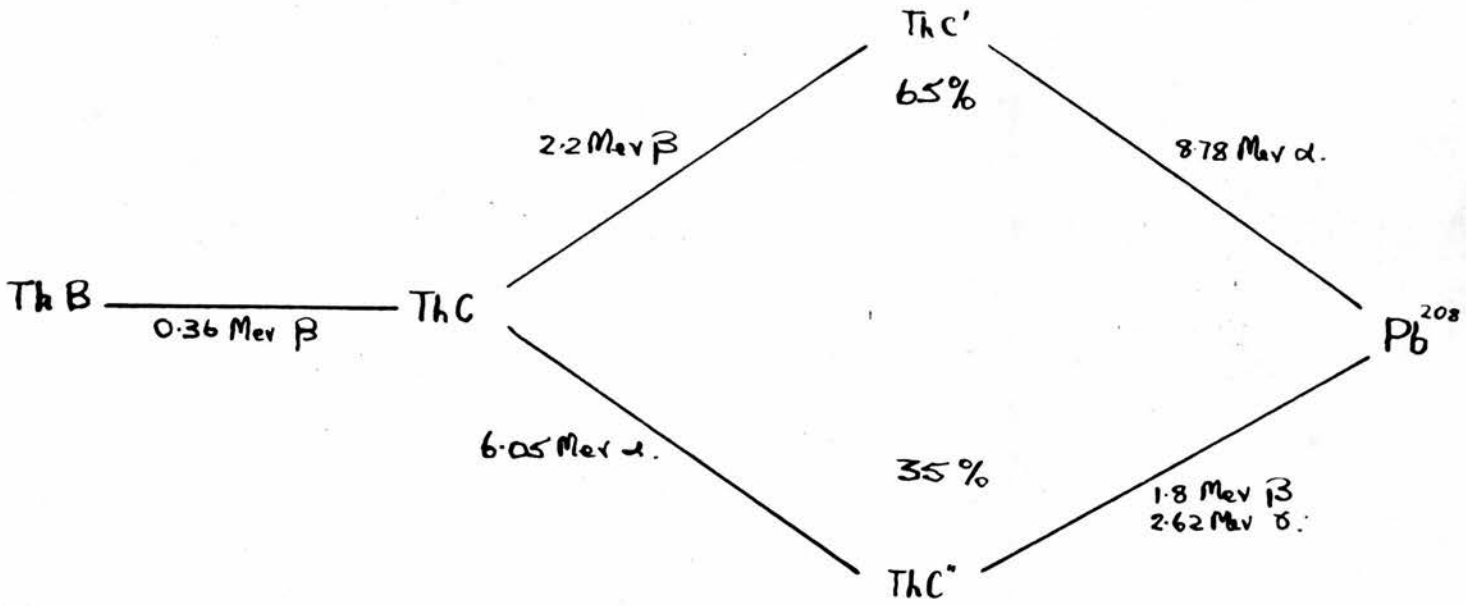

Figure 27. Diagram of disintegrations in the active deposit of Thorium.

many radiations present, and was not carried out.

Relatively low output pulses are obtained from fast Organic Phosphors with α particles, smaller than those due to β particles of equal energy.
It was not possible to discriminate in favour of the α particles, or between those of ThC and ThC', but when low coincidence resolution time is employed this becomes less necessary.

The decay of the source was, of course, governed by that of Thorium B, so its half-life was 10.6 hr.

Experimental Procedure.

The presence of γ radiation made it necessary to keep the γ sensitivity of the counters low. Naphthalene was chosen for the scintillating material because

(1) Its decay time for the emission of light is very short = 0.05 μs (13).
(2) It has a comparatively low sensitivity to γ radiation.
(3) It was readily available in suitable form.

After some preliminary experiments using large crystals grown from the melt, these were found to be unnecessary, and the method given below was used. A microscope slide was coated with a layer of Naphthalene about 1/16 in. thick by flowing molten material on to it when it was warm. The holes in the discs D of the

scintillation counters (see Fig. 23) were covered by suitable foils of Aluminium, 2.4 mg./sq. cm. for the α counter and 11 mg./sq. cm. for the β counter to form light tight windows for the particles. Then the microscope slides were attached, naphthalene side outwards, by means of paxolin straps secured by screws.

Thus when the counters were in position, with the source mounted between them, as described above, an α particle traversed $\frac{1}{2}$ cm. of air and 2.6 mg./sq. cm. of Aluminium, and a β particle $\frac{1}{2}$ cm. of air and 22 mg./sq. cm. of Aluminium, before reaching the scintillating material.

The coincidence unit used, A.E.R.E. type 1036, consists of three identical channels, two of which were used in this instance. Each channel comprises a discriminator, a pulse-shaping circuit, and a variable delay line, and these channels feed a mixer giving a variable resolving time, T. T was kept at the 10^{-7} sec. setting throughout the experiments, and, although it is not necessary to know its value provided it is kept constant, it was checked to be $1.1 \pm 0.06 \times 10^{-7}$ sec. by a subsidiary experiment with two sources. In order to ensure constancy of characteristics the apparatus was allowed ample warming-up time before each experimental run.

In these runs the coincidence rates were counted for equal intervals of time, actually 5 min., with

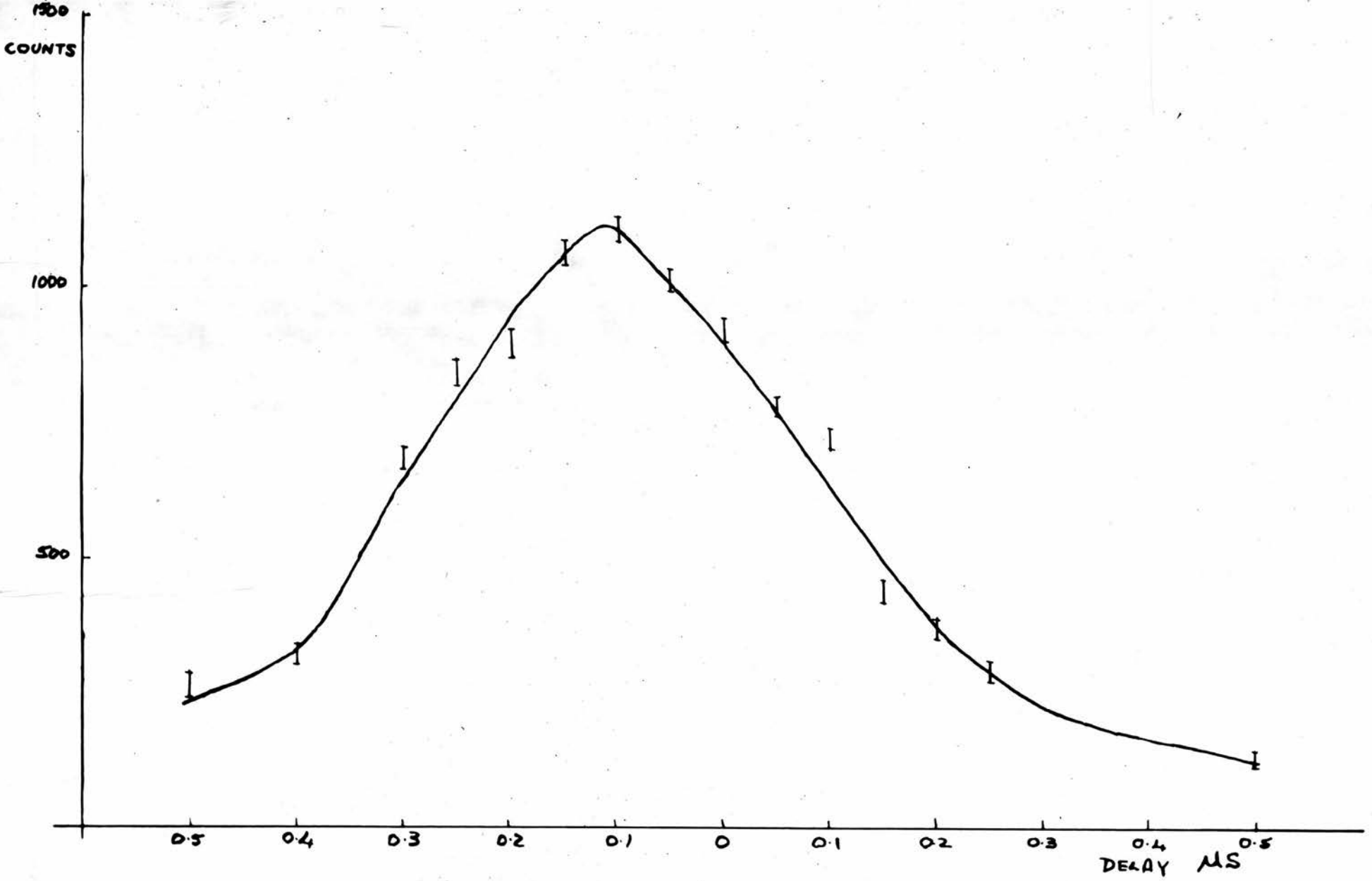

Figure 28. Prompt disintegration delay curve (P(td)). Source: Co^{60}.

different time delays introduced into the β channel varying between - 0.5 μS and + 1.0 μS in 0.05 μS steps. By "a negative delay" is meant one introduced into the α channel. One minute was allowed between each count for reading and resetting scalers and changing the delay, so that accurate normalization for the decay of the Thorium B could be carried out without difficulty. At both the discriminator settings used the background counting rates due to noise etc. were about 10 per minute and so entirely negligible. The random coincidence rate was calculated using the relation

$$N_c = 2N_1N_2T.$$

The single counting rates of each counter were taken at the beginning and end of the experiment, and were of the order of 3×10^5 per min. Subsidiary experiments using a weak source of Co_{60}, the γ rays from which follow one another with negligible delay, had shown that the delay curve was then highly symmetrical, Fig. 28, in agreement with theory(37).

Results.

Four sets of experimental results were obtained, and the curves of coincidence counts against delay time are shown in Figs. 29 and 30. The errors of representative points are marked and the curves are all of the same form. However the positions of the

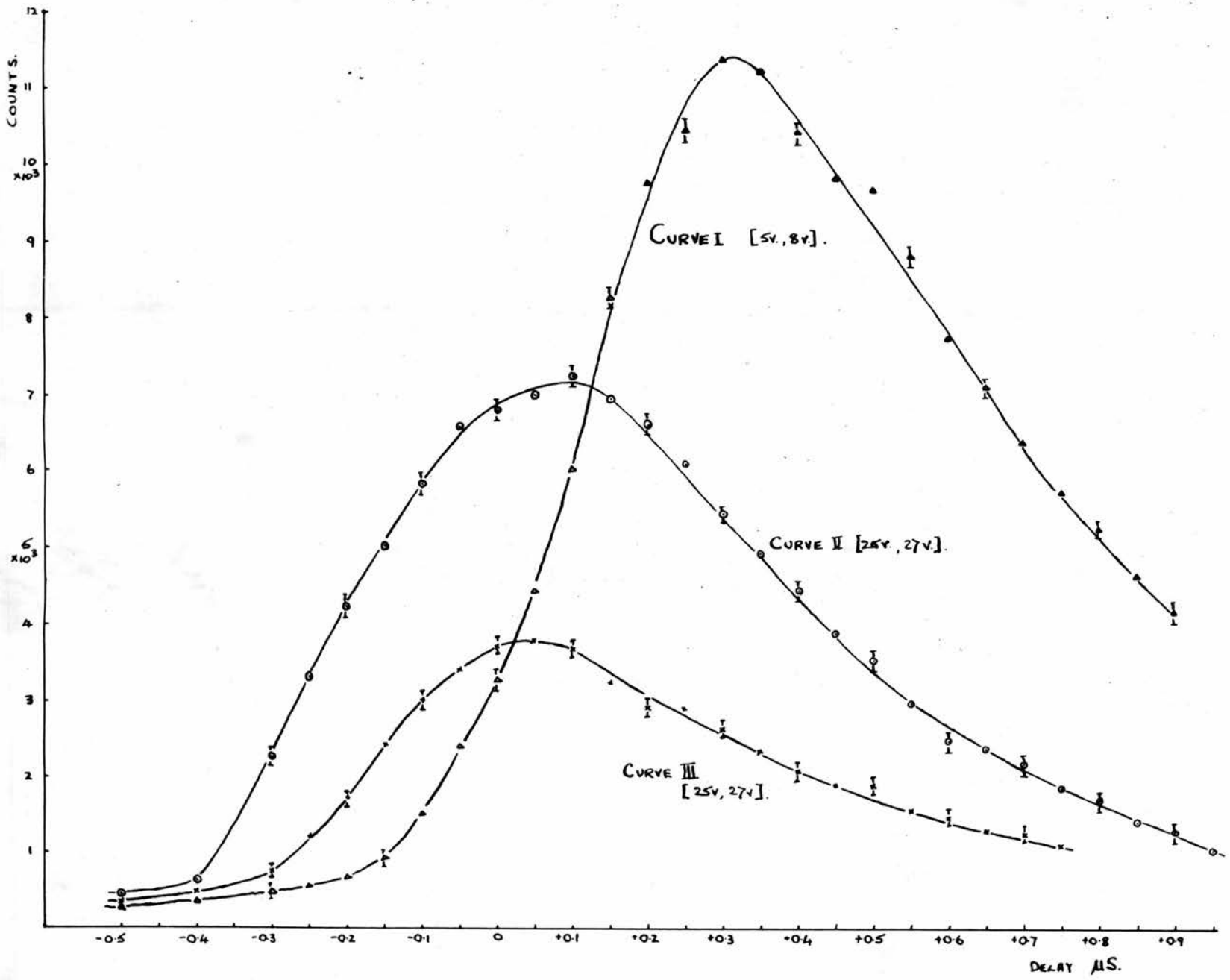

Figure 29. Results of ThC' experiments.

maxima do not fall at identical delay values. This effect is caused by the different discriminator settings used for different runs. Curve I of Fig. 29 and Curve IV, Fig. 30 were both taken with discriminator settings of 5 and 8v for the α and β channels respectively and the maxima occur at approximately 0.3 μS.

Curves II and III of Fig. 29 were taken with discriminator settings of 25 and 27 volts respectively and have maxima at approximately 0.5 μ S delay. The latter curves were counted first and the bias then lowered, to give more coincidence counts for each source.

The results were deduced by making plots upon logarithmic graph paper of the points on the R.H. side of the maxima. Straight lines were then fitted by means of least squares, and the final graphs are shown in Fig. 31. The straight line portion of the curve starts at a delay of 0.2 - 0.25 μ S from the maximum in each case. Since the measured half-life is 3×10^{-7} sec. and the resolving time is considerably less, $= 1 \times 10^{-7}$ sec., it is unnecessary to apply the more complicated analysis to be given below.

The values obtained were:-

Curve I	$T_{\frac{1}{2}}$ =	$3.23 \pm 0.08 \times 10^{-7}$ sec.
Curve II		$3.30 \pm 0.1 \times 10^{-7}$ sec.
Curve III		$3.27 \pm 0.1 \times 10^{-7}$ sec.
Curve IV		$3.08 \pm 0.05 \times 10^{-7}$ sec.

The weighted mean of these results is 3.19 ± 0.05 x 10^{-7} sec. This is higher than the most reliable of the previous values, and outside the probable errors.

The present results are consistent within themselves and so a systematic error may be indicated. The most likely reason is faulty calibration of the delay line. The coincidence unit used was newly calibrated by the manufacturers, and lack of suitable equipment prevented this being checked. The apparatus has subsequently been moved to India.

The table below includes the present results, and those of previous authors.

Table 5.

Author	Date	Method	Result	Ref.
Dunworth	1939	Integral	3 ± 1 x 10^{-7} sec.	31
Bradt & Scherrer	1943	Integral	2.6 ± 0.4 "	32
Van Name	1949	Differential	2.2 ± 0.1 "	33
Hill	1949	Differential	3.0 ± 0.15 "	36
Bunyan et al.		Differential	3.04 ± 0.04 "	37
Ogilvie	1950	Differential	3.19 ± 0.05 "	-

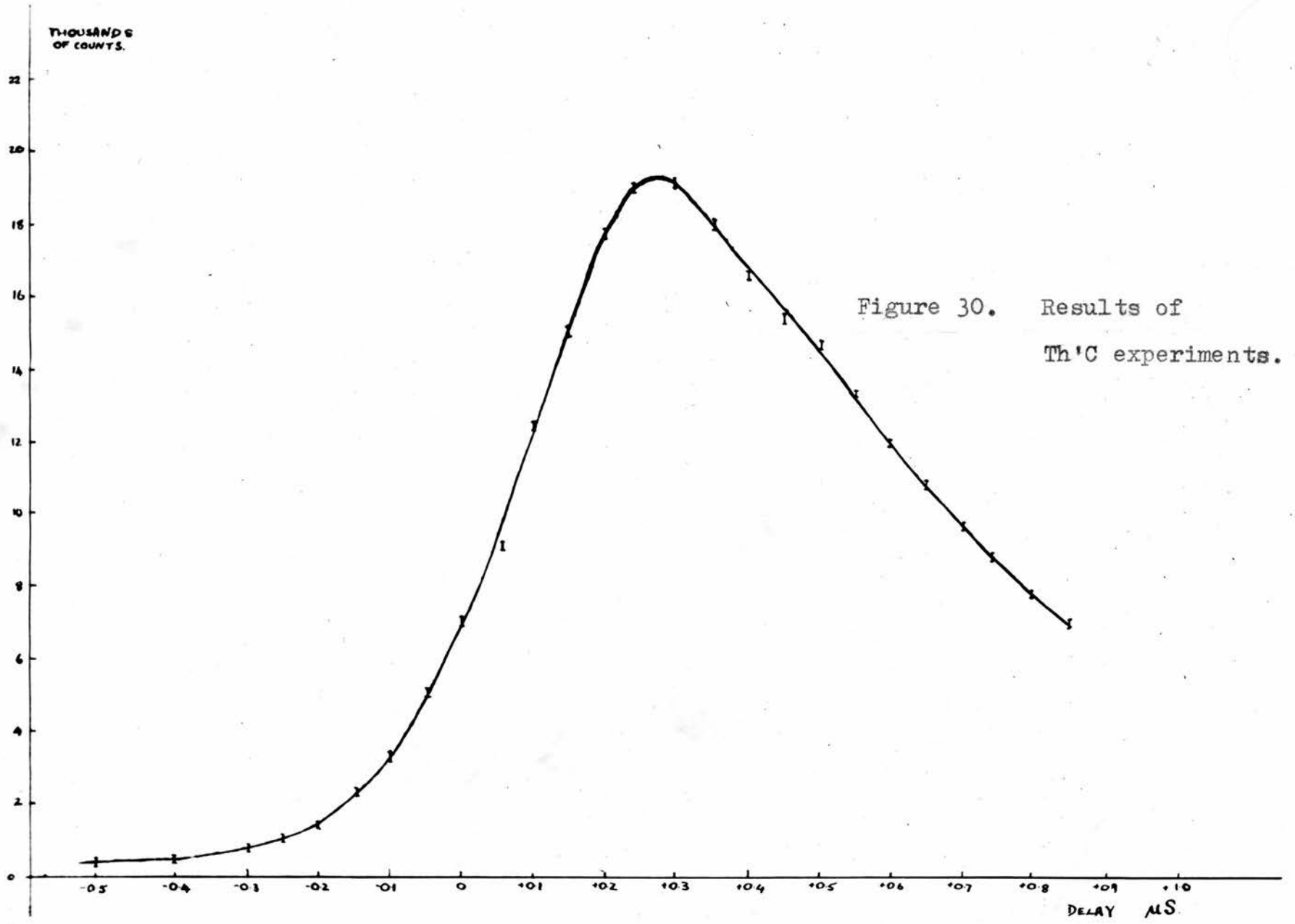

Figure 30. Results of Th'C experiments.

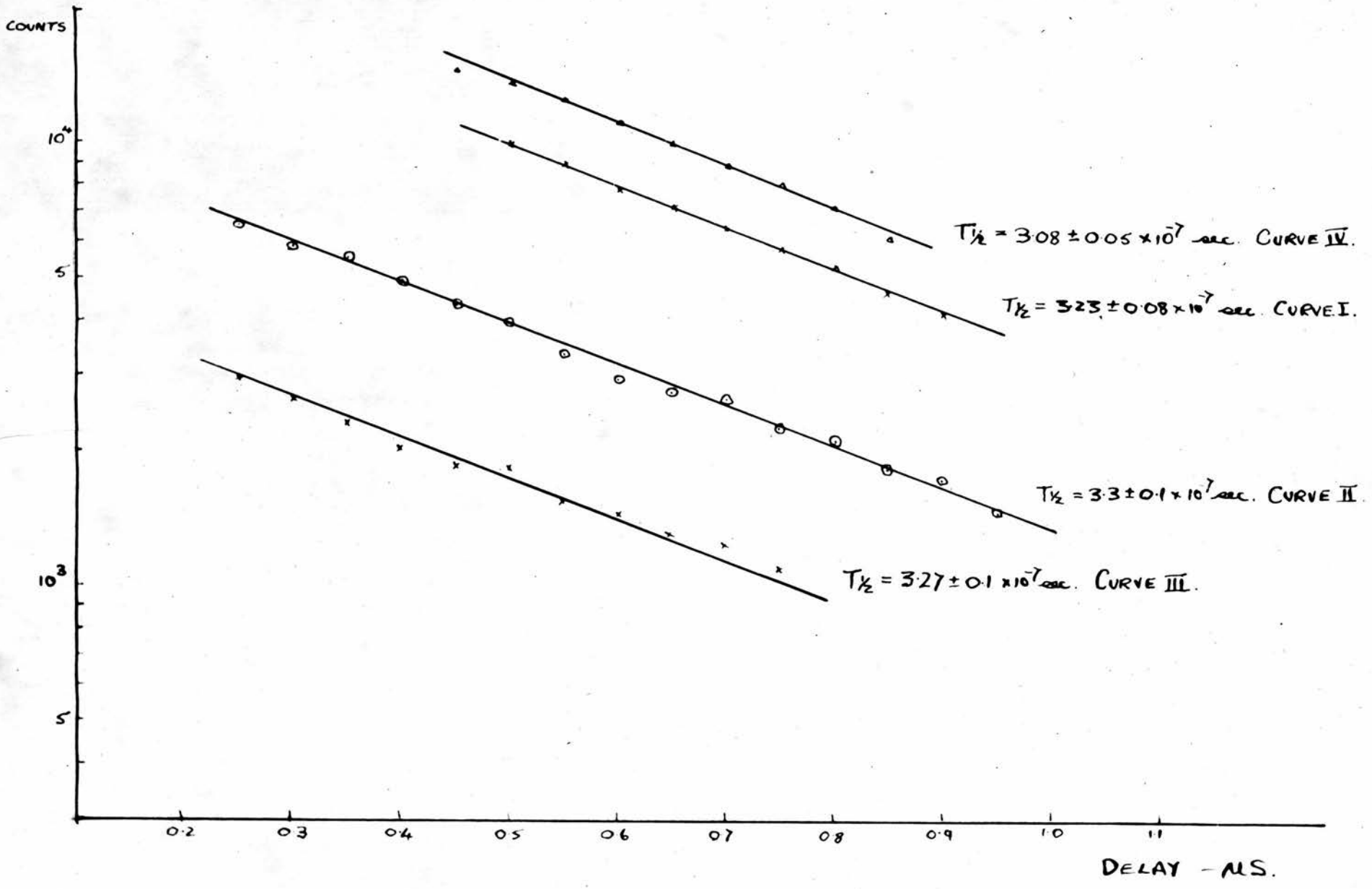

Figure 31. Semi-log plot of data from Figs. 29 and 30.

Chapter IV.

THE THEORY OF COINCIDENCE EXPERIMENTS.

In this section two topics will be considered. Firstly, the methods used by various authors for the evaluation of radioactive decay constants from the results of delayed coincidence experiments will be examined. Secondly, some deductions about the design of such experiments will be presented.

Radioactive decay constants from delayed coincidence experiments.

We shall denote by $F(\lambda, td)$ the curve of coincidence counting rate against inserted delay, td, for a substance with decay constant λ. Assuming this to have been found by experiment, the problem which must now be solved is that of obtaining the value of λ from the measurements, with the greatest accuracy. This can be done if the constants of the apparatus are known, the resolving time T, and the so-called prompt resolution curve P(td). This latter is the curve of coincidence counting rate against td, which is found when radiations enter the two detectors with a negligible time interval between them.

The simplest method by which λ may be obtained is to replot the curve $F(\lambda, td)$ using logarithmic ordinates. It will be shown below that this yields a straight line for values of td inserted between the

counter which responds to the preceding radiation and the coincidence unit. Least square methods then allow λ to be deduced at once. However, cases occur when this method does not make the best use of the data obtained. It is not satisfactory when the half-life, $T_{1/2} = \frac{0.693}{\lambda}$, is of the same order as or smaller than the least resolving time that can be employed. When these conditions occur it is necessary to analyse the whole delay curve. We must notice an assumption which is implied in the following theory. This is that the time lags which occur in the counters, between the entry of a charged particle and the output pulse, are the same for the radiations by means of which P(td) is measured as those for which F(λ, td) is counted. With photomultiplier counters it is considered that the time lags may depend upon the energy liberated within the crystal, but are likely to be small compared with the rise time of the output pulse, and need not concern us unless the resolving time used is less than 10^{-8} sec.

It is first necessary to normalize F(λ, td) and P(td) to unit area. We may then write

$$F(\lambda, t_d) = \int_{-\infty}^{+\infty} f(t)\, P(t_d - t)\, dt \qquad (10)$$

where f(t) represents the variation with time of emission of the delayed radiation. If only a single substance of short half-life is present, f(t) = 0 for $t < 0$ and $\lambda e^{-\lambda t}$ for $t > 0$.

Figure 32. Intersection of P(td) and F(λ,td) - after Bunyan, Lundby and Walker (37).

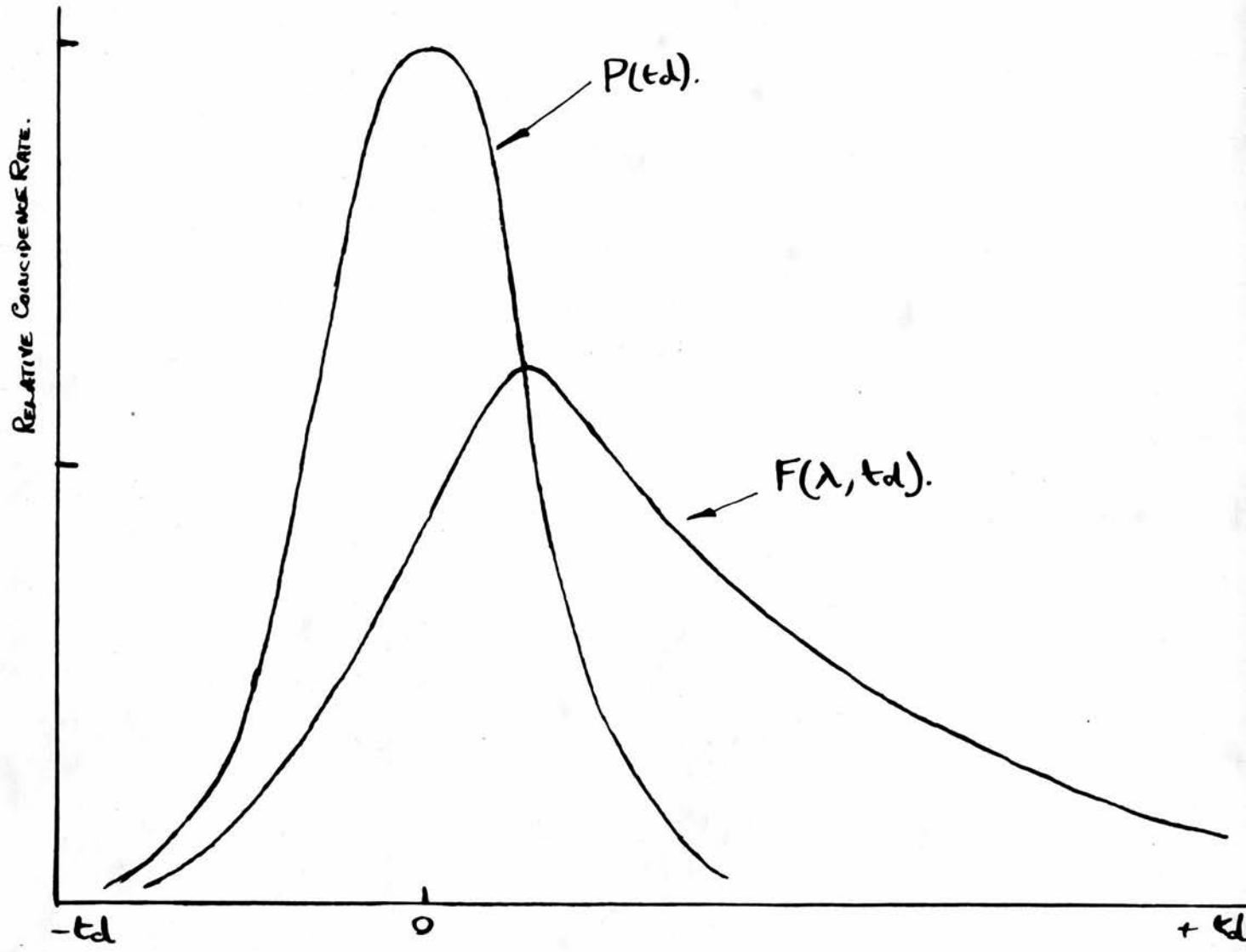

Following Newton (38) we write $y = td - t$ and obtain

$$F(\lambda, td) = \lambda e^{-\lambda td} \int_{-\infty}^{td} e^{\lambda y} P(y)\, dy.$$

and differentiating this,

$$\frac{d}{dtd}\left[F(\lambda, td)\right] = \lambda\left[P(td) - F(td)\right] \quad (11)$$

and also

$$\frac{d}{dtd}\ln\left[F(\lambda, td)\right] = -\lambda\left[1 - P(td)\left[F(td)\right]^{-1}\right] \quad (12)$$

From (11) we see that the maximum of $F(\lambda, td)$ occurs at its intersection with P(td), Fig. 32. Equation (12) shows how a logarithmic plot of the results has a slope of $-\lambda$. Integrating, we obtain

$$\lambda = \left[F(A) - F(B)\right]\left[\int_A^B \left[F(\lambda, td) - P(td)\right] dtd\right]^{-1} \quad (13)$$

This equation is useful because A and B may be chosen in several ways and thus several values for λ may be deduced from one set of data, to form mutual checks. Also the best determined portion of the curve may be used, and the errors of the other portion occur only in the normalization process where their effect is small.

As illustration of this point, Bell and Graham (39) quote some interesting figures. In an experiment to determine the mean life of a transition in Yb^{170}, they calculated the result in four different ways. If td' is the delay where P(td) and $F(\lambda, td)$ cross, equation 13 with $A = -\infty$, $B = td'$ gives $T = 1/\lambda =$ $(2.34 \pm 0.12) \times 10^{-9}$ sec. With $A = t'd$, $B = \infty$ it

yields $T = (2.31 \pm 0.09) \times 10^{-9}$ sec. The slope at large delay gives $T = (2.3 \pm 0.4) \times 10^{-9}$ sec., and an equation of Bay, to be deduced below, leads to $T = (2.28 \pm 0.08) \times 10^{-9}$ sec. The increase of accuracy to be gained by proper use of all the observations is thus considerable.

Z. Bay (40) has deduced a general relation between the moments of $F(\lambda, td)$, $P(td)$ and $f(t)$, where the n^{th} moment of $f(x)$ is defined by the equation

$$M^n\big(f(x)\big) = \int_{-\infty}^{+\infty} x^n f(x)\, dx .$$

This may also be obtained as follows from equation (10) above.

$$F(\lambda, td) = \int_{-\infty}^{+\infty} f(t)\, P(td - t)\, dt . \qquad (10)$$

$$td^n F(\lambda, td) = \int_{-\infty}^{+\infty} td^n f(t)\, P(td - t)\, dt .$$

$$\therefore \int_{-\infty}^{+\infty} td^n F(\lambda, td)\, dtd = \int_{td=-\infty}^{+\infty} \int_{t=-\infty}^{+\infty} td^n f(t)\, P(td - t)\, dtd\, dt .$$

$$= M^n\big(F(\lambda, td)\big) .$$

Now let $(td - t) = T$

$$M^n\big(f(\lambda, td)\big) = \int_{T=-\infty}^{+\infty} \int_{t=-\infty}^{+\infty} (T+t)^n f(t)\, P(T)\, dt\, dT .$$

$$= \int_{-\infty}^{+\infty} \int_{-\infty}^{+\infty} \sum \frac{n!}{j!\,(n-j)!}\, T^j t^{n-j} f(t)\, P(T)\, dt\, dT .$$

$$= \sum \frac{n!}{j!\,(n-j)!} \int_{-\infty}^{+\infty} T^j P(T)\, dT \int_{-\infty}^{+\infty} t^{n-j} f(t)\, dt .$$

Thus at last we arrive at Bay's result,

$$M^n(F(\lambda,t_d)) = M^n(P(t_d))\,M^0(f(t)) - \binom{n}{1} M^{n-1}(P(t_d))\,M^1(f(t)) + \cdots\cdots + M^0(P(t_d))\,M^n(f(t)). \qquad (14)$$

The Design of Delayed Coincidence Experiments.

In this section we shall consider how to choose the value of resolving time, and the manner of counting to be employed during delayed coincidence experiments. We must decide upon a suitable function to represent the prompt resolution curve of the apparatus. This is the curve of counts against inserted delay time when the source emits two radiations separated by an infinitesimal time interval. In Fig. 33 is shown the curve obtained with the coincidence unit to be described below.* The fall-off at each side is exponential in form, Fig. 34, and has a half width of approximately 1.3×10^{-8} sec. This form is in agreement with curves given by McGowan (9), Bell and Petch (41), and de Benedetti and Richings (28) and the half width is in

* see also Fig. 28, which gives such a curve for another apparatus.

Figure 33. Prompt disintegration delay curve (P(td)) for higher-resolution coincidence circuit. Source: Co^{60}.

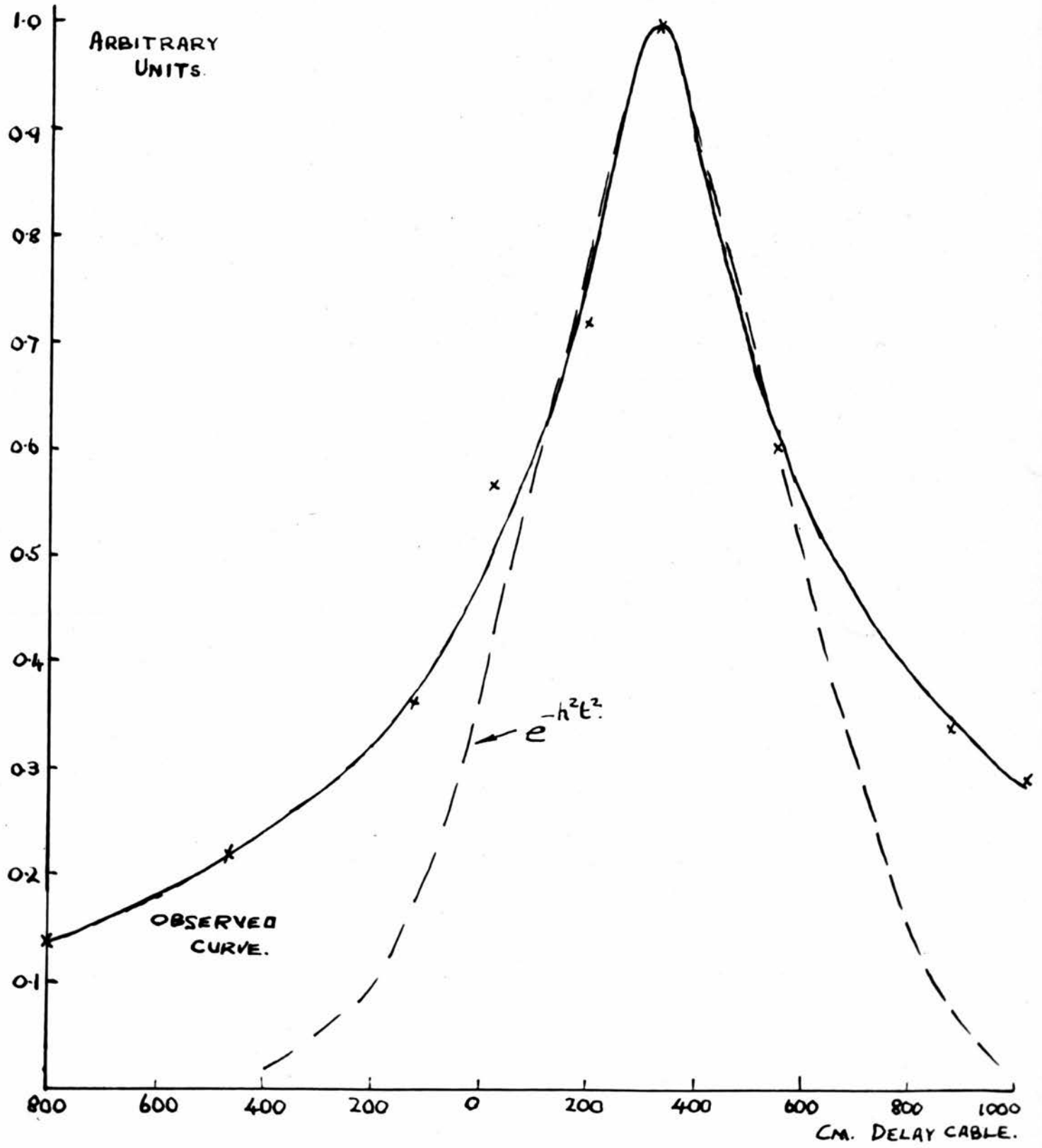

Figure 34. Semi-log plot showing exponential fall-off of curve shown in Fig. 33.

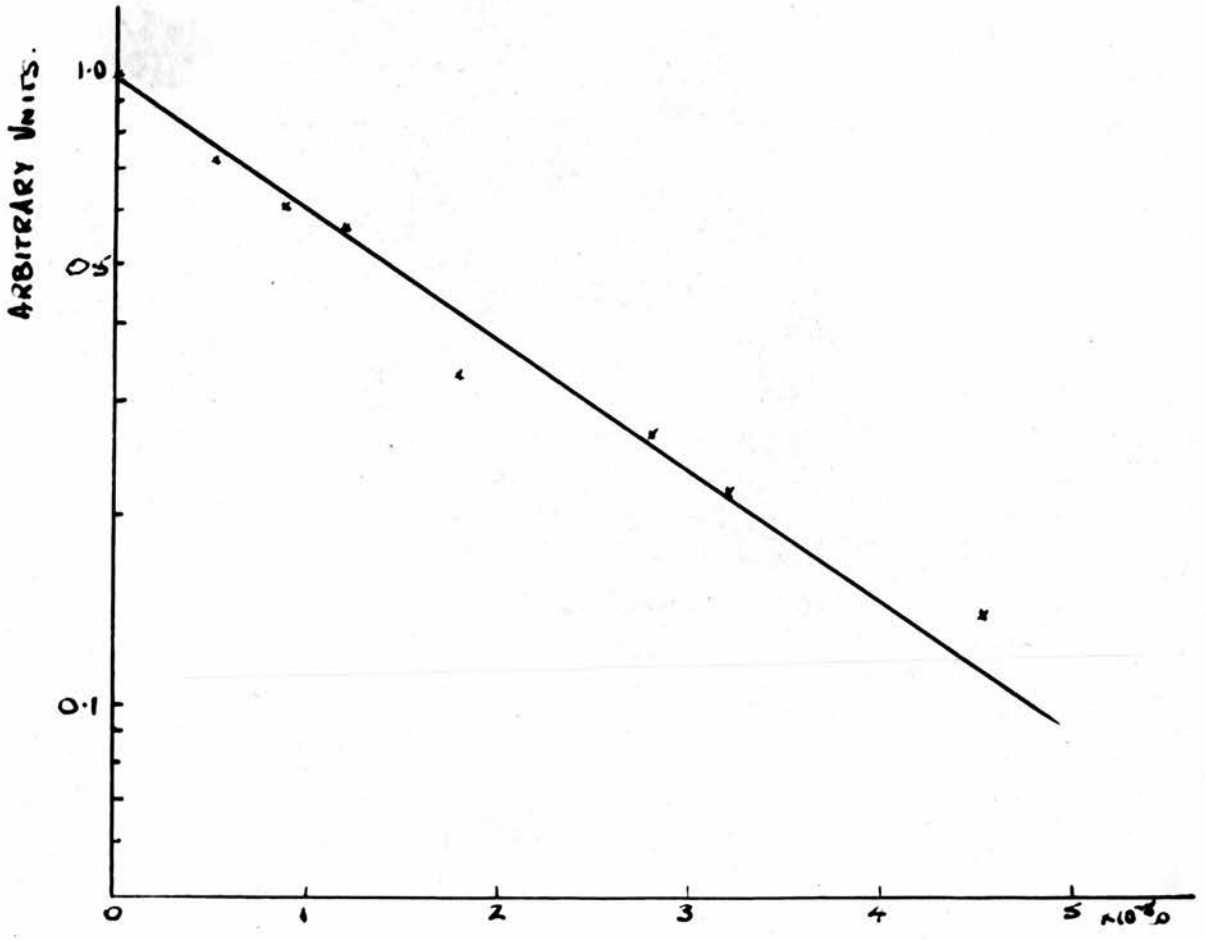

each case rather larger than half the resolving time obtained by the two source method. A square form is obtained for coincidence circuits where the resolving time is of a larger order of magnitude than the time lags which occur in the counters, and the rise time of the associated circuits. If these uncertainties are of the same order of magnitude as the resolving time, the square form is 'smeared' out into the exponential type of fall-off which is observed here. The form of the curve depends also upon the amplitude distribution of the pulses. If those from one detector are large compared to those from the other, the width of the prompt resolution curve will be increased, and it will be smallest when they are the same. (28, this effect has also been observed by the present author.) A form of P(td) which has been used by some authors (32), (37), is the error function $P(td) = Ae^{-h^2 td^2}$. This seems to apply when Geiger counters are used in conjunction with coincidence circuits having resolving times of about 10^{-7} sec.

For reasons of mathematical simplicity and because high accuracy is not required, we shall use for P(td) the following square function

$$-\infty \leq td < -T/2 \quad , \quad P(td) = 0.$$

$$-T/2 \leq td \leq +T/2 \quad , \quad P(td) = 1.$$

$$+T/2 < td \leq +\infty \quad , \quad P(td) = 0.$$

where T is the resolving time. If the first counter is affected only by the preceding radiation counting it with efficiency ϵ_1 while the second counter counts only the delayed radiation with efficiency ϵ_2 then

$$F(\lambda, t_d) = 2N\epsilon_1\epsilon_2 \int_{t_d - T/2}^{t_d + T/2} e^{-\lambda t}\, dt.$$

$$= 2N\epsilon_1\epsilon_2 e^{-\lambda t_d} \sinh \lambda T. \qquad (15)$$

The chance coincidence rate is given by the relation

$$N_c = 2N_1N_2T$$
$$= 2N^2\epsilon_1\epsilon_2T.$$

So that the ratio $\frac{\text{Real coincidence rate}}{\text{Total coincidence rate}}$ is

$$r = \frac{2N\epsilon_1\epsilon_2 e^{-\lambda t_d} \sinh \lambda T}{2N\epsilon_1\epsilon_2 e^{-\lambda t_d} \sinh \lambda T + 2N^2\epsilon_1\epsilon_2 T}$$

$$= \frac{e^{-\lambda t_d} \sinh \lambda T}{e^{-\lambda t_d} \sinh \lambda T + NT} \qquad (16).$$

It is not possible, by differentiating (16) with respect to T, to arrive at a maximum value for this quantity because it approaches unity monotonically. However, it is possible to deduce criteria for the optimum values of T and the counting rate in a given experiment if λ is known approximately.

(1) If we have a source which is constant in strength, to find conditions such that r does not fall below a given value we can proceed as follows.

In the delayed coincidence experiment, suppose t'd

to be the largest delay which we shall insert. This should be about 5 half-lives if the methods given above are to be used to calculate the results. Then $e^{-\lambda t_d'} =$ 0.03. If we require r not to fall below the value $\frac{1}{2}$, when the real and accidental coincidences will be equal, at the longest delay, then

$$e^{-\lambda t_d'} \operatorname{Sinh} \lambda T = N_m T .$$

or $$0.03 \operatorname{Sinh} \lambda T = N_m T \qquad (17).$$

It is obviously advantageous in a practical case that Sinh λT should not vary rapidly with T, in order that any variations in the value of T during an experiment will have the least effect upon the coincidence rate. Thus Sinh λT should be less than unity because it varies very rapidly with its argument for greater values. If we assume Sinh λ T = 0.4 we may also assume Sinh λ T = λ T with fair accuracy.

Then $0.03 \lambda T = N_m T$ (18)

and $\lambda T = 0.4$ (19).

We interpret these equations in the following way. To measure the half-life of a particular substance where $T_{\frac{1}{2}} = 0.693/\lambda$ is known approximately, a value of $T = 0.4/\lambda$ should be used. For the best conditions, Nm, the maximum counting rate, should be varied until $N_m = 0.03\lambda$.

If λ is very large this maximum value becomes too large to be practicable, but equation (19) still gives

the optimum value of resolving time. The largest practical counting rate may be used with confidence that r will be closely equal to unity for all points on the delay curve. For example, suppose that the half-life is 10^{-9} sec., so that $\lambda = 7 \times 10^{8}$ per sec.

Therefore $Nm = 2 \times 10^{7}$ per sec.

Using scintillation counters a counting rate of 2×10^{5} per second could be used and the ratio real/accidental coincidences would be approximately 300.

(2) Decaying Source.

Decay of the primary source makes no essential difference to the conclusions reached above, unless its half value period is of the same order as that of an experimental run. If this is so, the problem becomes complicated by the question of how long each run should be to get the best results from each primary source. We shall assume that the actual counting intervals at each delay are equal in length, since the practical difficulties of normalization are thereby reduced. The results of the experiment may be deduced from a least-squares plot on logarithmic ordinate scale, through points corresponding to each delay time. The long delays can either be taken while the source is fresh or at the end of the experiment, when it has decayed. If the first of these is done, then the smallest value of r is obtained when N and td are both large, at the beginning of an experiment, so that $Nm = 0.03\lambda$, $r = \frac{1}{2}$.

At the end of the experiment td is small and Nm becomes $Nme^{-\lambda st}$, where λs is the decay constant of the source. The value of r increases throughout an experiment and this offsets the decay of the primary source, for:

$$r_i = \frac{e^{-\lambda t_d'} \operatorname{Sinh} \lambda T}{e^{-\lambda t_d'} \operatorname{Sinh} \lambda T + N_m T}.$$

and r_n, at the n^{th} counting interval is

$$r_n = \frac{e^{-\lambda (t_d)_n} \operatorname{Sinh} \lambda T}{e^{-\lambda (t_d)_n} \operatorname{Sinh} \lambda T + N_m T e^{-\lambda s t_n}}$$

$$\therefore \quad \frac{r_n}{r_i} = \frac{\lambda e^{-\lambda t_d'} e^{-\lambda (t_d)_n} + e^{-\lambda (t_d)_n} N_m}{\lambda e^{-\lambda (t_d)_n} e^{-\lambda t_d} + N_m e^{-\lambda s t_n} e^{-\lambda t_d'}}$$

where t_n is the time at which the n^{th} counting interval is taking place.

$$= \frac{1 + 0.03 e^{\lambda t_d'}}{1 + 0.03 e^{-\lambda s t_n} e^{\lambda (t_d)_n}}$$

$$= \frac{\text{Const.}}{\text{Const.} + 0.03 e^{-\lambda s t_n} e^{\lambda (t_d)_n}} \qquad (20).$$

Thus the way in which r_n/r_i varies depends upon the value of $e^{-\lambda s t_n} e^{\lambda (t_d)_n}$ both factors of which decrease. r_n/r_i will vary slightly during a counting interval, the length of which is considered to be small compared to t_n.

In the opposite case of short delays counted first however,

$$r_1 = \frac{e^{-\lambda(td)_0} \sinh \lambda T}{e^{-\lambda(td)_0} \sinh \lambda T + N_m T}$$

$$r_p = \frac{e^{-\lambda(td)_p} \sinh \lambda T}{e^{-\lambda(td)_p} \sinh \lambda T + N_m e^{-\lambda st_p} T}$$

which give

$$r_p/r_1 = \frac{1 + 0.03\, e^{\lambda(td)_0}}{1 + 0.03\, e^{-\lambda st_p} e^{+\lambda(td)_p}}$$

$$= \frac{\text{Const}}{\text{Const} + 0.03\, e^{-\lambda st_p} e^{+\lambda(td)_p}} \quad (21).$$

The behaviour of r_p/r_1 depends upon that of the product $e^{-\lambda st_p} e^{\lambda(td)_p}$ the factors of which vary in opposite directions during an experiment, t_p always increasing and $(td)_p$ becoming larger as larger delays are inserted. General statements cannot be made about this, but it will be seen that it is always preferable to count the longer delay intervals first.

In many actual experiments counter 1 is sensitive to radiation other than that which precedes the transition whose half-life is to be found. In order to discuss this, suppose a substance S_1, the primary source, which decays to substance S_2 with a long half-life, emitting radiation A. Suppose it also to emit a radiation which is uncorrelated with A, such as in radioactive branching. Substance S_2 subsequently decays with constant λ and the emission of radiation B.

Delayed coincidences between A and B will allow us to measure λ , and so the half-life of substance 2. A diagram is given below.

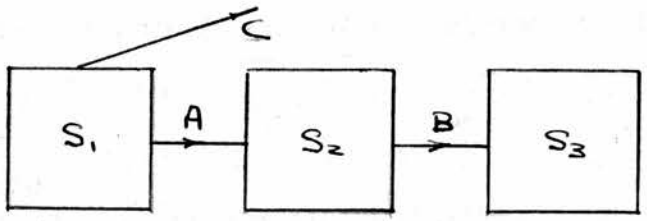

A may be called the preceding radiation, B the delayed radiation, and C the parallel radiation, and if N atoms of substance 2 are formed per second, so that N particles or quanta of radiations A and B are emitted and, say, XN particles or quanta of radiation C, then we have

$$N_1 = N[\epsilon_{1A} + \epsilon_{1B} + X\epsilon_{1C}] \qquad (21)$$

and

$$N_2 = N[\epsilon_{2A} + \epsilon_{2B} + X\epsilon_{2C}] \qquad (22).$$

Now

$$F(\lambda, t_d) = N\epsilon_{1A}\epsilon_{2B}\lambda \int_{t_d - \tau/2}^{t_d + \tau/2} e^{-\lambda t} dt.$$

$$= 2N\epsilon_{1A}\epsilon_{2B} e^{-\lambda t_d} \sinh \lambda\tau \qquad (23)$$

and

$$N_C = 2N_1N_2\tau$$

$$= 2N^2[\epsilon_{1A} + \epsilon_{1B} + X\epsilon_{1C}][\epsilon_{2B} + \epsilon_{2A} + X\epsilon_{2C}]\tau \quad (24).$$

Putting the product of the square brackets above equal to Z

$$N_C = 2N^2\tau Z.$$

and $$r = \frac{\epsilon_{1A}\epsilon_{2B}\, e^{-\lambda t_d} \sinh \lambda T}{\epsilon_{1A}\epsilon_{2B}\, e^{-\lambda t_d} \sinh \lambda T + N Z T}.$$

If we differentiate this equation with respect to T, simplify and equate to zero we obtain

$$\tanh \lambda T = \lambda T$$

This is the same equation which is obtained by differentiating equation (16) with respect to T and equating to zero. Thus the presence of this parallel radiation has no effect upon the results obtained above.

The three curves in Fig. 35, which are for constant primary source, and the two decaying source cases treated above, show diagrammatically how the counting rates vary.

This theory can be applied to the delayed coincidence experiments upon RaC' described in Chapter I to form an illustrative example. Here λ was known to be approximately 4.3×10^3 so that $0.4/\lambda = 90\ \mu s$ approximately, and Nm, the maximum counting rate $= 0.03\lambda = 8 \times 10^3$ per min. In the actual experiments the resolving time was held down to $30\ \mu s$ in order to reduce still further the effect of any variations, and Nm allowed to rise to about 2×10^4 per min. at the beginning of an experimental run. The value of r never dropped below $\frac{1}{2}$. Again referring to the experiments upon Thorium described in Chapter III, there $T_{\frac{1}{2}} = 3 \times 10^{-7}$ sec., $\lambda = 2.3 \times 10^6$ giving $T = 1.74 \times 10^{-7}$ sec. The maximum counting rate, 0.03λ, $= 4 \times 10^6$

per min., which was too high to be employed due to the losses which would have occurred due to overlapping. The pulses from the counters were 2.0 μ S in duration, so that the maximum counting rate for 1% loss was 3×10^5 per min. Using a source of the strength required to give this maximum counting rate resulted in a value of r which was never less than $\frac{1}{2}$.
It is thus apparent that the criteria deduced above are definitely useful in the design of such experiments to measure short radioactive half-lives.

All the foregoing work has assumed that P(td) has a square form. However P(td) often takes other forms, which may be approximated to closely by a superposition of functions such as we have used. In this way the results are of quite general application, at least to the degree of accuracy necessary for the design of experiments.

Figure 35. Diagram to illustrate coincidence counting with constant and decaying sources.

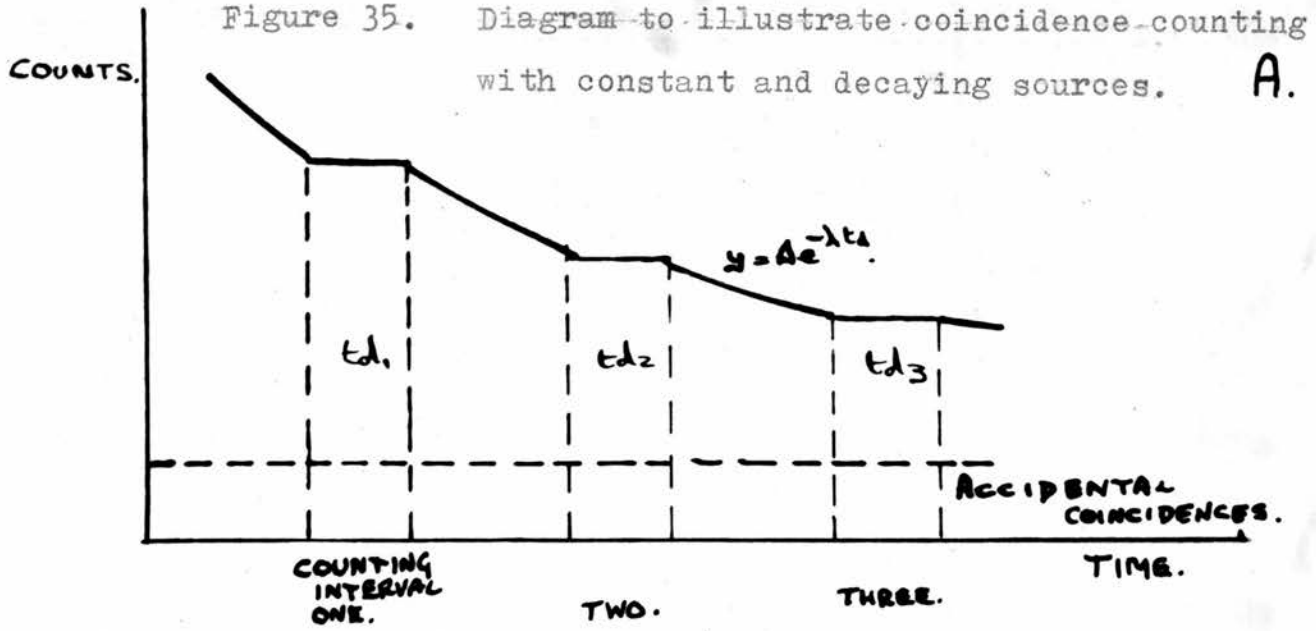

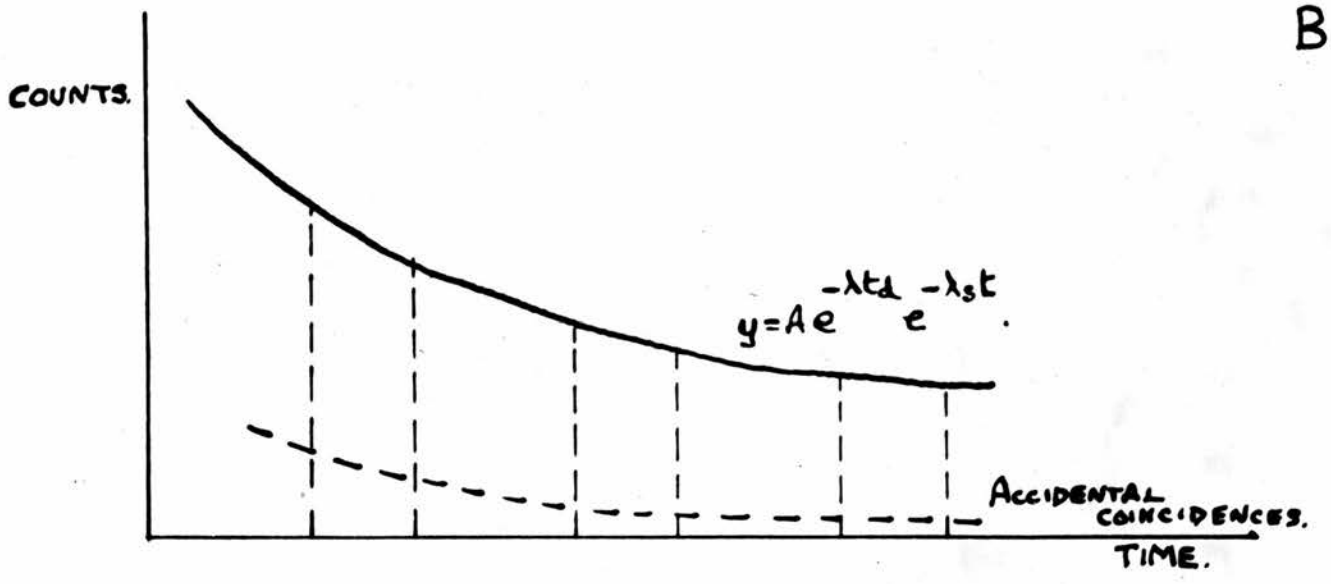

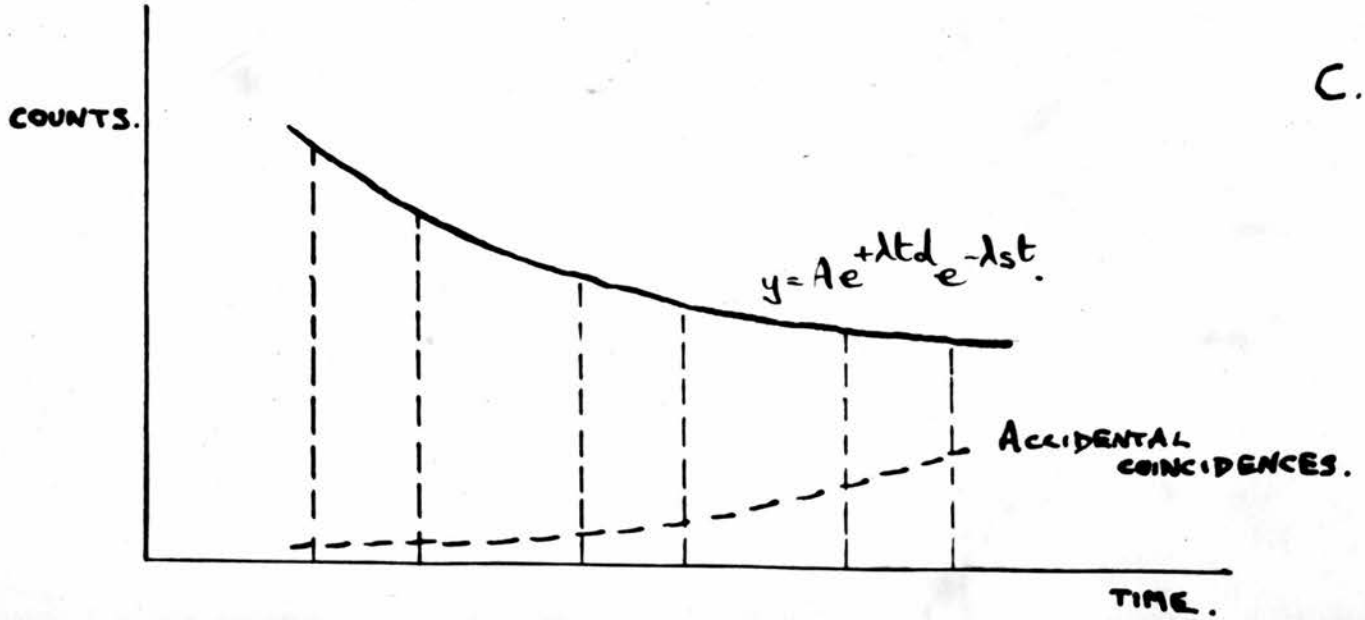

Chapter V.

A SIMPLE HIGH SPEED COINCIDENCE SYSTEM.

Design.

It was decided to construct a coincidence system with a smaller resolving time than that given by the A.E.R.E. type 1036 unit, used in the experiments described above. The component parts which make up such a system are the counters, the pulse shaping devices, and the coincidence circuit itself. Also methods must be devised, both for recording the single counting rate of each counter, and also for delaying the pulses from one counter relative to those from the other.

The photomultipliers available were E.M.I. type VX 5045, eleven stage tubes with a gain of approximately 10^7 times at their maximum rated potential and with photocathodes 5 cm. in diameter. These tubes have dynodes of the Venetian blind type, and the rise time of their thermionic noise pulses has been measured by Allen and Engelder (15)* and found to be 7×10^{-9} sec. This is greater than that found for multipliers of the focussed-beam type. They found the signal and noise pulses to be of much greater duration than those of multipliers of the focussed type. If a scintillating

* Allen and Engelder used type 5311 which is identical with type VX 5045 except for the size of the photocathode.

crystal with a decay time of 7×10^{-9} sec. were used in conjunction with such a tube, and the pulse shortened by a circuit such as that described on page 23 and illustrated in Fig. 9, triangular signal pulses could be obtained with a width of 7×10^{-9} sec. at half their maximum height. These pulses would be the shortest that could be produced using the tubes without additional gain, and they would be inseparable from any noise pulses of similar size which might occur. Two such counters in conjunction with a diode coincidence unit would provide a system with a resolving time somewhat greater than 1.5×10^{-8} sec., and this is the minimum resolving time to be expected.

Anthracene has a decay time for light emission of 1.0 to 1.5×10^{-8} sec., and was available in the form of purified powder, so it was decided to use this substance as scintillating material. Preliminary experiments showed that the γ radiation from Co^{60} (1.1 and 1.3 MeV) produced pulses of up to 0.5v amplitude at the collector plate, when the load resistance was 3×10^4 ohms. The stray capacitance at this electrode was 8 pf and the input capacitance of the succeeding cathode follower and wiring raised this to 20 pf. The output circuit time constant was thus 6×10^{-7} sec., allowing a maximum counting rate of 10^6 per minute without losing more than 1% of the counts by overlapping. An output circuit time constant equal to the

decay time of the phosphor, entailing a load resistance of 750 ohms, could not be used here because of the small pulses which would then have been obtained.

The pulses from the counters when counting the γ rays of Co^{60} were thus of $1.0 - 1.5 \times 10^{-8}$ sec. rise-time, and had an amplitude of up to $\frac{1}{2}$ volt. Their total duration was less than one microsecond.

To match the output impedance of the counters to the low input impedance of the coincidence circuit, a cathode follower was used. This device was also used to shape and shorten the pulses, as described above. The circuit was essentially that of Fig. 9, using a type 6J6 (C.V. 858) double triode valve with both triode sections connected in parallel. The band-width of a cathode follower circuit using this valve ($>$ 100 Mcs) is sufficient for the present purpose,(42).

The necessary length ℓ of cable between the cathode resistor Ro and the short circuit is given by

$$2\ell = Vt$$

where V = velocity of propagation of the pulses along the cable,

and t = half the total duration of the desired pulse.

The velocity of propagation along the cable used was $0.83C = 2.49 \times 10^{10}$ cm. per sec., and 125 cm. was used, giving a value of t of 1×10^{-8} sec. The total duration of the pulses was thus reduced to about twice their rise-time, the width at half height being approximately

1.0×10^{-8} sec. A minimum resolving time slightly more than 2×10^{-8} sec. was accordingly expected under these operating conditions.

The counter output stages were connected to the coincidence circuit by means of cable similar to that employed for pulse shaping. It was a 'twin feeder' cable manufactured by Messrs. Telcon Limited., and was selected because of its high characteristic impedance of 300 ohms. This ensured minimum loss of pulse amplitude in the shortening device. Complete information on the operation of the circuit could not be obtained directly, due to the lack of a suitable oscillograph, but it operated to some extent as a limiting device, reducing the spread of amplitude of the larger pulses.

Since without additional amplification the well tried coincidence circuits of Garwin (20) and Wells (29) could not be used, it was decided to investigate that of Bay (27). Bay reports that he has obtained minimum resolving time as low as 3×10^{-10} sec., using direct particle-multiplying tubes of high gain, and, what is more important for the present purpose, high sensitivity and a high discrimination against large single pulses breaking through into the coincidence output channel. The principle of this circuit has been described on page 28 and a circuit diagram appears in Fig. 19, while an account of its construction and opera-

tion forms the next section of the present chapter.

In order to calculate the number of accidental coincidences which are recorded by a coincidence circuit, the counting rates in the individual counters must be measured. It is interesting to contrast the situation when scintillation counters are used with that when Geiger counters are employed. The latter give pulses which are all closely equal in amplitude, so that if one, together with a coincident pulse in the other channel, has sufficient amplitude to operate the mixer, then all will do so. The scintillation counter, however, gives a range of pulse amplitudes even when counting monoenergetic radiation, and this range may be very wide. The effective counting rate of such a counter is then dependent upon the sensitivity of the mixer circuit which acts as a crude discriminator operating at an unknown level. An actual discriminator cannot be introduced between the counters and the mixer because of the low speed of response of such a device. This limitation has been overcome in an interesting way by Bell and Petch (41) and their arrangement is shown in Fig. 36. Each counter is connected through pulse shapers directly to the coincidence circuit C_1, but also to the 'slow' amplifiers A_1 and A_2. These have a restricted band width, and after passing through the discriminators D_1 and D_2, their output pulses and those of the amplifier A_3 are put into triple coincidence in

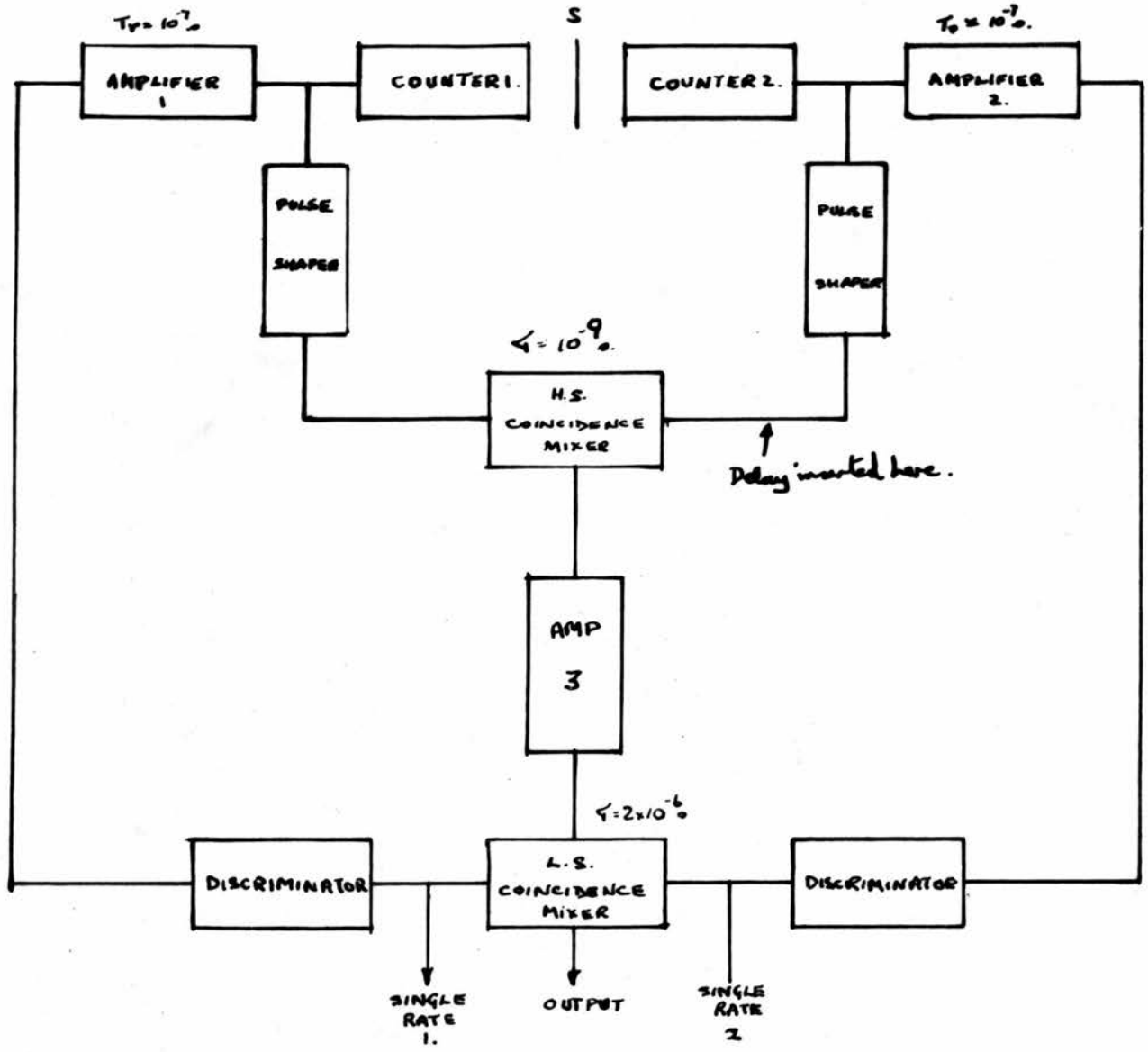

Figure 36. Block diagram of the coincidence counting arrangement of Bell and Petch.

the circuit C_2. Thus only those coincidences are recorded which are due to pulses large enough to pass through discriminators D_1 and D_2 respectively. This scheme has two advantages. Firstly, it allows selected radiations only to be put into coincidence, which simplifies the interpretation of the results of delayed coincidence experiments. It is especially helpful if one or both of the discriminators be replaced by 'kick-sorters', which pass only pulses whose amplitudes lie between two limits which may be varied. Also the single counting rates may be recorded without difficulty as shown in Fig. 36, as the number of recorded coincidences is determined by the discriminator settings and not by the mixer sensitivity. In the event of multipliers with sufficient gain being available, the amplifiers A_1 and A_2 are not required.

A method which can be used, if the problem to be investigated does not require the complication of two coincidence circuits as described above, is to count the single rates by connecting each counter in turn to both inputs of the fast coincidence circuit. The correct single counting rate is the number of pulses occurring per minute which if, by chance, coincident with a pulse in the other channel, could operate the coincidence recorder. Let us suppose that a pulse in one channel with an amplitude less than V volts, will not operate the recorder even when coincident with a

pulse of the largest amplitude which occurs in the other channel. Then we require to count all pulses with amplitudes greater than V, which we may do by connecting the same counter to both inputs of the mixer circuit. The distribution in size of the pulses so obtained will be the same as those from the counter direct, but cut off at a lower limit of amplitude.

The resolving time of a coincidence circuit may be measured by using the two source method. It may also be measured by connecting one input to a counter directly, and the other to the same counter by a cable of variable length. As the length of this cable is increased the number of counts recorded decreases, and from a graph of the readings the resolving time may be evaluated (28), using the equation

$$T = \sqrt{\pi}/2\,\delta \qquad (25)$$

where δ = half-width of the curve at 1/e from the peak.

This method of measuring the resolving time is open to the same two objections as the method of counting single rates outlined above. One of these is that the circuit is not working under the same conditions as obtain in practice, since there is then no correlation between the amplitude of the two pulses which together give rise to a coincidence, and the other is that any random delays occurring in the operation of the counters might lead to loss of counts. The second objec-

tion is not valid for the order of resolving time to be used here, and since both methods are found to give closely equal results (27), the first seems not to be valid either.

In the delayed coincidence experiments to be described, the lengths of delay cable were introduced by means of plugs and sockets. These were found not to cause reflections of the pulses. For example, in a particular experiment the counting rate was the same when an 800 cm. length of cable was used, as when four 200 cm. lengths were inserted in series.

Construction and Tests.

The counters were of the type shown in Fig. 23, although used here with the cathode at the high potential and the collector plate earthed through the load resistor. They were mounted as shown in Fig. 26 and the source was placed coaxially between them. High voltage was supplied by two A.E.R.E. type 1033 power packs, in which the D.C. supply was obtained by rectification of the output of a highly stable radio-frequency oscillator. The cathode followers were rigidly attached to the counters by the radial tubes shown in Fig. 23 and were supplied with H.T. and heater current by a power pack stabilised against voltage changes. The counting rates were found to be altered by voltage variations in the cathode follower high-tension supply.

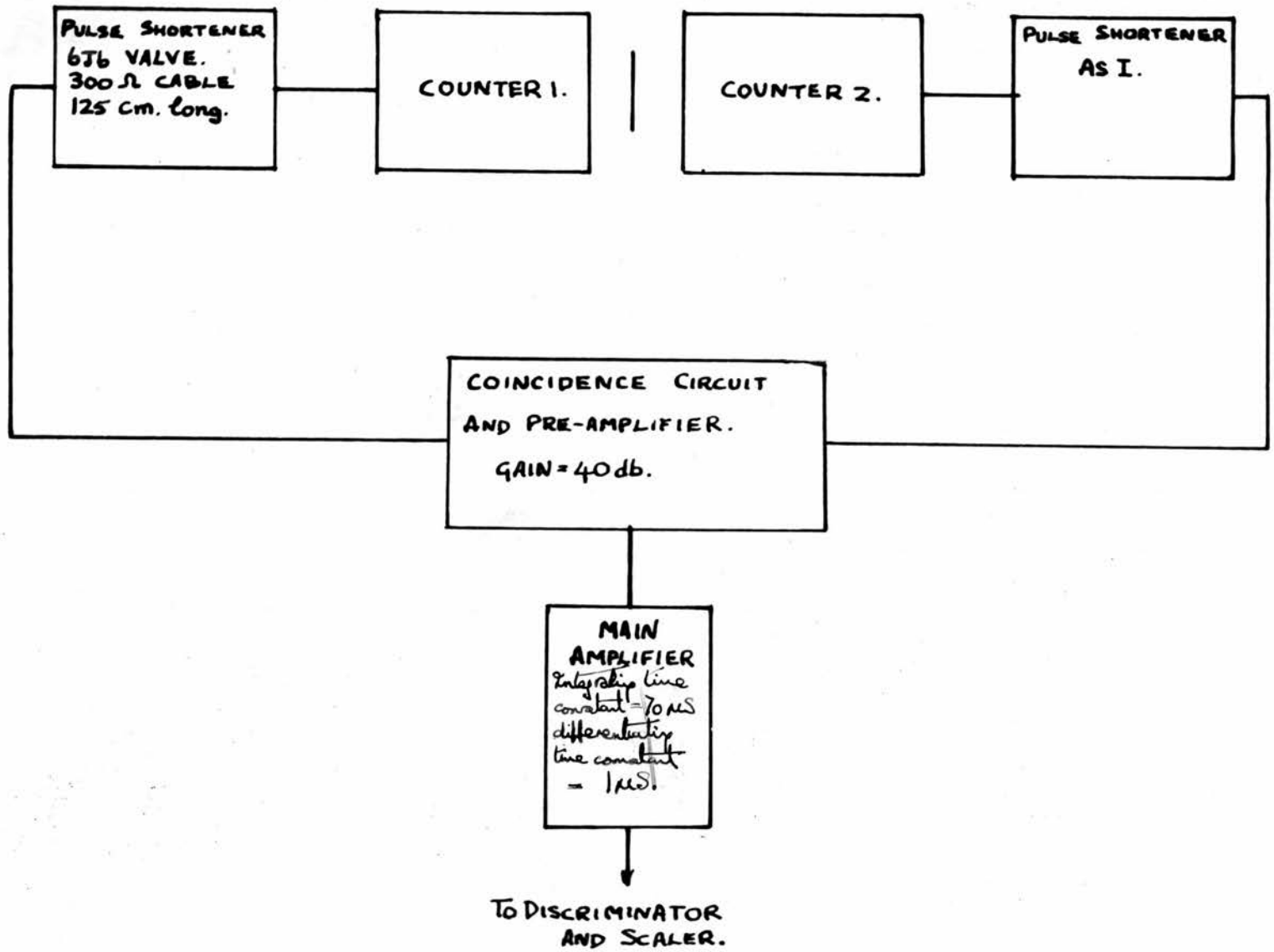

Figure 37. Block diagram of coincidence system.

The coincidence circuit, built in a tinplate screening box, was secured to the case of the head amplifier and placed alongside and equidistant from both counters.

Bay specifies Sylvania type 1N34 germanium diodes for use in his circuit, but as these are not available in this country, G.E.C. type G.E.X. 45/1, a close equivalent, were substituted. It is possible that a slight improvement in performance could be obtained by selecting crystal diodes (28). The output of the head amplifier was taken to the main amplifier, the head and main amplifiers together forming a complete A.E.R.E. type 1008 amplifier. This was very suitable since its coupling circuits could be varied to differentiate or integrate the pulses passing through them, which assisted in obtaining the optimum performance from the coincidence circuit. A block diagram of the complete system forms Fig. 37.

The Adjustment of the Coincidence Circuit.

After building the coincidence circuit it was necessary to adjust the potentiometers R_A and R_B, Fig. 19. R_B is used to equalise the input pulses, and R_A to adjust the time constants R_AC_1 and R_BC_2, until they are equal. The procedure for preliminary adjustment was as follows. Both inputs were fed by separate cables from the same counter and the output of the amplifier examined with a monitor oscillograph. With

one input disconnected the potentiometer R was adjusted to give minimum output pulse size. Coincidence action was then observed by reconnecting the other input, and R_A adjusted to give large output pulses. The average coincidence pulse should be at least 20 db. above the average single pulse in the coincidence channel. This was measured by setting the output discriminator about 10v below coincidence pulse cut-off, and counting for a short period. The amplifier gain was then increased by 20 db., and one input disconnected. The counting rate was now less than in the previous case. The adjustment of the potentiometers was repeated several times, going round in order.

Some experiment was required, to find the optimum values for the differentiation and integration time constants in the amplifier, aiming at the best rejection of large single pulses. This is of particular importance when using scintillation counters, since the large spread in the size of noise pulses and low resolving time may lead to a break-through rate of the same order as the accidental coincidence counting rate.

When this procedure has been followed through, readings of delayed coincidences were taken for Co^{60}, which emits two γ rays in cascade with a negligible time interval between them. The result is shown in Fig. 38, curve A being obtained with one counter, to be referred to as counter 1, connected to input 1 of

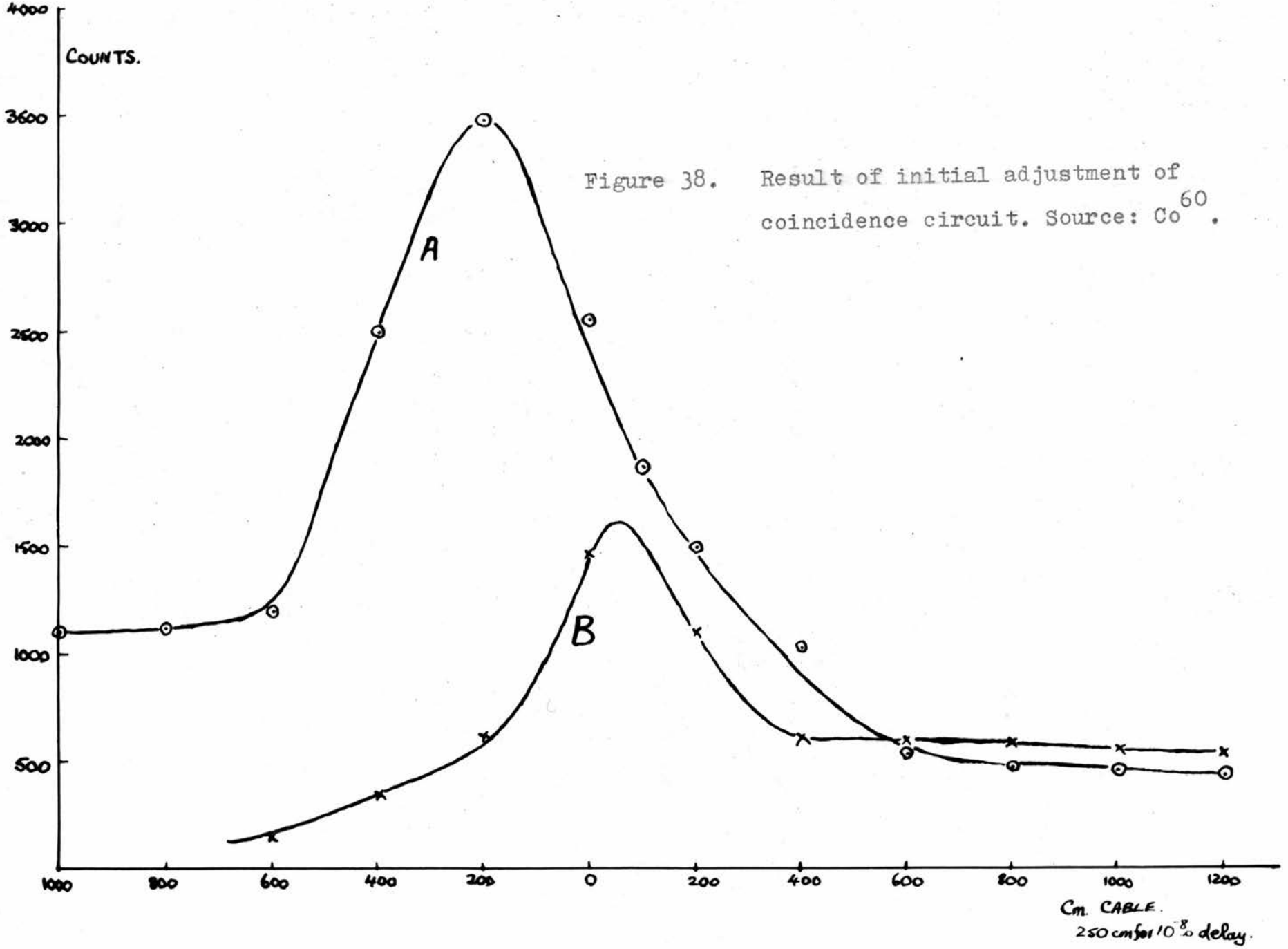

Figure 38. Result of initial adjustment of coincidence circuit. Source: Co^{60}.

the coincidence circuit, and counter 2 to input 2. The curve is not symmetrical. Curve B was then obtained by connecting counter 1 to input 2 and counter 2 to input 1. It is similar to curve A, with all the ordinates decreased in a constant ratio, and transposed left to right. This indicated that the adjustment was still not correct, so it was continued until the curve shown in Fig. 33 was obtained. This is highly symmetrical, and has a half width at half the maximum ordinate of 1.3×10^{-8} seconds. A small displacement of the zero of delay is still apparent, due probably to the counters not having exactly identical characteristics.

Once the circuit has been correctly set up in this way, since wire wound resistors and potentiometers are used, the adjustment is retained for long periods of time, although the potentiometer settings are highly critical. Because of the high temperature coefficient of back-resistance of the diodes and the position of the coincidence circuit on top of the head amplifier, an hour was allowed to elapse between switching-on and taking readings. In Fig. 39 the same points as those in Fig. 33 are plotted as circles, and points obtained after another independent setting-up procedure are shown as triangles. Agreement between these is satisfactory, showing that the correct adjustment is unique.

In Fig. 40 curves are presented which show the

Figure 39. Curves obtained after two separate adjustments of coincidence circuit. Source Co^{60}.

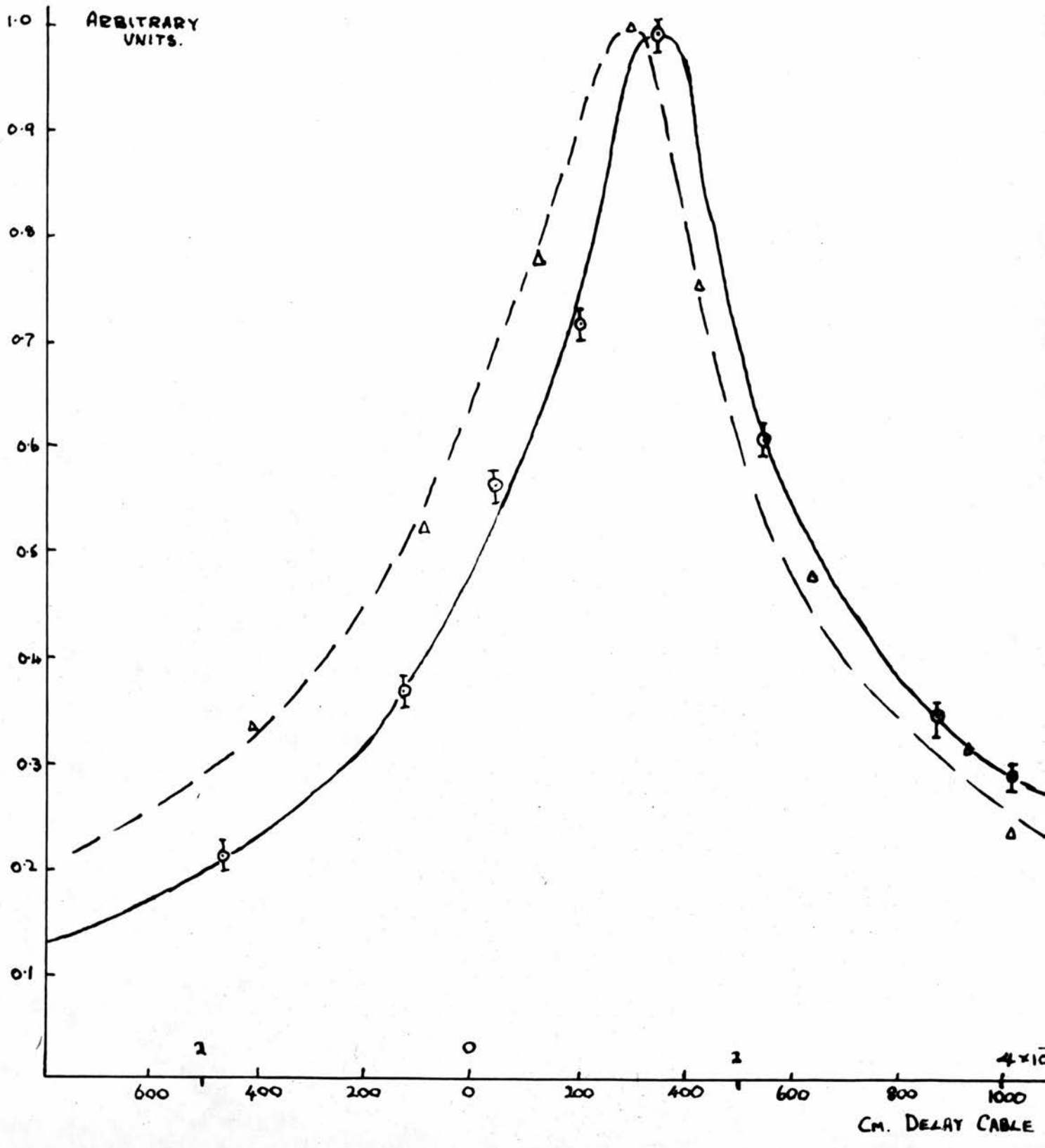

variation of resolving time with the setting of the discriminator which precedes the scaler. Both inputs to the coincidence circuit were fed with pulses from one counter and the abscissa shows the excess of length of the cable joining input one to the counter, over that connecting the same counter to input two. The ordinates represent the number of counts observed. It will be seen that the resolving time decreased as the discriminator bias was raised, the lowest recorded resolving time being 6.8×10^{-9} seconds, calculated using equation (25). This is less than was expected taking into account only the duration of the pulses given by the counters. The effect has also been obtained by Bay (27), who attributed it to the sensitivity of the circuit for pulses of both signs. As will be seen in Fig. 10, pulses formed by a short-circuited line technique have an overswing of small amplitude, which helps the charge on the capacitors to leak away more rapidly.

Table 6.

Discriminator bias	Resolving Time (Equation 24).
5v	1.6×10^{-8} sec.
10v	1.5 "
20v	1.27 "
30v	1.13 "
40v	0.87 "
50v	0.68 "

Figure 40. Results of measurements of resolving time, at several discriminator bias settings, by the inserted cable method.

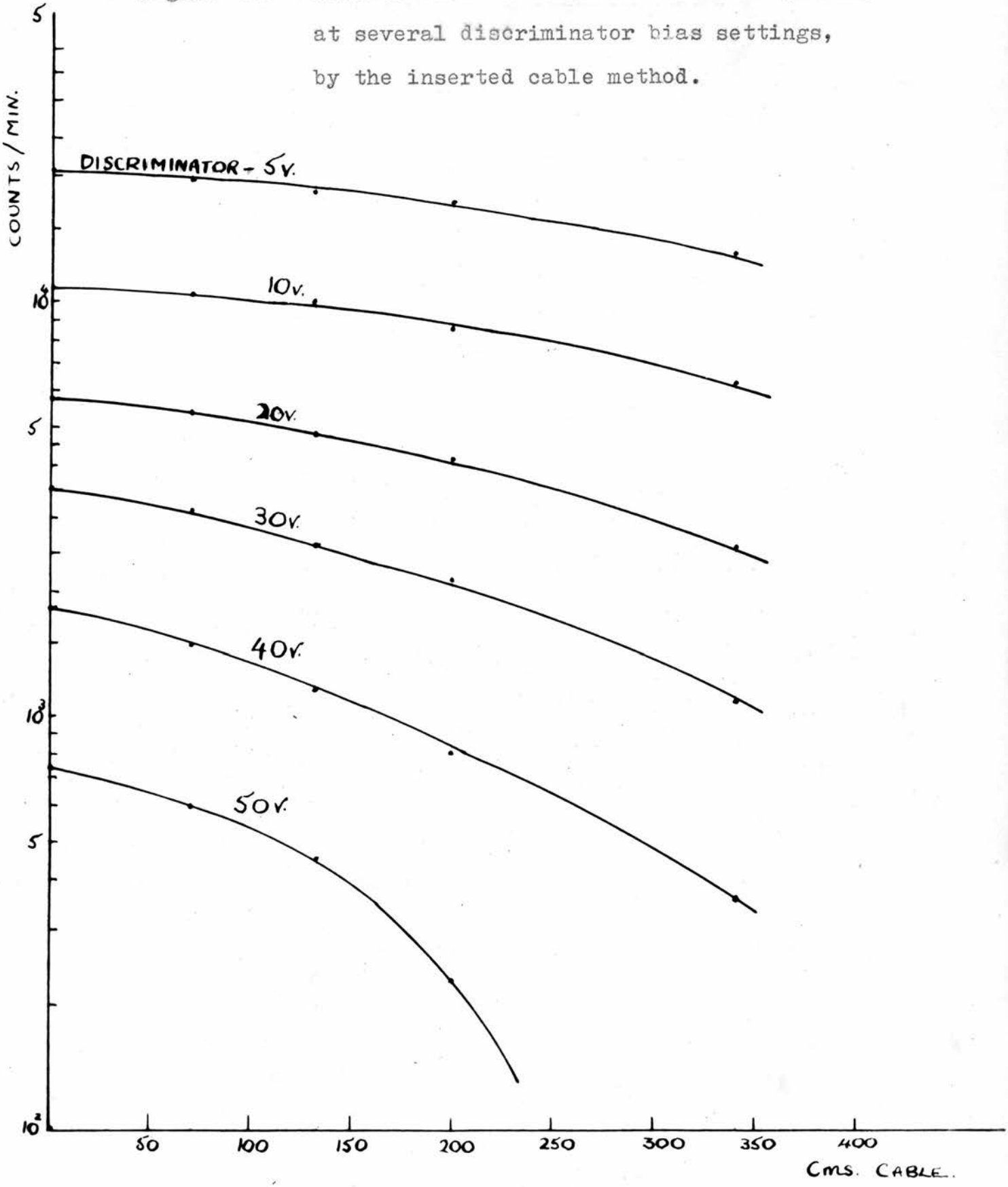

Experiment indicates that the curves shown in Fig. 40 are symmetrical about the origin.

Before using the apparatus for delayed coincidence experiments, the effect of altering the potential applied to the counters was investigated. Using a source of Co^{60}, the curves shown in Fig. 41 were obtained. For a change in the supply voltage of counter 1 from 2.1 to 1.9 kV, the position of the peak of the curve was moved 60 cm., corresponding to a time of 2.38×10^{-9} seconds in the direction corresponding to an increase in transit time in counter 1. If the expected change is calculated, assuming that the electrons start from rest at each dynode, and that their path between dynodes is 1 cm. long, 1.8×10^{-9} seconds is obtained. Since the details of the paths are unknown, this is reasonable agreement. Bell and Petch (41) carrying out similar experiments, obtain a result of the same order of magnitude. As an additional test of the operation of the coincidence apparatus, and, more especially, to check the correction for attenuation of pulses in the delay cable, measurements of delayed coincidences were taken for the active deposit of thorium.

When cable was inserted between a counter and the coincidence circuit, the amplitude of the spectrum of pulses from the counter was reduced by a constant

Figure 41. Showing the shift of the prompt disintegration delay curve with change of counter potential. Source: Co^{60}.

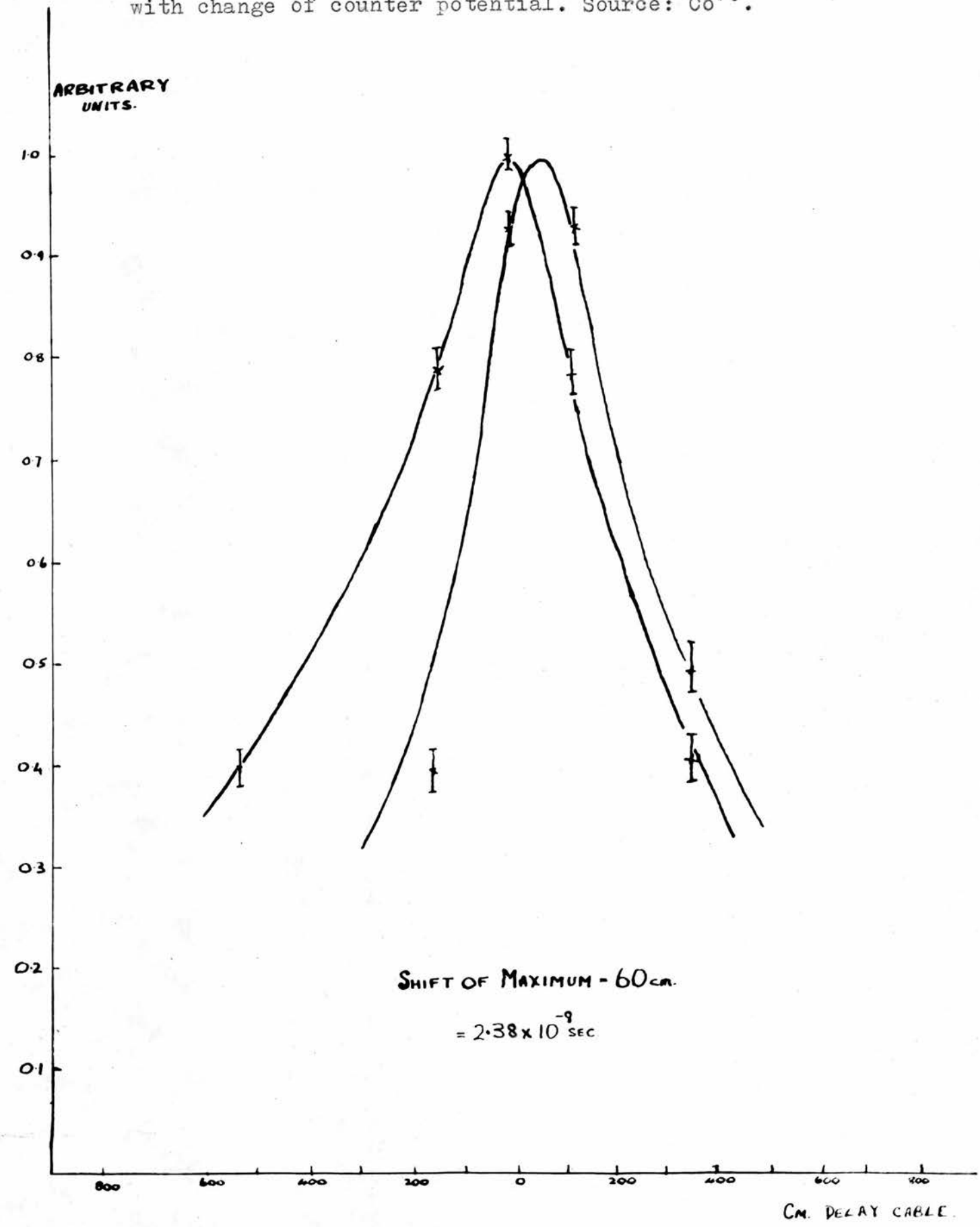

factor for each cm. of line introduced. Thus fewer of the coincidences which occurred were between two pulses which together delivered enough charge to the circuit to give an output pulse which overcame the bias of the output discriminator. In consequence, the number of coincidences observed, when using two separate sources, one actuating each counter, was less when delay was introduced than when the counters were connected to the mixer directly, although all were accidental. The attenuation correction was obtained in this way. Two β ray sources were set up before the counters, shielded one from another, so that all the coincidences counted were accidental. With no cable in circuit, the observed coincidence rate was given by the equation

$$N_c = 2N_1N_2T.$$

When an equal length of cable was inserted in each channel this became

$$N_c' = 2f_1N_1f_2N_2T$$

where f_1 and f_2 are fractions representing the loss of coincidences due to attenuation in the two cables. Since the cables in each channel were of equal length and the average height of pulses from the two counters was initially adjusted to be equal, we may assume $f_1 = f_2$

$$\therefore f = \sqrt{N_c'/N_c}$$

the attenuation factor for the inserted length. It

was found in this way that when a 340 cm. length of cable was used in each channel, $f = 0.925 \pm 0.032$. The manufacturers of the cable give the attenuation as 1 db. per 100 ft., when carrying sinusoidal currents at a frequency of 50 Mcs. This represents a ratio of 0.891 for 3050 cm. and a check was considered necessary in view of the large difference, although the pulses used here are of triangular shape, and thus have component frequencies much higher than 50 Mcs, at which the attenuation is presumably much greater. No figures were available of the variation of attenuation with frequency for frequencies above 50 Mcs.

Fig. 42 shows a plot of readings obtained in an experiment with the active deposit of thorium. The ordinates are the number of counts, and the abscissae are the lengths of delay cable in cm., inserted in the β channel. From 1300 cm. onwards, the fall-off is approximately linear, and the two straight lines drawn represent good agreement with the points. The triangle points represent the readings obtained in the experiment, uncorrected for attenuation, and the circles are the same points when corrected. The full line is calculated using the decay constant of ThC', and fits the corrected experimental points well. Thus the value for the attenuation constant deduced above is correct within the experimental error. Due to the straight portion of the curve representing only 8×10^{-8} seconds

Figure 42. Results of ThC' experiments with higher-resolution circuit. Circles are corrected points, triangles uncorrected.

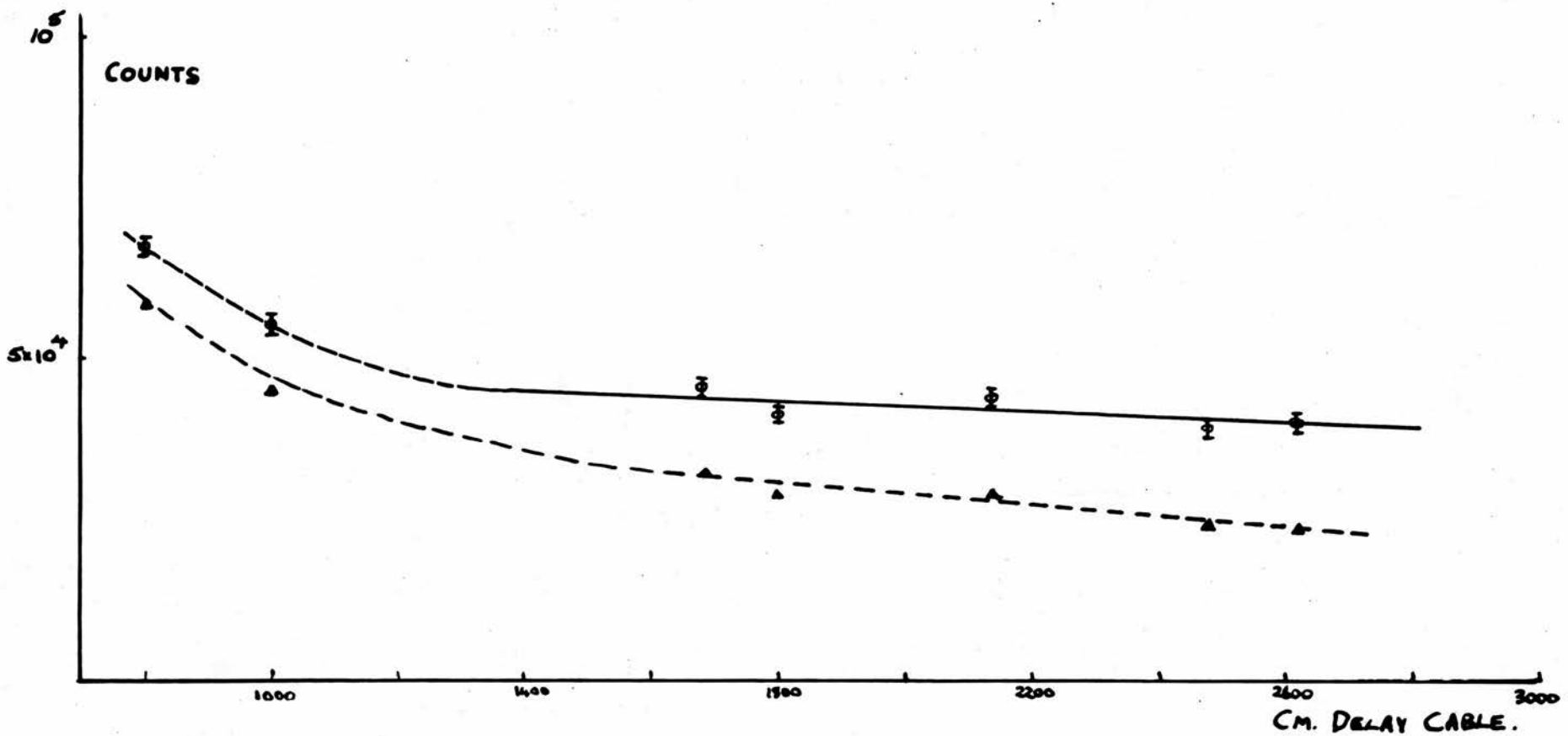

delay, a large number of counts were necessary to obtain the indicated degree of accuracy, and the exponential decay of ThC' could be approximated by a straight line. It is possible that the value of f may depend upon the distribution in size of the pulses from the multipliers, so that its value is not regarded as a constant of the apparatus. However in the following work we shall be concerned only with sources of the active deposit of thorium and Co^{60}, so that it may be considered to be constant for our purposes. If photomultipliers with greater gain had been available, the pulses could have been arranged to drive the cathode followers beyond cut-off, so that they would act as limiters as described by de Benedetti and Richings (28). This would be advantageous because the pulses from them would then be of a constant size and shape, the correction for attenuation would be smaller, and constant for each experimental arrangement. The rest of the decay curve, joining on to the left of that of Fig. 42, is shown in Fig 43. (Curve 1, full line). The curves 2 and 3 indicate how its shape may be interpreted.

They are, respectively, a curve of delayed coincidences for a prompt transition, P(td) for Co^{60}, taken under the same conditions of photomultiplier voltage and discriminator bias as curve 1, and a theoretical curve calculated from the formula for delayed coincidence curves given by Bunyan, Lundby and Walker (37).

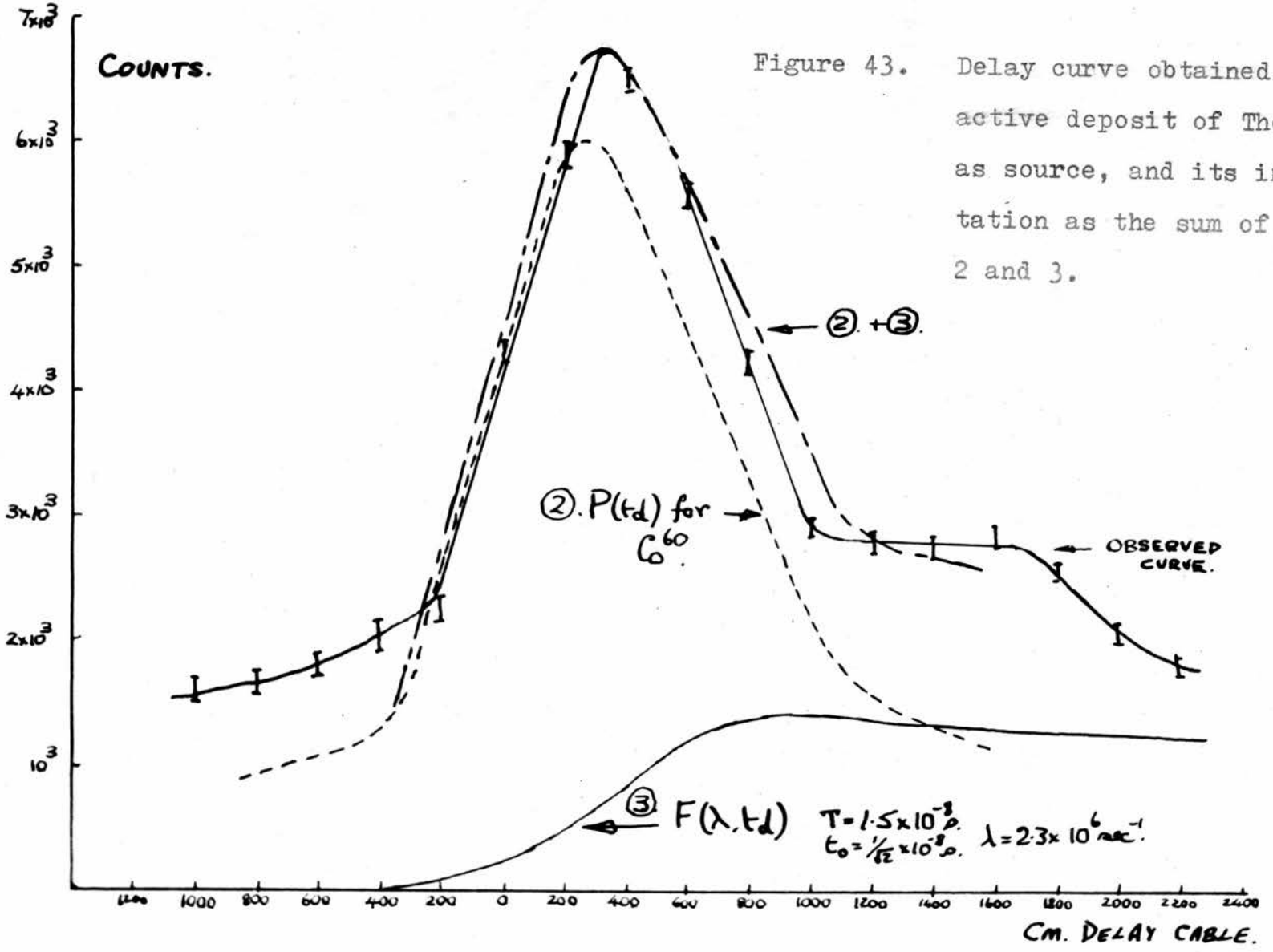

Figure 43. Delay curve obtained with active deposit of Thorium as source, and its interpretation as the sum of curves 2 and 3.

Their formula is free from any approximations, and they assume only that the pulses from the counters A and B suffer time lags distributed about their mean value $\bar{t}_A$ and $\bar{t}_B$ according to a Gaussian law, with a standard deviation $t_0/\sqrt{2}$. Their result is

$$F(\lambda,t_d) = \tfrac{1}{2}\left\{\phi\left(\frac{t_d+T+\Delta}{t_0\sqrt{2}}\right)+\phi\left(\frac{t_d-T+\Delta}{t_0\sqrt{2}}\right)\right\}$$
$$+\tfrac{1}{2}\left[\left\{1+\phi\left(\frac{t_d-T+\Delta}{t_0\sqrt{2}}-\frac{\lambda t_0}{\sqrt{2}}\right)\right\}e^{\lambda T}\right.$$
$$\left.-\left\{1+\phi\left(\frac{t_d+T+\Delta}{t_0\sqrt{2}}-\frac{\lambda t_0}{\sqrt{2}}\right)\right\}e^{-\lambda T}\right]e^{-\lambda t_d-\Delta\lambda+\frac{\lambda^2 t_0^2}{\sqrt{2}}}$$

$$\phi(x) = \frac{2}{\sqrt{\pi}}\int_0^x e^{-z^2}dz.$$

The first term is P(td) and $\Delta = \bar{t}_A - \bar{t}_B$.

In order to apply this formula to our case we put $\Delta = 1.2 \times 10^{-8}$ sec., corresponding to the shift of the zero of delay by 300 cm. of cable noted above, and $T = 1.5 \times 10^{-8}$ sec., the resolving time employed. Because the pulses from the counters have a wide distribution in size, they grow to an amplitude sufficient to operate the coincidence circuit after a time which is short for a large pulse and longer for a small one. This time will always be less than the rise time of the pulse and in calculating curve 3, Fig. 43, t_0 was put equal to $1/\sqrt{2} \times 10^{-8}$ sec., about half the pulse rise time. The ordinate scales of curves 2 and 3 were adjusted so that the sum of their ordinates at the zero of delay (300 cm. of cable $= 1.2 \times 10^{-8}$ sec.) in the β particle counter channel, fitted that of curve 1.

The fit between curve 1 and the sum of curves 2 and 3 is then within the experimental error.

Adopting this interpretation we must assume that, besides the $\alpha-\beta$ coincidences due to the decay of ThC', there are present in the radiations from the source at least two, whose mean separation in time is very small. Such radiations have been reported by Feather, Kyles and Pringle, (43). They found that 95% of the coincidences which they detected from a source of thorium active deposit in a double β spectrometer, other than those corresponding to the decay of ThC', had a half-life of less than 10^{-7} seconds. These were β-photoelectron coincidences between the 330 keV β particles from ThB and the photoelectrons of 148 keV energy due to internal conversion of the succeeding 238 keV γ ray (F line). In these experiments with the active deposit of thorium, the two counters were arranged coaxially with the source between them. This was in the form of a foil carrying the deposit, with the active side facing one counter, to be called the α counter. The thickness of this foil was 3 mg./sq. cm. and the foils which excluded the light from the counters were 3 mg./sq. cm. and 30 mg./sq. cm. for the α and β counters respectively. Thus a β particle had to penetrate approximately 33 mg./sq. cm. of aluminium before reaching the crystal, which was a layer of anthracene powder 2 mm. thick, held on to the end

face of the photomultiplier envelope, directly opposite to the photocathode, by Canada balsam. Since the effective photocathode diameter was reduced to 4 cm. by the ring connection to the cathode, and the source was separated from it by approximately 1.5 cm., the fractional solid angle of the counters was about 0.15.

We therefore see that neither the 148 keV photoelectrons nor the β particles of 330 keV maximum energy, emitted by ThB, could penetrate into the β counter. Coincidences observed here due to the F line must have been between 238 keV γ rays counted in the β counter and 330 keV β particles counted in the α counter, into which would penetrate some 75 $\pm$ 5% of those striking the foil. There are 0.6 238 keV γ rays and 0.9 330 keV β particles per disintegration of ThB.

The remainder of the coincidences of very short life-time reported by Feather, Kyles and Pringle, were between the β particles of 1.79 MeV maximum energy of ThC'' and a γ ray, to which the sensitivity of their counters was low. According to the energy level diagram for ThC'' given in the collection of nuclear data by the National Bureau of Standards (44), the 2.62 MeV γ ray, emitted in every disintegration, is in cascade with a 582 keV γ ray. This latter γ ray is only internally converted to the extent of 1.5%, but the efficiency of a scintillation counter, especially one using the present type of photomultiplier, is high

Figure 44. Curve 1: delay curve with α counter absorbing foil 10.5 mg./sq. cm. thickness.
Curve 2: delay curve with α counter absorbing foil 33 mg./sq. cm. thickness.

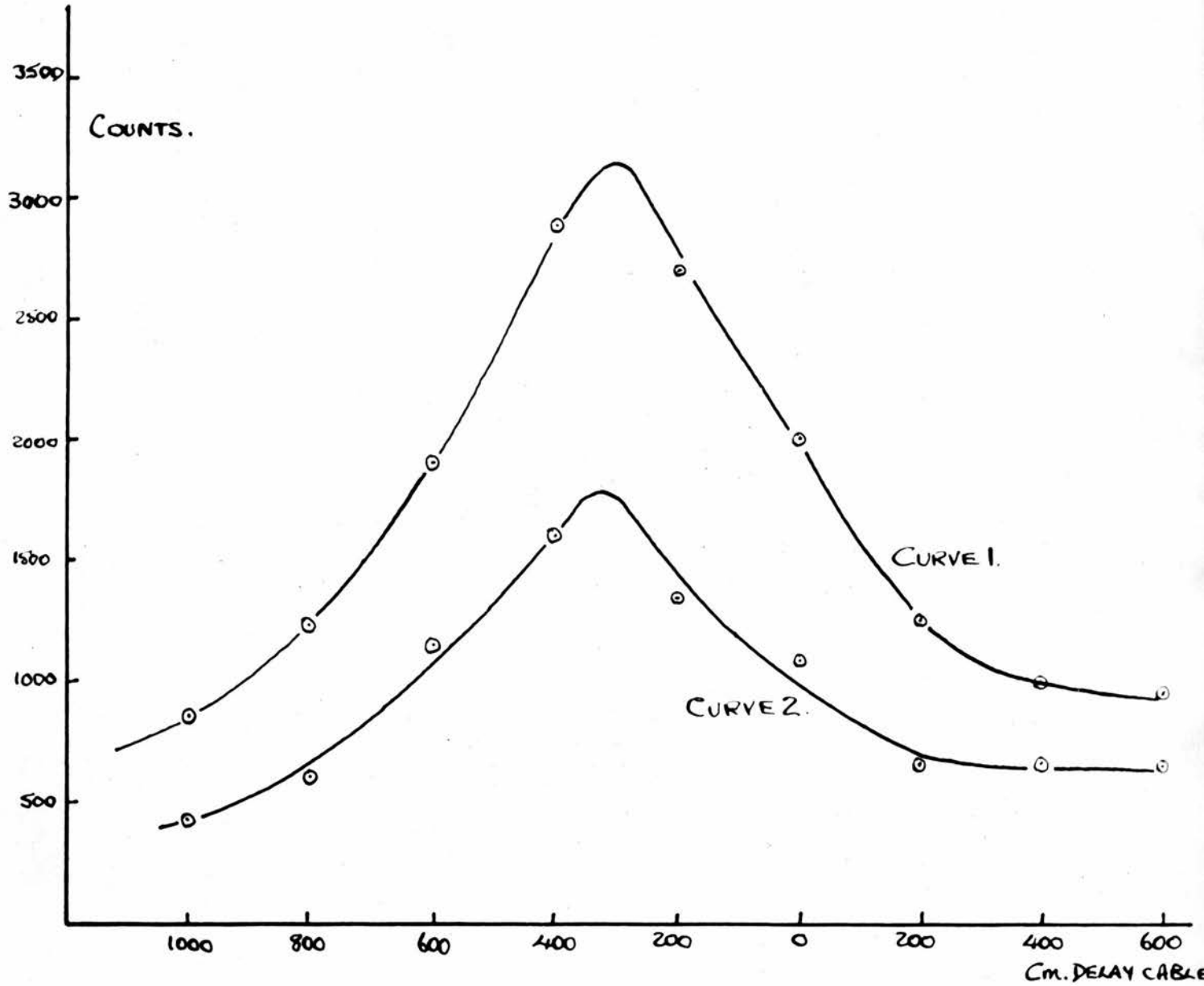

enough to low energy γ radiation, for a considerable proportion of the observed instantaneous coincidences to be assigned to this cause.

Thus the prompt coincidences observed, other than those due to the disintegration of ThB, were due to 1.79 MeV β particles in coincidence with 582 keV γ rays. An experiment will be described which allowed the relative contributions of the two causes to be estimated.

In Fig. 44, curve 1 is a delayed coincidence curve obtained under the same operating conditions, and with the same source as that of Fig. 43, except that the thickness of the foil before the α counter had been increased from 3 mg./sq. cm. to 10.5 mg./sq. cm. The spectrum of the β-photoelectron coincidences from ThB, obtained by Feather, Kyles and Pringle and reproduced from their paper in Fig. 45, yields a straight-line Fermi plot. Therefore, using the method given by Bleuler and Zünti (45), an absorption curve may be deduced for the β particles of 330 keV maximum energy. This showed that replacing the 3 mg./sq. cm. foil before the α counter by one of 10.5 mg./sq. cm., reduced the proportion of such incident particles penetrating into the counter from 75 $\pm$ 5% to 46 $\pm$ 5%, leaving the other radiations largely unaffected. Curve 2 shows similar experimental results obtained when the α counter foil had been increased in thickness to 33 mg./

Figure 45. Coincidence spectrum reproduced from Feather, Kyles and Pringle's paper.

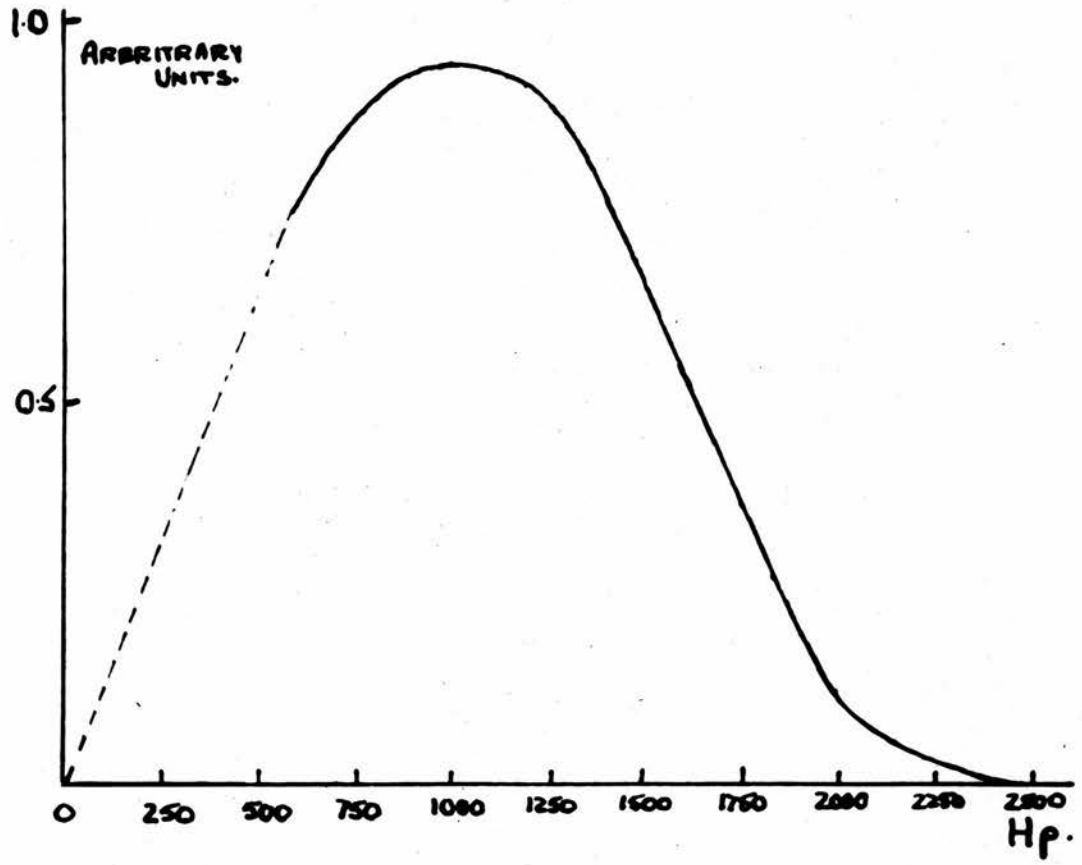

sq. cm., thus cutting off the 330 keV β particles completely. The areas under the curves 1 and 2 are in the ratio 2:1 so that, of the original immediate coincidences illustrated in Fig. 43, a fraction $\frac{1}{1+75/46} = 0.38$ were due to the ThC'' transition. This leaves the long-range α particles out of account, but the single counting rate in the β counter showed that less than 1 in 10^3 of the coincidences making up curve 1, Fig. 43, could be ascribed to them.

The ratio of the areas of the calculated curve and the 'prompt' delay curve in Fig. 43, which together add up to the observed curve, is 1.85:1. Thus one immediate coincidence was detected for every 1.85 α-β coincidences counted. It is important, for the interpretation of experiments to be described later, to note that one ThC'' immediate coincidence was counted for every 1.85/0.36 = 4.9 ThC' α-β coincidences.

The energy level diagrams (44) of ThB and ThC'' are reproduced below.

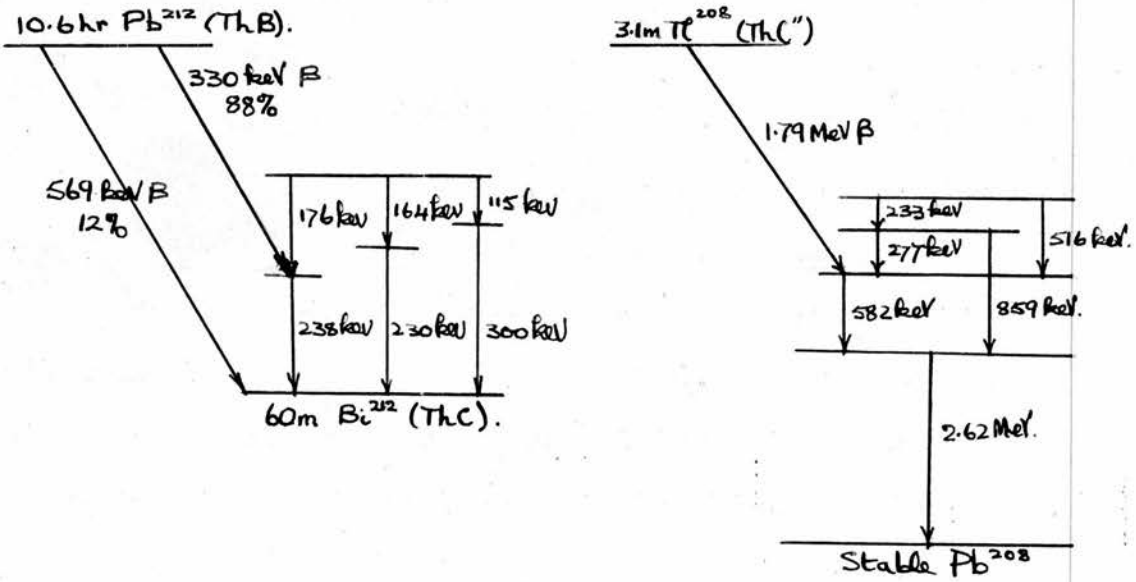

Chapter VI.

AN ATTEMPT TO PUT AN UPPER LIMIT TO THE HALF-LIFE OF ONE OF THE LONG-RANGE α PARTICLE GROUPS EMITTED BY ThC'.

The ThC' nucleus may be formed in one of three excited states and these can decay to Pb^{208} by the emission of α particles directly, in competition with the emission of a γ ray leading to the ground state of ThC' followed by ordinary α emission (44). Besides the α particles of 8.78 MeV energy, ThC' emits three other groups of α particles, with energies of 9.48, 9.6 and 10.58 MeV. The intensities of the first and third groups are 34 and 200 per 10^6 α particles respectively, and that of the second is very small.

We can calculate the half-life of the long-range α transition of energy 10.58 MeV, using the Geiger-Nuttall law in the form given by Fermi, (46).

$$1/T = 10^{-44.2}\, R^{57.5}$$

Here R is the α particle range and T the mean life of the transition. The result is approximately 10^{-17} sec.

Fermi also gives (47) the following equation for the mean life-time of a nucleus having charge Z and emitting an α particle of energy E,

$$1/T = 10^{21} \exp.\left\{-\left(\frac{8\mu Z 3e^2}{h^2} b\right)^{1/2}\left[\cos\sqrt{R/b} - \sqrt{R/b - R^2/b^2}\right]\right\}$$

(26),

where R is the nuclear radius, and z the α particle charge. μ is the reduced mass of the particle and nucleus. This formula gives approximate values for the mean life, and the value of T is strongly dependent upon the value of R. Therefore, in order to give a more reliable result, R has been calculated using equation (26) and substituting the known life time and energy of the ordinary α particles. In this way a value for R of 9.4×10^{-13} cm. was obtained, while the relation

$$R = 1.5 \times 10^{-13} A^{1/3},$$

where A is the nuclear mass number, gives $R = 8.95 \times 10^{-13}$ cm. When the former value was used in equation (26) to calculate the half-life of the transition leading to the α particles of 10.58 MeV energy, the result was

$$T_{\frac{1}{2}} = 8 \times 10^{-12} \text{ sec.}$$

A coincidence counting system with a resolving time of 5×10^{-11} sec. would be necessary before such a half-life could be detected, so that it is evident that the apparatus described above could do no more than show that the life-time is less than about 5×10^{-9} seconds.

From the results of the experiments described in the previous chapter, it was clear that to enable the coincidences due to long range α particles to be studied the sensitivity of the system to other coincidences must be considerably reduced. If they could

be entirely eliminated, a counting rate of 10^6 per minute in the β counter, which was the maximum permissible, would lead to a coincidence counting rate of the order of $10^6 \times 200/10^6 \times 0.15 = 30$ per minute, a quite reasonable figure. This, of course, assumes that all the β particles counted would be associated with an α particle of short or long range and that the intrinsic efficiency of the α counter was 100%. If, however, a high counting rate occurred in the α counter due to any unwanted radiations, then the required coincidences would be detected with difficulty due to the accidental coincidence rate. For example, with the resolving time used, 30 accidental coincidences per minute would occur with a β counting rate of 10^6 per minute and an α counting rate of 6×10^4 per minute.

Experimental results.

In these experiments, the counter and source arrangement were as described in the accounts of previous work, and the long-range α particles were separated from those of normal range by means of aluminium foil. A long-range α particle reaching the anthracene layer at the photocathode thus had an energy of only 1.5 MeV. The table below gives the relative pulse heights to be expected for various relevant radiations with an anthracene scintillator, taken from the curves given by Taylor et al., (48).

Table 7.

Electrons	Pulse heights - arbitrary units.
150 keV	10
240 keV	13.5
330 keV	20
780 keV	48
1.79 MeV	105
α particles	
1.5 MeV	7
4 MeV	20

From these figures we can see that many of the low energy electrons and gamma rays which could penetrate the 10.5 mg./sq. cm. foil before the α counter, gave rise to pulses as large as those due to the required α particles. It was found to be possible to suppress the immediate coincidences due to ThB, by reducing the counter potential until the 238 keV gamma rays were no longer counted. However, because of the immediate coincidences from ThC'' which were discussed above, and the relatively large number of chance coincidences due to the high counting rate occurring in the α counter, β particle-long range α particle coincidences still contributed only 1% to the total.

Two methods were tried to decrease the efficiency of the α counter to low-energy β and gamma radiation.

It is well known (49) that some inorganic phosphors transform into light the energy dissipated in them by α particles more efficiently than anthracene, thus giving larger pulses in a scintillation counter. However their decay-times are longer so that they are not generally suitable for fast counting. It was thought possible that shortening the pulses by the technique described above might give short pulses while still retaining the discrimination in favour of α particles. In Fig. 46 are shown integral bias curves plotted from the results of experiments with three inorganic phosphors and anthracene, using both an α particle and a β particle source.

These sources were mounted upon brass plugs which screwed into hole D, Fig. 23 , so that they were positioned 1 cm. in front of the centre of the photocathode of the photomultiplier. The α particle source was of Polonium, energy 5.3 MeV, and the β particle source was of Thallium, the isotope of mass 204 emitting β particles of maximum energy 0.78 MeV. The area of the sources was 15 sq. mm., and the β source was carried on a foil of thickness 3 mg./sq. cm. mounted across a hole $\frac{3}{4}$ in. diameter and $\frac{1}{8}$ in. deep. The phosphors were deposited on the flat glass end of the photomultiplier envelope, by settling them out of a suspension of fine powder in distilled water, to form a deposit of thickness approximately equal to the range

Figure 46. Bias curves for various scintillating materials,

Sources; α - Polonium

β - Thallium.

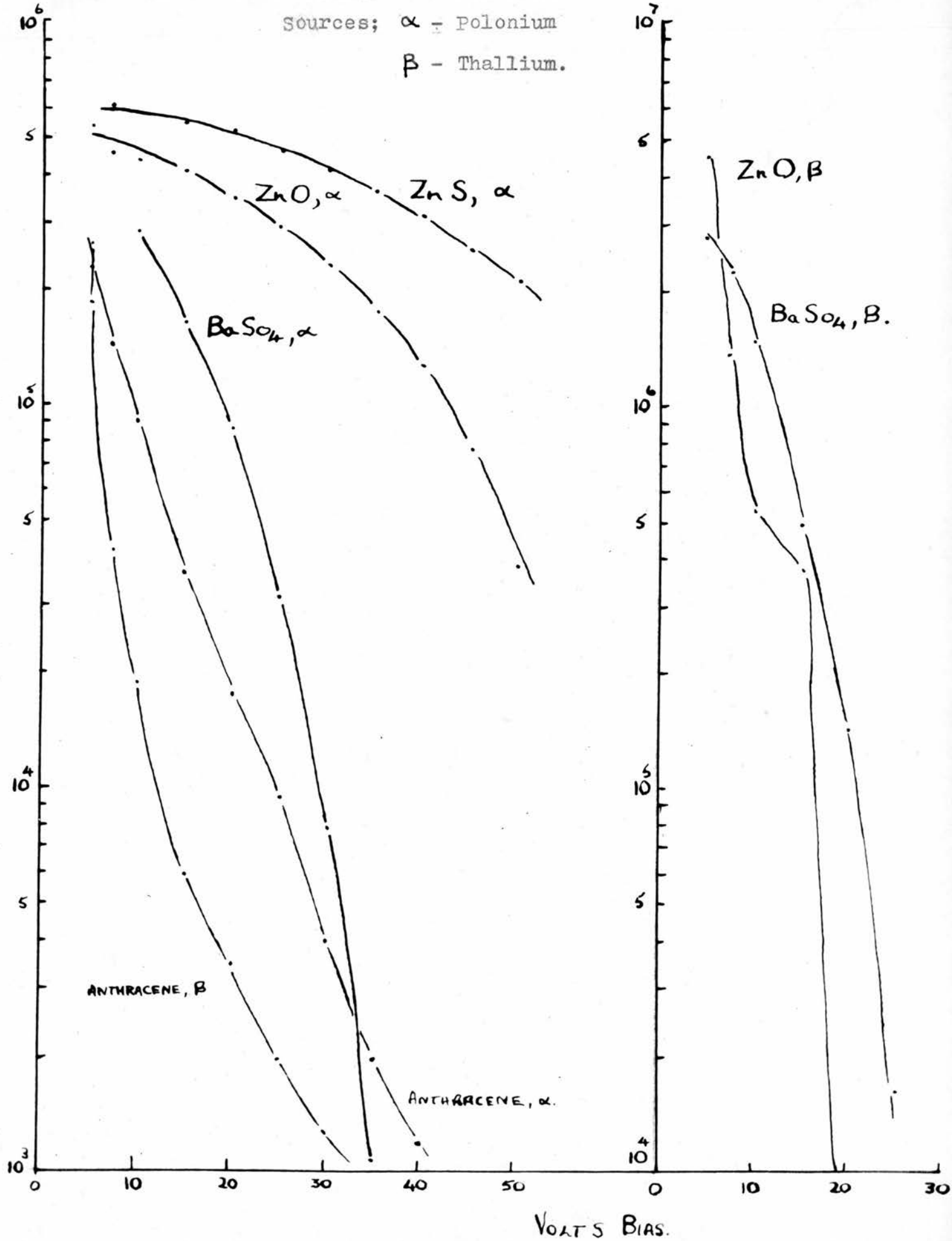

in the substance of an α particle of energy 4 MeV. This was the energy with which the 5.3 MeV α particles struck the scintillating substance. From these curves it is clear that such a phosphor would allow the counting of 4 MeV α particles alone in the presence of β particles of 780 keV maximum energy, and, therefore, 1.5 MeV α particles alone in the presence of β particles of 330 keV maximum energy, by lowering the counter potential until the latter were not counted.

However, tests showed that the long decay time for light emission of, for example, ZnS-Ag, which is 10μS, prevented the correct operation of the shortening circuit. With such long input pulses of slow rise, the amplitude of the overswing of the shortened pulse becomes as large as that of the shortened pulse itself. Since the coincidence circuit is sensitive to pulses of both sign, the effective pulse is not shortened at all by the counter output stage, and the resolving time is no longer small.

The second attempt to reduce the counting rate of the α counter and the sensitivity to coincidences of short life-time from ThC'', was by reducing the thickness of the anthracene deposit. A very thin layer was put on to the tube by evaporating a benzene solution drop by drop. This produced a uniform layer of very small crystals less than 1 mm. in thickness.

When this had been done and the 'soft' immediate

coincidences from ThB eliminated by adjustment of the counter potential, experiments still revealed so many coincidence counts that the long-range α coincidence rate, deduced from the counting rate of the β counter, was less than the probable error in the total coincidence rate. In order to investigate why the sensitivity of the α counter to unwanted radiations could not be reduced by reducing the phosphor thickness, the counting rate of this counter was measured with and without the thin anthracene layer. Using a source of thorium active deposit, giving a counting rate in the α counter of 3.41×10^5 counts per minute; under the conditions of the experiment, (with 10.5 mg./sq. cm. foil before it), removal of the anthracene reduced the counting rate to 3.1×10^5 per minute. This can only be explained by assuming that the photomultipliers in use have an appreciable efficiency for counting low energy γ radiation without a phosphor. The effect is less surprising when we consider that the dynodes are 5 cm. in diameter. Subsidiary experiments, with a source of Co^{60} indicate that the intrinsic efficiency of the photomultipliers for γ rays of 1.2 MeV energy is approximately 5×10^{-4}.

Thus, in the experiments, most of the immediate coincidences recorded were between 1.79 MeV β particles, counted principally in the β counter, and γ radiation counted in the α counter. The sensitivity of this counter to 2.62 MeV was much less than to 0.58 MeV γ radiation. A 2 mm layer of anthracene was then

reapplied to the α counter, and with an aluminium foil of thickness 33 mg./sq. cm. in front of each counter, a long series of observations was taken. The delayed coincidence curve obtained was indistinguishable from that shown in Fig. 33, each point being determined with a probable error of less than 2%. The readings are shown in Table 8.

Table 8.

cm. delay cable	400	200	0	200	400	600	800	1000
counts	4593	4578	8442	14918	15178	10403	7028	5398

By dividing the curves into strips and integrating numerically, the readings shown above and those represented by Fig. 33 were compared. Equation (13) was used to show that the half-life of the present transition was

$$= 7 \pm 8 \times 10^{-9} \text{ sec.},$$

assuming that the γ rays from Co^{60} follow one another with negligible delay. Thus the half-life of the transition, 1.79 MeV β to 582 keV γ ray, in ThC'' is less than 7×10^{-9} sec.

Conclusion.

Although the apparatus was capable of putting an upper limit of the order of 5×10^{-9} sec. to the half-life of a transition, the sensitivity of the photo-

multipliers to low energy γ radiation, and possibly also to low energy β particles, prevented the procedure being applied to the long range α particles of ThC'. Evidence has been advanced to show that the 582 keV γ ray of ThC'' follows the β particles of maximum energy 1.79 MeV with a half-life of less than 7×10^{-9} sec. It is interesting to consider how it might be possible to carry out successfully the experiment which forms the subject of this chapter. A counter is required which produces pulses with a rapid rate of rise, although it is unnecessary that these should be very short in duration, since the long-range α particle counting rate will be low. It should have a high efficiency for 1.5 MeV α particles but substantially zero efficiency for low energy β particles and gamma radiation.

In his paper on the properties of spark counters of the Rosenblum type, Connor (50) states that the rise time of the voltage pulse delivered by such a counter is less than 10^{-7} sec. The amplitude of the pulse is about 3 kV, and it thus reaches 3v in a time less than 10^{-9} sec. It is possible that such a counter, which has a high efficiency for counting α particles of low energy and a very low efficiency for counting β and γ rays, could operate a high resolution coincidence circuit in conjunction with a scintillation counter. However, the difficulty of shielding the other parts

of the system to prevent induced pulses would be very great.

Wilkinson (51) states that proportional counters have been used in coincidence systems with resolving times as low as 4×10^{-8} seconds. The pulse delivered by such a counter rises rapidly, corresponding to the collection of the electrons by the anode, and in order to retain this rise, the high-gain amplifiers required must have a large bandwidth. The pulse could then be shaped by a short-circuited line technique, before reaching the coincidence mixer. It would probably be advantageous still, to separate the long-range from the normal α particles by foils, and so reduce the ambient level of ionization in the counter. It is unlikely that even as small a resolving time as has been achieved above, could be reached with this arrangement.

Acknowledgment.

I should like to thank Professor Feather for his interest in my work; and Mr. Dainty, also of the Department of Natural Philosophy of the University of Edinburgh, for suggesting the radium problem and for many helpful discussions. I must also thank Dr. Garlick of the Physics Department of the University of Birmingham for giving me samples of the three inorganic phosphors referred to in Chapter VI.

Appendix.

THE EFFICIENCY OF A SCINTILLATION COUNTER AS A γ RAY DETECTOR.

The sensitive volume of a scintillation counter is occupied by a solid or liquid substance, rather than a gas, and it is often of the same order of size as that of a Geiger counter. Thus, the efficiency of a scintillation counter for γ radiation is much higher than that of a Geiger counter. An experiment is described below to determine the efficiency of one of the counters referred to in the text, using a medium-sized crystal of naphthalene grown from the melt.

It is first of all necessary to calculate the fraction of the incident radiation which is absorbed by the crystal. We suppose a small source at the origin distant x_0 cm. from the first face of a cylindrical crystal, lying with its axis along the x axis, of length ℓ cm. We assume the absorption coefficient of the material at the energy of the incident γ radiation to be μ cm.$^{-1}$, and the cross-sectional area of the crystal to be A sq. cm.

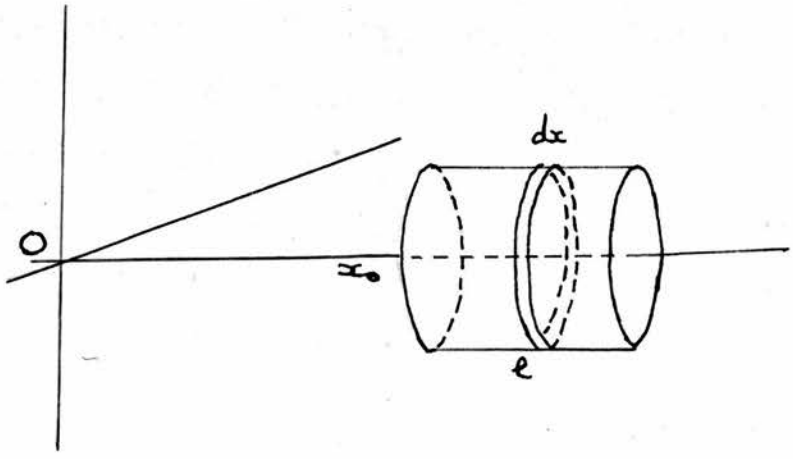

Then considering a slice of thickness dx at x, as shown in the diagram above, we obtain,

$$dI = -\mu dx \, A/4\pi x^2 \, I \, e^{-\mu(x-x_0)}$$

provided that the crystal does not subtend more than 15° at the source. We must evaluate the integral

$$\frac{dI}{I} = \frac{-\mu A e^{\mu x_0}}{4\pi} \int_{x_0}^{x_0+\ell} \frac{e^{-\mu x}}{x^2} \, dx .$$

Now $$\int_a^b \frac{e^{-\mu x}}{x^2} dx = \left[-\frac{1}{x} e^{-\mu x} \right]_a^b - \int_a^b \mu/x \, e^{-\mu x} \, dx .$$

Putting $\mu x = t$ in the second integral we have,

$$\left[\frac{1}{a} e^{-\mu a} - \frac{1}{b} e^{-\mu b} \right] - \mu \int_a^b \frac{e^{-t}}{t} \, dt .$$

$E_i(-\alpha)$, the sine integral $= \int_\alpha^\infty \frac{e^{-t}}{t} \, dt .$

$$\therefore \int_{\mu a}^{\mu b} \frac{e^{-t}}{t} \, dt = E_i(-\mu a) - E_i(-\mu b)$$

so that

$$\frac{dI}{I} = \frac{-\mu A}{4\pi} \left[\frac{1}{x_0} - \frac{1}{x_0+\ell} e^{-\mu \ell} \right]$$

$$- \frac{\mu^2 A}{4\pi} e^{\mu x_0} \left[E_i(-\mu x_0) - E_i(-\mu(x_0+\ell)) \right] \quad (27)$$

The crystal, 1.3 cm. long and 2.2 cm. in diameter, was cemented to the glass envelope opposite the photocathode, of an E.M.I. type VX5045 photomultiplier; and a small source of Co^{60} of strength 10 μC set up on the axis of the cylinder 5.6 cm. from its nearer end. The foil closing the end of the counter was of thickness 10 mg./sq. cm. Substituting the values in the result (27) above we obtain $dI/I = 0.0032$. The value of μ used was obtained from the curve, Fig. 47, calculated for naphthalene and anthracene from the data of Davisson and Evans, (52). The source of Co^{60} emits one γ ray of 1.1 MeV and one of 1.3 MeV per disintegration, so 1.2 MeV was taken as the energy of the radiation.

The number of γ rays interacting with the crystal is thus $2 \times 3.7 \times 10^5 \times 0.0032 = 2.37 \times 10^3$ per sec. On taking a bias curve, and extrapolating to zero pulse height, the counting rate was 280 per second. Thus, the efficiency was $2.8/23.7 = 11.8\%$. The surface of the crystal was not coated with reflecting material.

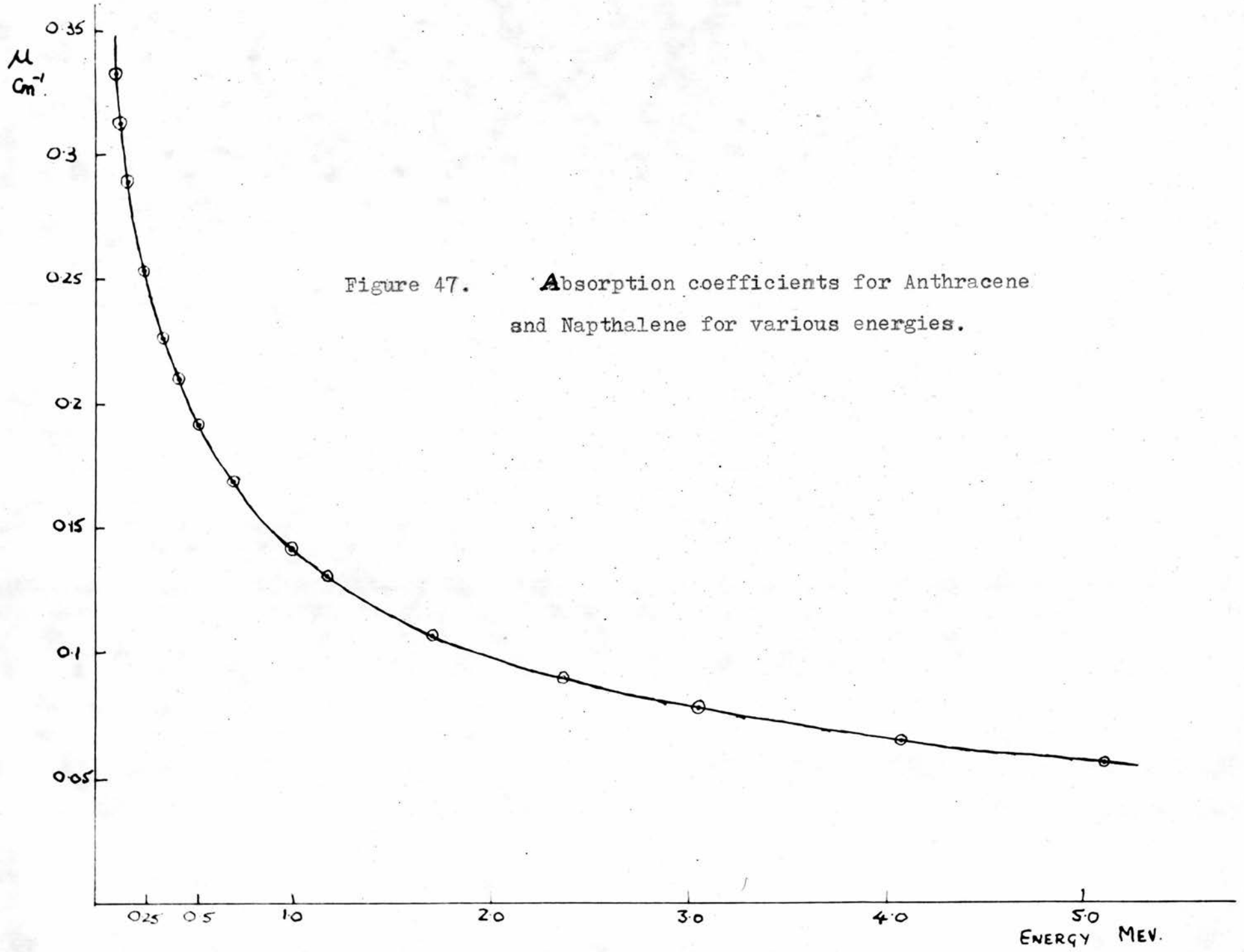

Figure 47. Absorption coefficients for Anthracene and Napthalene for various energies.

References.

Ref. No.		Page No.
1	Dunworth, J.V., 1939, Nature, Lond., 144, 152.	1
2	Ward, 1942, Proc. Roy. Soc., A, 181, 183.	1
3	Rotblat, J., 1941, Proc. Roy. Soc., A, 177, 260.	1
4	Jacobsen, J., and Sigurgiesson, T., 1943, Det. K. Danske Vidensk. Selsk. Nat.-Fys., 20, 11.	1
5	Von Dardel, G., 1950, Phys. Rev., 79, 734.	2
6	Von Dardel, G., 1950, Arkiv för Fysik, 2, 32, 337.	2
7	Hevesy, G., and Paneth, F., 1938, "A Manual of Radioactivity", Oxford.	11
8	Bond, "Probability and Random Errors", Edward Arnold, London.	14
9	McGowan, F.K., 1951, "Short-Lived Isomeric States of Nuclei", O.R.N.L., Report No. 952.	15
10	Von Dardel, G., Private Communication.	18
11	Morton, G.A., 1949, R.C.A. Review, Vol. X, 4.	22
12	Coltman, J W., 1949, Proc. I.R.E., 37, 671.	22
13	Martinson, O., Isaacs, D., Brown, H., and Rudeman, I.W., 1950, Phys. Rev., 79, 178.	22
14	Collins, G.B., 1948, Phys. Rev., 74, 1543.	22
15	Allen, J.S., and Engelder, T.C., 1951, Rev. Sci. Instrum., 22, 401.	22

Ref. No.		Page No.
16	Grington, E.L., Hewlett, W.R., Jasberg, J.H., and Noe, D., 1948, Proc. I.R.E., 36, 956.	23
17	Rudenberg, M.G., and Kennedy, F., 1949, Electronics, 22, 106.	23
18	Bay, Z., 1941, Rev. Sci. Instrum., 12, 127.	23
19	Bay, Z., and Papp, G., 1948, Rev. Sci. Instrum., 19, 565.	25
20	Garwin, R.L., 1950, Rev. Sci. Instrum., 21, 569.	25
21	Wiegand, C., 1950, Rev. Sci. Instrum., 21, 975.	26
22	Dicke, R.H., 1947, Brookhaven Conference Report, p.29.	26
23	Dicke, R.H., 1947, Rev. Sci. Instrum., 18, 907.	26
24	Elmore, W.C., 1950, Rev. Sci. Instrum., 21, 649.	27
25	Shrader, E.F., 1950, Rev. Sci. Instrum., 21, 883.	28
26	Baldinger, E., Huber, P., Meyer, K.P., 1948, Rev. Sci. Instrum., 19, 473.	28
27	Bay, Z., 1951, Rev. Sci. Instrum., 22, 397.	28
28	de Benedetti, S., and Richings, H.J., Rev. Sci. Instrum., 23, 37.	29
29	Wells, F.H., 1951, Proc. Brit. I.R.E., 11, 491.	30
30	A series of articles commencing Nucleonics, 1952, 4, 28.	30
31	Dunworth, J.V., 1939, Nature, Lond., 144, 152.	31
32	Bradt, H., and Scherrer, P., 1943, Helv. Phys. Acta, 16, 259.	31

Ref. No.		Page No.
33	Van Name, J.H., 1949, Phys. Rev., 75, 100.	31
34	Mandansky, L., Pidd, R., 1848, Phys. Rev., 73, 1215.	32
35	Stevenson, A., 1952, Rev. Sci. Instrum., 23, 93.	33
36	Hill, J.M., 1948, Proc. Camb. Phil. Soc., 44, 440.	33
37	Bunyan, D.E., Lundby, A., and Walker, D., 1949, Proc. Phys. Soc., A, 62, 253.	33
38	Newton, T., 1950, Phys. Rev., 78, 490.	46
39	Bell, R.E., and Graham, L., 1950, Phys. Rev., 78, 491.	46
40	Bay, Z., 1950, Phys. Rev., 77, 419.	47
41	Bell, R.E., and Petch, H.E., 1949, Phys. Rev. 76, 1409.	62
42	Schlesinger, K., 1945, Proc. I.R.E., 33, 843.	60
43	Feather, N., Kyles, J., and Pringle, R.W., 1948, Proc. Phys. Soc., 61, 466.	75
44	"Nuclear Data", 1950, N.B.S. circular No. 499, p. 245.	76
45	Bleuler, E., and Zünti, W., 1946, Helv. Phys. Acta, 19, 375.	77
46	Fermi, E., 1950, "Nuclear Physics", Univ. of Chicago Press, p. 66.	79
47	loc. cit., p. 58.	-
48	Taylor, C.J., Jehtschke, W.K., Remley, M.E., Eby, F.S., and Kruger, P.G., 1951, Phys. Rev., 84, 1034.	81
49	Jordan, W.H., and Bell, P.R., 1949, Nucleonics, 5, 10, 30.	83

Ref. No.		Page No.
50	Connor, R.D., 1951, Proc. Phys. Soc., B., 64, 30.	87
51	Wilkinson, D.H., 1950, "Ionization Chambers and Counters", C.U.P., p.162.	88
52	Davisson, C., and Evans, R., 1952, Rev. Mod. Phys., 24, 79.	92.